Adaptation for Climate Change

Sediment-Biota Interactions (Experimental Protocols)

Deliverable Number 9.3

Status: Final Version

Version: 2.0

Date: April 2018

EC contract no 654110, HYDRALAB+

DOCUMENT INFORMATION

Title	Sediment-Biota Interactions (Experimental Protocols)
Lead Author	Hannah Williams (University of Hull)
Contributors	Robert Houseago (University of Hull) Stuart McLelland (University of Hull) Wietse van de Lageweg (University of Hull) Florent Grasso (IFREMER) Pierre-Yves Henry (NTNU) Moritz Thom (LUH)
Distribution	
Document Reference	

DOCUMENT HISTORY

Date	Revision	Prepared by	Organisation	Approved by	Status
January 2018	V1.1	H.E. Williams	University of Hull	S.J. McLelland (UoH)	
February 2018	V1.2	H.E. Williams	University of Hull	S.J. McLelland (UoH)	
March 2018	V1.3	H.E. Williams	University of Hull	S.J. McLelland (UoH)	
April 2018	V2.0	H.E.Williams	University of Hull	S.J. McLelland (UoH)	

ACKNOWLEDGEMENT

The work described in this publication was supported by the European Community's Horizon 2020 Programme through the grant to the budget of the Integrated Infrastructure Initiative HYDRALAB+, Contract no. 654110.

DISCLAIMER

EXECUTIVE SUMMARY

This deliverable details a number of experiments carried out as part of HYDRALAB+ investigating the interaction between sediment and various biota. By conducting these experiments, a number of recommended protocols have been developed to help inform future experiments in these areas. This document firstly consists of an overall introduction to the rationale behind the deliverable. The document is then divided into further sections looking at the interaction between sediment and different types of biota namely; biofilms, vegetation and animals. Within each of these sections, details of the experiments including methodology and where available results will be provided, along with the developed protocols.

The first section looks at two sets of experiments that investigated the use of biofilms within flume experiments. One set of these experiments was carried out at the University of Hull and concentrated on comparing the behaviour of natural biofilms with extracted EPS substances that could be used as surrogates in experiments. The second set of experiments were carried out at Leibniz Universität Hannover, and looked at the development of a novel technique to determine the adhesiveness of different extracted EPS substances, to compare against previous results obtained using natural biofilms.

The next section also details two sets of experiments, this time utilising vegetation or surrogates for vegetation. The first set of these experiments were collaborative work, carried out between the University of Hull and the University of Aberdeen. These have used plastic surrogates representing seagrass to investigate the role of vegetation blade flexibility on wave induced flow velocities and turbulence, above and within the seagrass canopy. The second set of experiments using vegetation looked at seaweed, and consisted of investigations into the dependency of drag forces on different levels of complexity of seaweed morphology to allow characterisation of its hydrodynamics.

The final section consists of a single set of experiments looking at the interaction between animals and sediment, in this case the marine gastropod, *Crepidula*. These experiments quantified the key processes driving the sediment dynamics associated with the presence of these creatures, both when living and dead.

Contents

1 INTRODUCTION

Traditionally physical modelling within the remit of hydraulics has been carried out in sterile conditions, however natural environmental systems are inherently more complex and their attributes and responses are a product of the interactions among hydraulic, ecological and geomorphological processes. There is limited understanding of how these can all be appropriately and successfully incorporated into experimental methods and procedures to give more realistic and comprehensive results. The objective of this task was to address these gaps by developing and testing new protocols for reproducing mobile bed experiments that include biota at suitable scales.

It is generally understood that sediment surfaces affected by biological activity (from growing vegetation to animal activity) provide greater resilience to wave and current action compared to bare (sterile) sediment surfaces. Biota can therefore be considered as a natural adaptation to varying climatic conditions and may also be useful in adaptation strategies that follow the principles of 'working with nature'. However, the interactions driven by biota are also likely to introduce significant non-linearities in system response to environmental change, particularly in terms of sediment transport dynamics which are critical to understanding morphological change.

There is clearly a high degree of complexity present when modelling these interactions experimentally, and the strategy of HYDRALAB+ was to address a number of fundamental aspects, including the representation of sediment-biota interactions through the use of simple surrogate versus real vegetation / fauna and the application of novel instrumentation to enable observation in the near bed areas and complex boundary regions (e.g. under or near moving vegetation / fauna) where measurements have not been possible previously.

All these considerations led the partners to carry out complementary experiments in a number of different available facilities to test new methodologies and improve existing protocols:

- Experiments on biostabilisation effects of biofilm-secreted and extracted extracellular polymeric substances (EPS) on sandy substrate (University of Hull)
- Experimental study of adhesion forces of surrogate EPS (Leibniz Universität Hannover)
- Experimental assessment of surrogate flexible seagrass canopies on wave hydrodynamics (University of Hull / University of Aberdeen)
- Experimental investigations of kelp hydrodynamics (NTNU)
- Experimental study of sediment-biota interactions under wave-current conditions: Application to the ecosystem engineer species *Crepidula fornicata* (IFREMER)

All these tests are described and discussed in the present document, along with specific protocols and recommendations developed from the test results.

2 PROTOCOLS FOR EXPERIMENTS WITH BIOFILMS

2.1 BACKGROUND

Micro-organisms are a fundamental feature of aquatic environments providing a range of ecosystem services (Gerbersdorf et al. 2011; Gerbersdorf and Wieprecht 2015). These micro-organisms can assemble and form what are generically known as "biofilms". Microphytobenthos and microbial mats are representations of these type of microbial communities found in aqueous environments. The microbes in these biofilms live in a self-formed matrix of glue-like and hydrated extracellular polymeric substances (EPS) such as polysaccharides (often 40-95%), proteins (up to 60%) and minor amounts of acids, lipids and biopolymers (Decho 1990; Flemming 2011; Gerbersdorf et al. 2011).

The ecosystem functions of EPS includes sediment particle aggregation, increasing sediment stability, altering chemical properties to enable contaminant release or adsorption, and providing a food source for invertebrates. These functions are well established for marine environments (Decho 1990; Passow 2002; Bhaskar and Bhosle 2006; Paterson et al. 2008), but remain less well understood for freshwater systems (Gerbersdorf et al. 2011).

The ability of biofilms to stabilize sediment and protect sedimentary surfaces against erosion is often referred to as 'biostabilisation' (cf. Paterson 1989). This may result from coverage by microbial mats which protect underlying sediments from fluid forces (Noffke and Paterson 2007) or from micro- to macroscopically thin biofilms that coat, bridge or permeate single grains and pore spaces with their EPS (Gerbersdorf and Wieprecht 2015) which increases both the sediment adhesion / cohesion and the entrainment threshold in two ways: 1) by physically binding both cohesive and non-cohesive sediment grains together (Tolhurst, Gust, and Paterson (2002)), and 2) by molecular electrochemical interaction with cohesive clay particles (Chenu and Guérif 1991).

Many studies have attempted to quantify biostabilisation in a variety of environments (Paterson 1989; Dade et al. 1990; Amos et al. 1998; Tolhurst et al. 1999; Tolhurst et al. 2003; Friend et al. 2003; Friend, Collins, and Holligan 2003; Droppo et al. 2007; Righetti and Lucarelli 2007; Vignaga, Haynes, and Sloan 2012; Graba et al. 2013; Thom et al. 2015). These studies generally show a positive correlation between EPS content and sediment stability measured using an erosion threshold, although variations in space and time (Friend, Collins, and Holligan 2003; Thom et al. 2015) and between cohesive and non-cohesive sandy environments are large.

Biofilm formation affects sediment erosion, transport, deposition and consolidation (Righetti and Lucarelli 2007; Gerbersdorf and Wieprecht 2015). There is, for example, evidence that diatom blooms alter estuarine sediment dynamics (Kornman and De Deckere 1998) illustrating the potential effects micro-organisms can have on system-wide sediment fluxes. At a smaller scale, the introduction of the extracted EPS Xanthan Gum in flume experiments investigating bedform dynamics has been shown to change bedform morphology and behaviour (Malarkey et al. 2015; Parsons et al. 2016). Changes in delta morphology and behaviour were also observed in flume experiments where EPS was added to the sediment mixture (Hoyal and Sheets 2009; Kleinhans et al. 2014). Furthermore, evidence is growing that biofilms alter their local environment by affecting hydrodynamics (Vignaga et al. 2013), since the biofilm surface changes the bed roughness to either dampen or increase turbulence production (Gerbersdorf and Wieprecht 2015), and sometimes their protruding structures create a buffer layer between the flow and the sediment bed that can enhance settling rates (e.g. Augspurger and Küsel 2010).

The corollary of the evidence showing the impact of biofilms on sediment stability and flow behaviour is that the inclusion of biological processes and responses is critical to modelling sediment dynamics because micro-organisms are an integral component of the functioning of water and sediment transfer systems. Predicting the potential impacts of climate change on aquatic environments and applying bio-engineering adaptation strategies like 'Building with Nature' for coastal defence (de Vriend et al. 2015) or flood resilience (Temmerman et al. 2013) requires an understanding of i) the response of micro-organisms to changes in climate-induced hydrodynamic forcing, and ii) the role of micro-organisms in water and sediment transfer systems. Even though it has been demonstrated that the extracted EPS Xanthan Gum is not a perfect analogue for natural biofilms (Perkins et al. 2004), it is useful for modelling biological interactions with sediment dynamics (e.g. Hoyal and Sheets 2009; Kleinhans et al. 2014; Malarkey et al. 2015; Parsons et al. 2016). Extracted EPS also has the advantage that enables time scales of physical modelling experiments to be reduced and biostabilisation effects to be controlled.

This work in this section aims to summarise key steps and findings from various experiments to develop protocols informing future work on the usage and expected biostabilisation effects of these biofilms and surrogates.

2.2 EXPERIMENTS BIOSTABILISATION EFFECTS OF BIOFILM-SECRETED AND EXTRACTED EXTRACELLULAR POLYMERIC SUBSTANCES (EPS) ON SANDY SUBSTRATE (UNIVERSITY OF HULL)

2.2.1 Objectives

The objective of these experiments was to evaluate biostabilisation effects of existing extracted EPS, compared with those of a reference natural biofilm, for a range of conditions commonly used in physical modelling experiments. In doing so, the study solely focused on the sediment stabilising aspect of biofilms and explicitly did not intend to replicate and evaluate natural biofilm behaviour and effects. A sandy substrate was used in this study since this grain size range is most commonly used in physical models of coastal and fluvial systems to date. The specific aims of this study were to:

- Quantify the biostabilisation effects (i.e. erosion threshold) of diatom biofilm-secreted EPS on sandy substrates in a physical model experiment.
- Using the same sandy substrate, quantify the biostabilisation effects of four extracted EPS.
- Assess the sensitivity of the biostabilisation effects of the four extracted EPS to:
  - The preparation procedure;
  - The time after application; and
  - Environmental factors that may differ between flume facilities such as salinity, pH and temperature.

2.2.2 Experiments

Natural Biofilm Experiments

The biofilm experiment was setup in the Total Environment Simulator flume facility at the University of Hull (Figure 2.2.1). Nine parallel channels without an initial gradient were constructed for colonisation. Each channel was 9m long, 0.48m wide and contained a 0.1m thick layer of substrate. With a typical flow depth of 0.1m, the width-to-depth ratio of the channels was about 5. For five of the channels, the substrate consisted of 110 micron sand. One channel contained a coarser 1mm

sand and one channel contained a fifty-fifty mixture of the 110 micron sand and 1mm sand. The two remaining channels contained a patterned substrate with alternating patches of the 110 micron sand and 1mm sand, these patches were different lengths for the two channels. Here, we will focus on the five channels with the 110 micron sandy substrate that allowed us to investigate the temporal dynamics involved in biofilm colonisation and stabilisation. Importantly, the same 110 micron sand was also used in the auxiliary tests with extracted EPS.

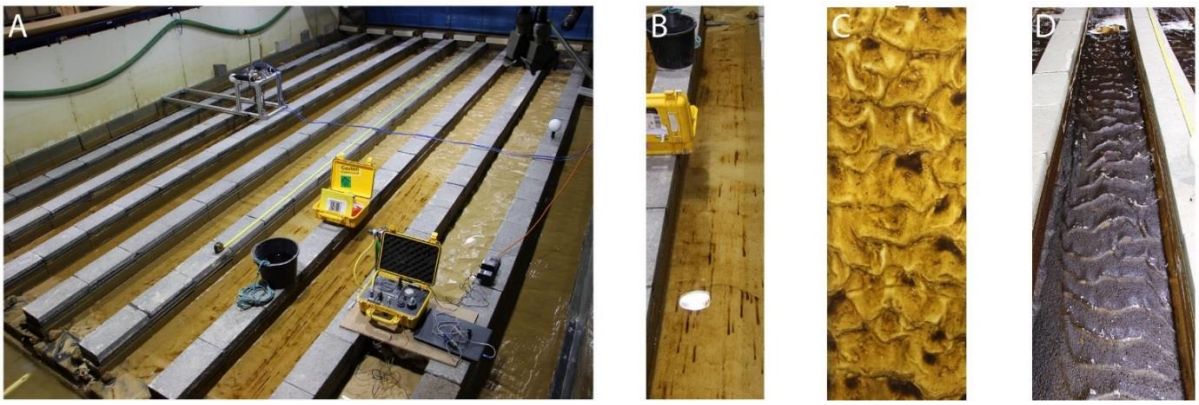

Figure 2.2.1: Biofilm experiment in Total Environment Simulator flume facility. A) Overview of experimental setup showing nine (9) parallel channels for biofilm colonisation. Channels are 9 meters long, 0.48 m wide and contain a 0.1 m thick substrate layer consisting of uniform 110 micron sandy sediment. Also visible in the yellow cases is the CSM erosion device. Panels B) – D) show colonisation and development of a diatomaceous biofilm on the sandy substrate from early onset in (B) to a mature and dark biofilm after 6 weeks. Flow in panels A), C) and D) is towards viewer, and away from viewer in panel B).

Brackish water (~30g of salt per litre) representative of estuarine, mangrove and deltaic settings was re-circulated at a constant rate. Typical flow velocities were 0.01–0.05m/s with higher flow velocities for the central channels due to the inlet conditions. The Reynolds number was generally between 5000 and 10000, indicating turbulent flow conditions. Lighting consisted of ten grow lamps, positioned in two parallel lines of five. Illuminance tests showed that the central channels received the highest light intensity (~3000 lux) with lower intensities towards the periphery channels (~1500 lux). Such light intensities correspond to an overcast day. The grow lamps were alternately switched on and off for 12 hours, although the experiment was never completely dark due to fluorescent lighting around the flume remaining switched on during the night for safety purposes.

The total experimental duration was seven weeks. During the first two weeks, the biofilm community was allowed to establish and no measurements were made. In this two-week period, inoculation of the flume proceeded from using eutrophic waste water from the local aquarium and by placing rocks with a biofilm sampled from the local Humber estuary in the flume. Then, weekly measurements of EPS content and sediment entrainment were made over the latter five-week period. The measurements required partial draining of the flume and therefore about 20% of the water volume was replaced weekly with new waste water from the aquarium. This also ensured that high nutrient levels were maintained during the entire experimental duration. Sediment samples from the top 0.01m of each channel were taken to determine the EPS content from (see section content for details on methodology to determine EPS from sediment samples). In total, 80 sediment samples were collected in this way. Similarly, two sediment entrainment measurements for each channel were collected using the Cohesive Strength Meter (CSM) erosion device (see section device for details on the CSM erosion device). In total, 61 successful CSM measurements were made.

Determination of EPS content

EPS content was calculated using the phenol sulphuric acid method, employing colour differences to determine the amount of carbohydrates (Dubois et al. 1956). The methodology can be subdivided into two main steps. First, 1.5g of each sediment sample were weighed out and placed into 15ml centrifuge tubes. Five millilitres of 0.5Mm Ethylene Diamine Tetra-acetic acid (EDTA) solution was added to each tube. The sediment-EDTA solution was then centrifuged at 5000rpm. Following centrifuging, the supernatants were pooled and placed in a 50ml centrifuge tube. This was repeated two more times. Then, 35ml of ethanol was added to the 15ml of supernatant and left overnight.

The second step started with a 30 minute centrifuge at 5000rpm of the ethanol-supernatant solution. Then, the precipitate was dissolved in 1ml of MilliQ (an ultrapure water) from which the amount of carbohydrates was measured using the phenol sulphuric acid method. This method uses a set of standards to produce a calibration curve. In this study, the standards had glucose concentrations ranging between 0µg/ml and 40µg/ml. Standards were produced by mixing 200µl of the respective glucose solution with 200µl of phenol solution and 1ml of concentrated sulphuric acid. The samples were prepared according to the same procedure, but by replacing the glucose solution with the aqueous solution. Finally, the absorbance was measured using a spectrophotometer at 490nm. Using the glucose calibration curve, the measured absorbance was converted to a carbohydrate amount that was assumed equal to the amount of EPS. Dry weight of the sediment sample was used to calculate the EPS content.

Extracted EPS experiments

The effect of varying amounts of four different types of extracted EPS on the sediment entrainment threshold and erosion behaviour was tested. The four different EPS selected were Xanthan Gum, Alginic Acid, Carrageenan and Agar for their ease of availability, differences in chemical properties, and absence of safety issues ensuring the potential for wide usage in future work. Xanthan Gum ($C_{35}H_{49}0_{29}$) is a polysaccharide commonly used as a food additive and has also been included in earlier laboratory tests (Tolhurst, Gust, and Paterson 2002; Parsons et al. 2016). Alginic Acid $(C_6H_80_6)_n$, also known as alginate, is a carbohydrate produced by brown algae and also widely used in food. Carrageenan is a sulphate polysaccharide extracted from red seaweeds and also widely used as a food additive. We used the Iota variety that has two sulphate groups per disaccharide ($C_{24}H_{36}0_{25}S_2$). Agar is used as a gelling agent and is obtained from the polysaccharide agarose found in some species of red algae.

Petri dish sediment sample tests with extracted EPS

A protocol similar to the one used in Tolhurst, Gust, and Paterson (2002) referred to as 'wet mixing' was applied to prepare the petri dish sediment samples for CSM testing. A control test with no EPS, and four tests with increasing EPS contents of 1.25g, 2.5g, 5g and 10g per kg of sediment were performed for the four different EPS. The required EPS amount was added to 330ml of distilled water and mixed thoroughly by a magnetic stirrer. The EPS solution was then added to 650g of dry 110 micron sand and mixed with an electric stirrer to distribute the EPS solution throughout the sand. The sand-EPS mixture was then poured into plastic petri dishes (5cm diameter) to a depth of 1cm. Irregularities on the sediment surface increase the bed roughness and stress (Tolhurst, Gust, and Paterson 2002), therefore care was taken to create a level surface by tapping the side of the petri dishes before testing. All test conditions were repeated five times and all tests were performed under fully saturated conditions.

Preparation procedure

Protocol development on the application and effects of different extracted EPS required an assessment of the impact of the preparation procedure on the sediment entrainment threshold. To this end, the Wet Mixing preparation procedure described above, was complemented by a preparation procedure referred to as 'Dry Mixing'. Both procedures used the same sand, EPS and amounts but the order in which they were combined and mixed, was changed. In contrast to the Wet Mixing procedure, in the Dry Mixing procedure the required amount of EPS was first added to the sand and mixed with an electric stirrer. Then, 330ml of distilled water was added to the dry sand-EPS mixture and further mixing with the electrical stirrer was performed. Note that the risk of dust formation and associated loss of EPS powder was greater in the Dry Mixing procedure.

Environmental conditions

Protocol development on the application and effects of different EPS also required an assessment of the impact of the different environmental conditions on the sediment entrainment threshold. As temperature, salinity and to a lesser extent pH commonly vary between flume facilities, a sensitivity analysis on the effectiveness of extracted EPS to impact the sediment entrainment threshold was performed. For temperature, tests were performed at 10°C and 40°C in addition to the control tests at room temperature of 20°C. For pH, tests were performed with a pH of 4 and a pH of 10 in addition to the control tests of a pH of 7. For salinity, tests with a salinity of 30 ppm corresponding to brackish conditions were performed in addition to the control tests with distilled fresh water.

Cohesive Strength Meter (CSM) erosion device

The CSM is an erosion device (https://partrac-csm.com/) that allows for quantification of sediment entrainment thresholds and erosion rates in the laboratory as well as in the field across a variety of environments (Paterson 1989; Tolhurst et al. 1999; Tolhurst, Gust, and Paterson 2002). The CSM uses a vertical jet of water that impinges on the sediment surface generating a normal and tangential stress at the interface. These stresses were converted to a critical horizontal shear stress (τ_c) according to the calibrated formulation (Tolhurst, Gust, and Paterson 2002):

$$\tau_c = 66.67 \cdot \left(1 - \mathrm{e}^{\frac{-C}{310.09}}\right) - 195.28 \cdot (1 - e^{\frac{-C}{1622.57}}) \quad (1)$$

Where C is the CSM measured vertical threshold stress (kPa).

The CSM allows 39 different test routines making it possible to vary the jet pulse duration, the pressure increments and the maximum applied pressure. For all data reported in this study, CSM test routine S7 was used as it strikes a balance between fine pressure increments while reaching a high maximum pressure, thus covering a large erosional range within the same setting. Another motivation for the selection of CSM routine S7 is that it was used in Tolhurst, Gust, and Paterson (2002), allowing for a direct comparison between the data. The CSM S7 test routine starts at 0kPa, incrementing by 2.068kPa per step up to 82.74kPa with a jet being fired for 1s.

2.2.3 Results

Colonisation of biofilm

The eutrophic water used in the experiment resulted in rapid colonisation and growth of a diatomaceous biofilm on the substrate materials (Figure 2.2.1a). After two weeks, biofilm colonisation and growth were localised and organised into darker stripes running parallel to the main flow (Figure 2.2.1b). Colonisation and development of the biofilm continued over the next five

weeks resulting in a more widespread biofilm coverage (Figure 2.2.1c). At the end of the experiment after seven weeks, the sandy substrate in the channels was covered by a few millimetres thickness of black biofilm crust (Figure 2.2.1d). At this stage, mortality of the biofilm had set in locally, which was illustrated by greyish patches within the black healthy biofilm that were sometimes eroded. This observation ensured that we observed the full life cycle of a diatomaceous biofilm from early colonisation to mortality and subsequent crust erosion.

Microscope investigations of the species ecology confirmed a saline environment that was dominated by halophilous diatoms, which are common in coastal zones (Pan et al. 2004). The diverse flora was dominated by five main species: a) Nitzschia pellucida, b) Nitzschia sigma, c) Mastogloia sp, d) Navicula perminuta, and e) Amphora pediculus. The Nitzschia species are considered early colonisers (Ledger et al. 2008; Ros, Marín-Murcia, and Aboal 2009), and were indeed found primarily in the samples of the early stages of the experiment. Furthermore, all taxa were benthic rather than planktonic, as expected in lotic conditions (Passy 2001; Schmidt et al. 2016). Some diatoms were attached whilst some diatoms were mobile and therefore not attached to the sediment grains. Also, ciliates were present and presumably eating the diatoms. Importantly, many of the species observed were obligate and cannot tolerate freshwater, in agreement with the designed experimental conditions.

Sediment stability from biofilm-secreted EPS

Figure 2.2.2 shows a cumulative probability distribution of the CSM sediment stability measurements made during the flume experiment. The average shear stress entrainment threshold was $0.69 N \cdot m^{-2}$ with a standard deviation of $0.82 N \cdot m^{-2}$. The distribution is highly skewed towards lower shear stresses, as evidenced by a median shear stress entrainment threshold of $0.23 N \cdot m^{-2}$. This median value was just above the CSM measured entrainment threshold for the uncolonised sand of $0.18 N \cdot m^{-2}$, which is in close agreement with the theoretical entrainment threshold for the applied 110 micron sand of $0.15 N \cdot m^{-2}$ (Zanke 2003). Notably, 42% of the measurements were smaller than the entrainment threshold of the uncolonised sand, even when a biofilm was clearly visible at the substrate surface. A maximum entrainment threshold of $3.84 N \cdot m^{-2}$ was measured, which represents a more than 21 times higher erodibility threshold compared to the uncolonised sand. Entrainment thresholds were higher in the first three weeks (~ $1 N \cdot m^{-2}$ on average) in comparison to the last two weeks (~ $0.3 N \cdot m^{-2}$ on average).

The average carbohydrate content, here equated to EPS content, was 7.8µg per g of sand with a standard deviation of 7.8µg per g (Figure 2.2.3). The measurements were best described by an exponential fit with a mean parameter µ of 7.88, highlighting the skewed character of the data with many lower content observations and fewer towards higher EPS contents. The maximum measured EPS content was 34.6µg per g of sand. In contrast to the sediment entrainment threshold (Figure 2.2.2), the average EPS content increased on a weekly basis from 5.6µg per g of sand in the first week to 11.6µg per g of sand in the final week.

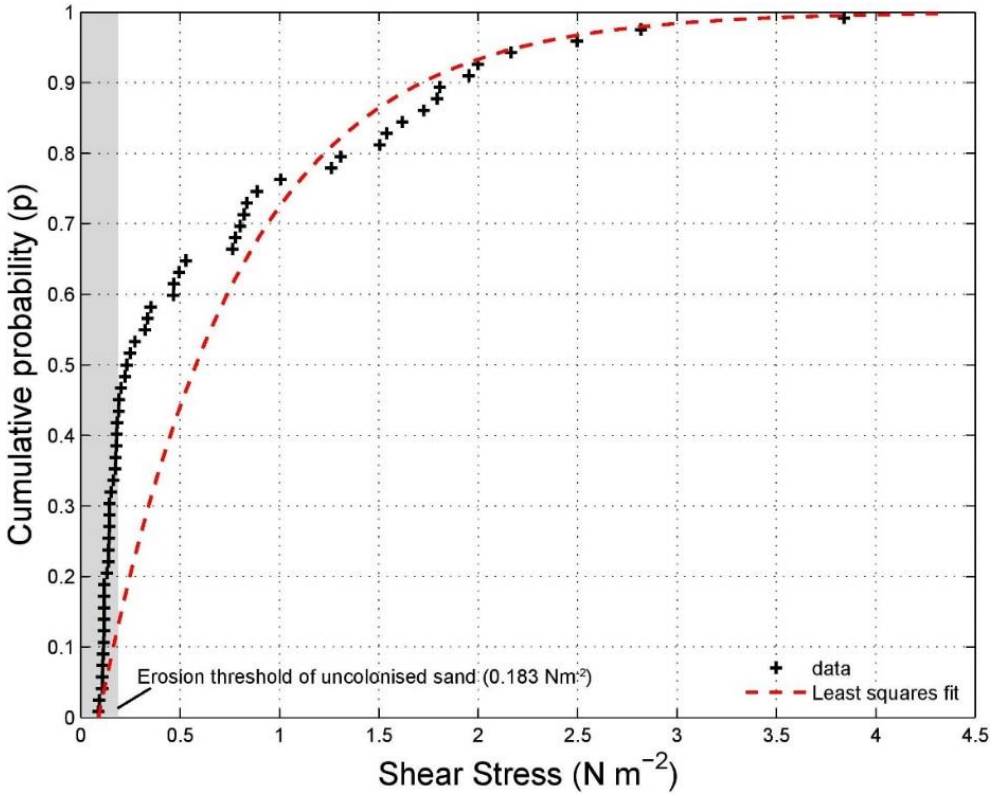

Figure 2.2.2. Shear stress measurements made with CSM erosion device during natural biofilm growth experiment. The measurements (n = 61) are best described by a least squares exponential fit with a mean parameter μ of 0.71.

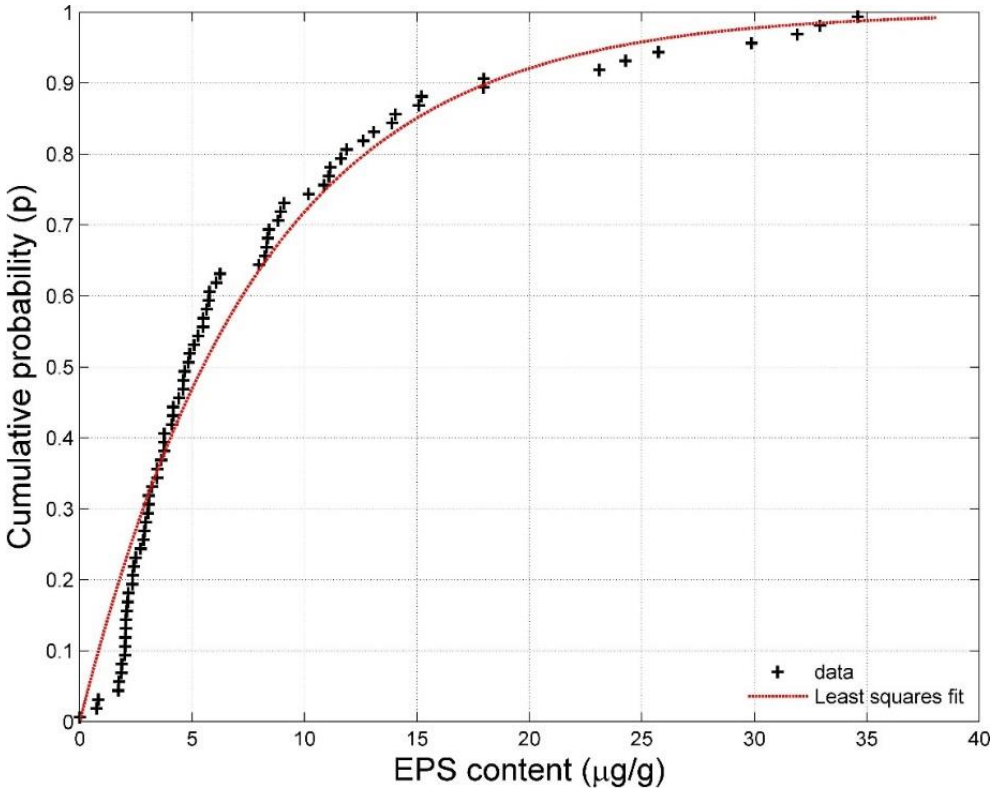

Figure 2.2.3. Extracellular polymeric substances (EPS) content measurements made during natural biofilm growth experiment. The measurements (n = 80) are best described by a least squares exponential fit with a mean parameter μ of 7.88.

Sediment stability from extracted EPS

The above section illustrated that experiments involving natural biofilms typically take multiple weeks to capture the complete life cycle. As such flume experiments are costly, extracted EPS has the potential to provide an effective alternative to reproduce the sediment stabilising effects on natural biofilms in a fast and controlled manner. Below, small-scale experiments are described quantifying 1) the effect of the different concentrations of four extracted EPS, 2) the effect of the preparation procedure, and 3) the effect of environmental factors such as temperature, salinity and pH. All three tests were intended to contribute towards the development of the protocol to guide the use of extracted EPS in experiments as a surrogate to replicate sediment stability from natural biofilms. The applied concentrations of the extracted EPS were based on the measured EPS contents in the natural biofilm experiment (Figure 2.2.3) and reported values in the literature (Taylor, Paterson, and Mehlert 1999; Tolhurst, Gust, and Paterson 2002).

Effects of extracted EPS content on sediment stability

The four extracted EPS had different effects on sediment stability (Figure 2.2.4). Alginic Acid and Agar did not increase the sediment stability above the erosion threshold of the sand without EPS, for all applied concentrations. For Xanthan Gum and Carrageenan, the erosion threshold generally increased with increasing EPS content (Table 2.2.1). For these EPS, the relation between the critical shear stress for erosion and EPS content was best described using linear models (Figure 2.2.4), where the slope of the linear model for Xanthan Gum (0.28) was more than double the slope of the linear model for Carrageenan (0.11).

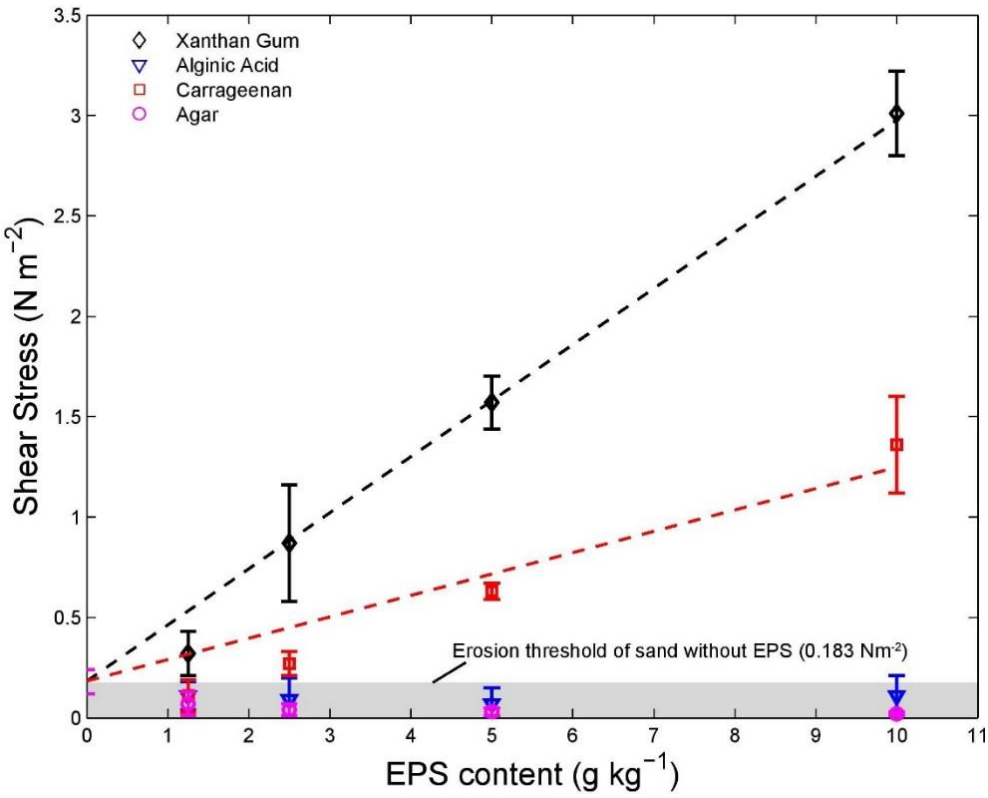

Figure 2.2.4. The erosion thresholds of 110 micron sandy substrate with different contents for four extracted EPS as measured with the CSM erosion device. Best fit curves were fitted using linear models for Xanthan Gum (Shear stress threshold = 0.28 EPS content + 0.18) and Carrageenan (Shear stress threshold = 0.11 EPS content + 0.18). Error bars are standard deviation from n =5 repeat measurements.

Table 2.2.1. Erosion thresholds for four extracted EPS measured with the CSM erosion device.

	Average ± St. deviation erosion threshold (N·m-2)			
EPS (g·kg-1)	*Xanthan Gum*	*Carrageenan*	*Agar*	*Alginic Acid*
0	*0.18 ± 0.06*	*0.18 ± 0.06*	*0.18 ± 0.06*	*0.18 ± 0.06*
1.25	*0.32 ± 0.11*	*0.11 ± 0.08*	*0.07 ± 0.06*	*0.11 ± 0.08*
2.5	*0.87 ± 0.29*	*0.27 ± 0.06*	*0.04 ± 0.03*	*0.09 ± 0.11*
5	*1.57 ± 0.13*	*0.63 ± 0.04*	*0.03 ± 0.02*	*0.07 ± 0.08*
10	*3.01 ± 0.21*	*1.36 ± 0.24*	*0.02 ± 0.01*	*0.11 ± 0.10*

Effects of preparation procedure on sediment stability

The preparation procedure adopted for adding the extracted compounds to the sediment material had an impact on the resultant erosion threshold (Figure 2.2.5). 'Dry mixing' the extracted EPS powder with the sediment prior to adding water resulted in a higher erosion threshold than 'Wet mixing' the EPS powder with sediment in water for all tested EPS. The difference was greatest for Xanthan Gum with a 67% higher threshold for the dry mixing procedure compared to the wet mixing procedure.

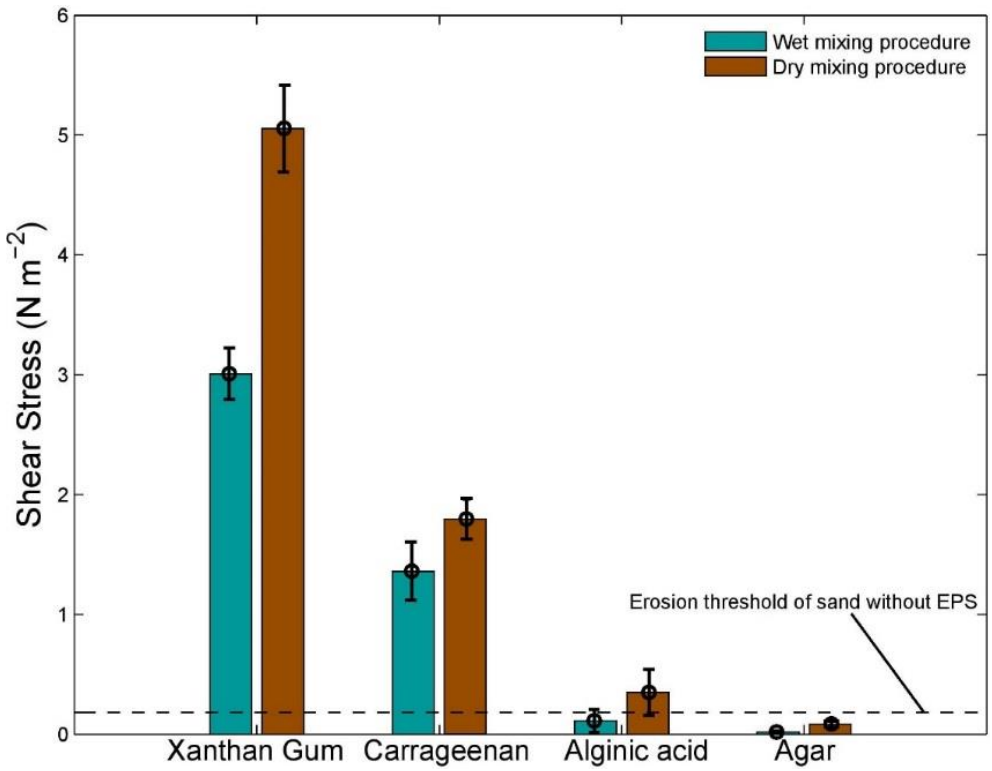

Figure 2.2.5. The erosion thresholds as a function of the preparation procedure for four surrogates as measured with the CSM erosion device. Wet mixing involves dissolving the extracted EPS powder in water and stir, then add sediment and mix. Dry mixing involves the addition of extracted EPS powder to sediment and mix, then add water and stir. Error bars are standard deviation from n =5 repeat measurements.

Temporal effects on sediment stability

Time elapsed from initial mixing also affected the sediment stabilising capacity of extracted EPS (Figure 2.2.6). Repeat measurements after one day, seven days and fifteen days demonstrated that the erosion thresholds remained constant throughout the first week. However, the repeat measurements after fifteen days showed a decrease in the erosion threshold below the erosion

threshold of sand without EPS. This effectively meant that after about two weeks of initial application of EPS, the impact on the erosion threshold of the sediment ceased to exist.

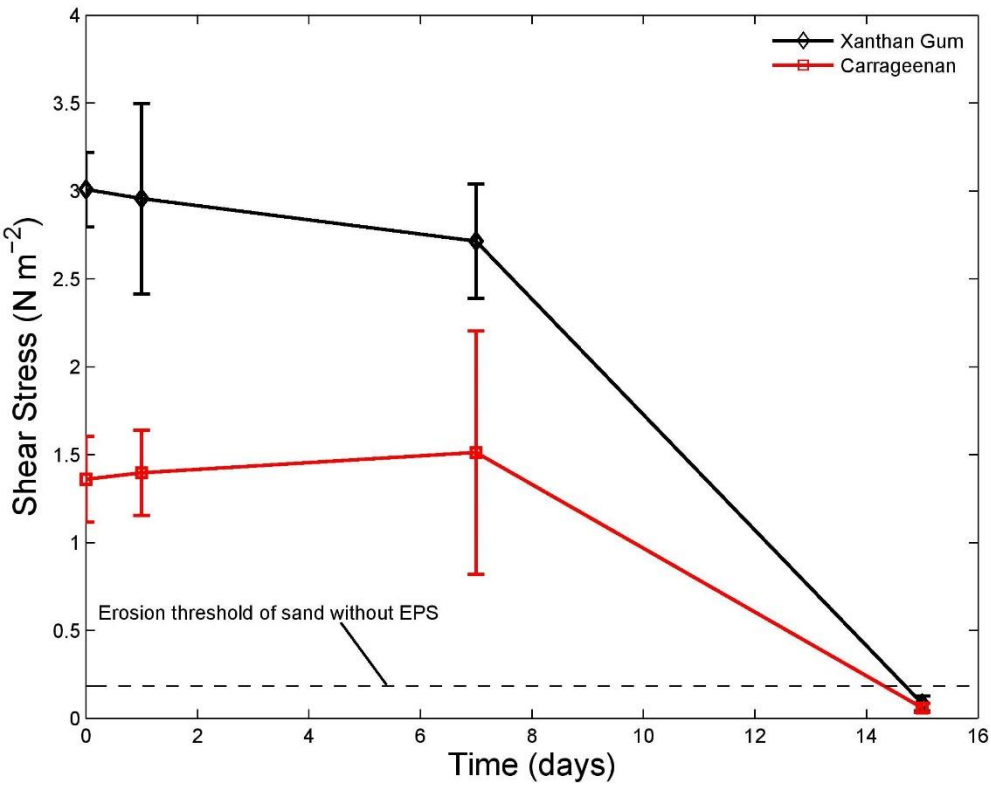

Figure 2.2.6. The erosion thresholds as a function of time for Xanthan Gum and Carrageenan as measured with the CSM erosion device. Error bars are standard deviation from n =3 repeat measurements.

Effects of salinity on sediment stability

Salinity had a limited effect on the erosion thresholds (Figure 2.2.7). Saline water tended to decrease the erosion threshold compared to freshwater conditions, though the differences are statistically insignificant for all four EPS. The erosion thresholds for Alginic Acid and Agar remained below the erosion threshold of sand without EPS independent of the salinity of the water.

This implies that the findings of this study that were mostly obtained for freshwater conditions can be extrapolated to saline conditions.

Effects of pH on sediment stability

The pH of the applied solution had variable effects on the erosion threshold (Figure 2.2.8). An acid solution with a pH of 4 resulted in a higher erosion threshold for Xanthan Gum, but in a lower threshold for Carrageenan. An alkaline solution with a pH of 10 resulted in lower erosion thresholds for Xanthan Gum as well as Carrageenan. The erosion thresholds for Alginic Acid and Agar remained below the erosion threshold of sand without EPS, independent of the pH of the solution.

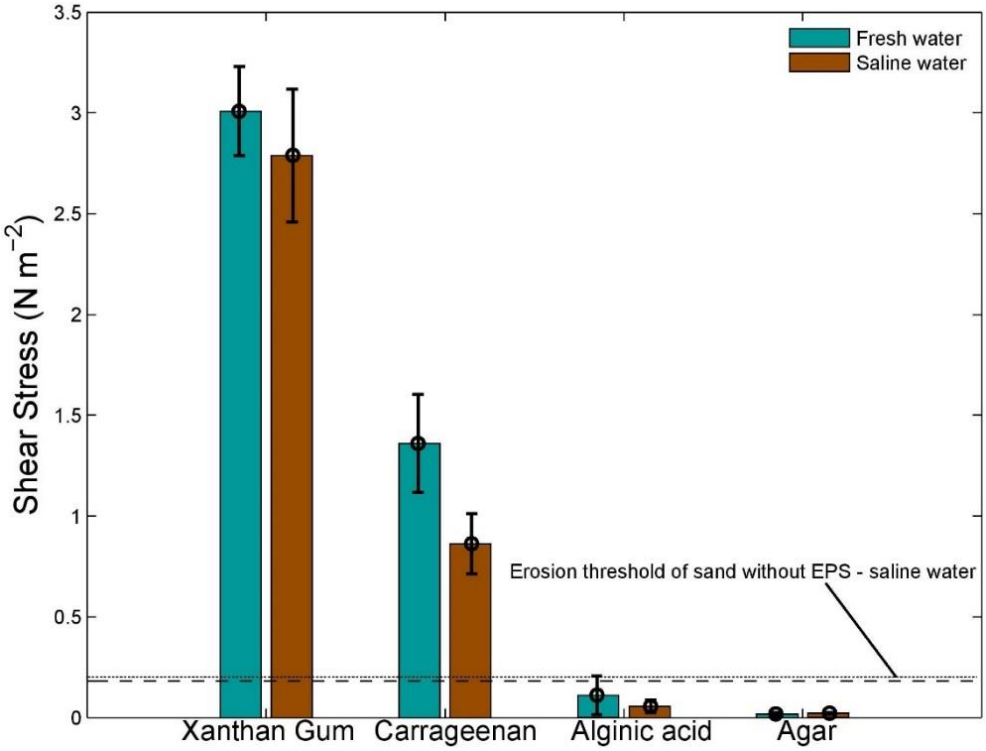

Figure 2.2.7. The erosion thresholds as a function of salinity for four extracted EPS as measured with the CSM erosion device. Tap water was used for the freshwater tests and a salinity of 30ppt was used for the saline water tests. The horizontal lines correspond to the erosion thresholds of sand without EPS for freshwater (dashed) and saline water (dotted). Error bars are standard deviation from n =3 repeat measurements.

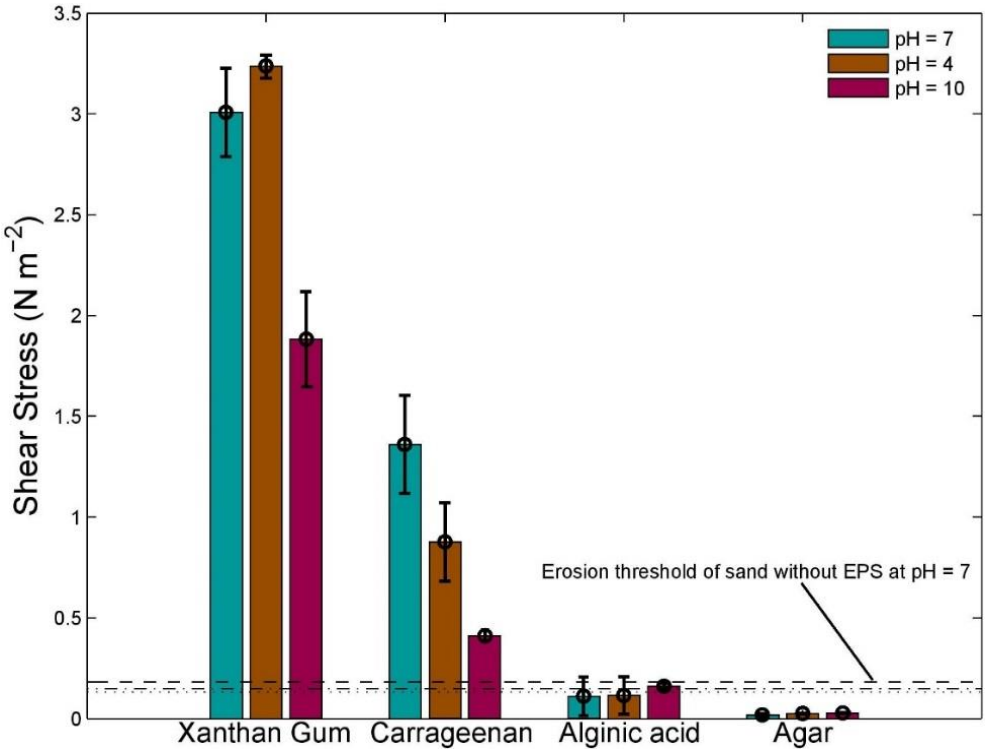

Figure 2.2.8.. The erosion thresholds as a function of pH for four extracted EPS as measured with the CSM erosion device. The horizontal lines correspond to the erosion thresholds of sand without EPS for water with a pH of 7 (dashed), a pH of 4 (dotted), and a pH of 10 (dash-dotted). Error bars are standard deviation from n =3 repeat measurements.

Effects of temperature on sediment stability

Temperature impacted the measured erosion thresholds (Figure 2.2.9). Both a lower temperature of 10°C and a higher temperature of 40°C resulted in lower erosion thresholds. For Xanthan Gum as well as Carrageenan, the erosion thresholds were about half under 10°C and 40°C test conditions compared to 20°C test conditions. The erosion thresholds for Alginic Acid and Agar remained below the erosion threshold of sand without EPS independent of the temperature.

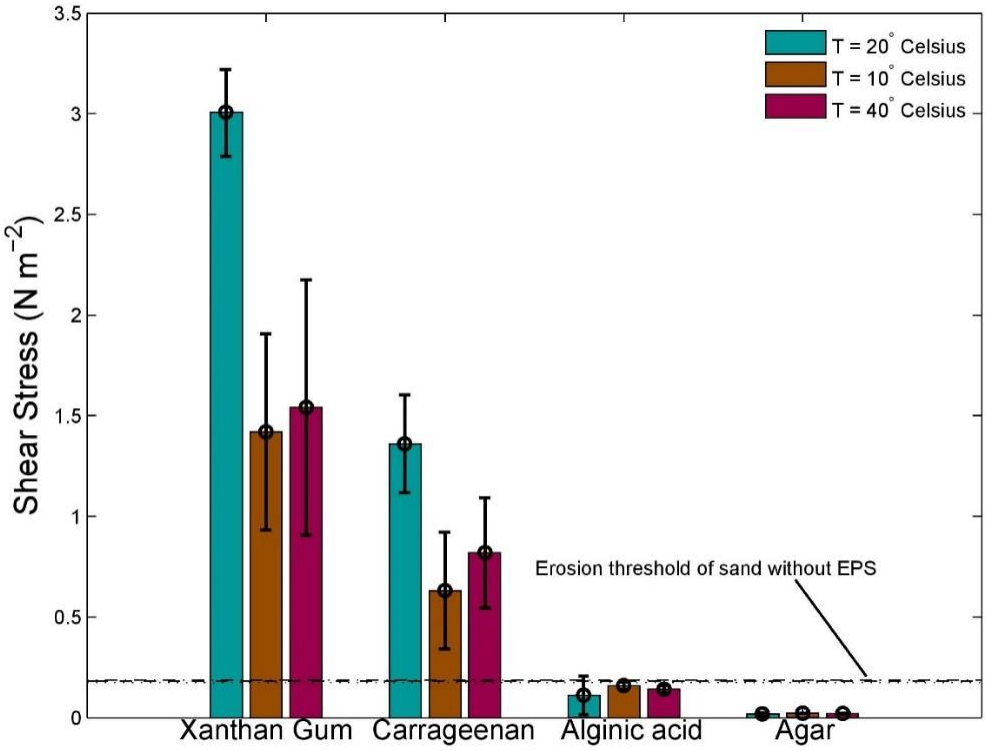

Figure2.2.9.The erosion thresholds as a function of temperature for four extracted EPS as measured with the CSM erosion device. The horizontal lines correspond to the erosion thresholds of sand without EPS for a temperature of 20° Celsius (dashed), a temperature of 10°C (dotted), and a temperature of 40°C (dash-dotted). Error bars are standard deviation from n =3 repeat measurements.

Synthesis of the effects of extracted EPS on sediment stability

In summary, extracted EPS Xanthan Gum and Carrageenan increased the erosion threshold with higher EPS content (Table 2.2.1). For these two EPS, the relationship between erosion threshold and EPS content was linear and predictable (Figure 2.2.4). In contrast, the extracted EPS Alginic Acid and Agar did not increase the erosion threshold (Table 2.2.1), independent of the applied concentration (Figure 2.2.4), preparation procedure (Figure 2.2.5) or environmental condition such as salinity, pH and temperature. Yet, this study demonstrated that the preparation procedure, environmental conditions and time impacted on the resultant erosion threshold for the EPS Xanthan Gum and Carrageenan. A dry mixing procedure increased the erosion threshold while saline water, alkaline solutions and non-room temperature test conditions of 10°C and 40°C decreased the erosion thresholds. The tests also showed that the effects of adding Xanthan Gum and Carrageenan on the erosion thresholds ceased to exist after about two weeks following initial application (Figure 2.2.6Figure). These findings indicate that the effectiveness of extracted EPS to stabilise sediment is sensitive to the applied concentration, the preparation procedure, time and environmental conditions.

2.2.4 Discussion

The CSM data show that the addition of extracted EPS Xanthan Gum and Carrageenan increases the critical erosion threshold, even at low EPS concentrations (Figure 2.2.4 and Table 2.2.1). The observation that the erosion threshold increased approximately linearly with EPS content for Xanthan Gum is in agreement with the findings reported in Tolhurst, Gust, and Paterson (2002). We find a similar linear increase in erosion threshold with EPS content for Carrageenan, though the rate of increase is smaller compared to Xanthan Gum. The approximately linear relation between EPS content and erosion threshold across the measured range for Xanthan Gum and Carrageenan simplifies the prediction of biostabilisation effects due to extracted EPS. Two other extracted EPS, Alginic Acid and Agar, were also tested and showed negligible biostabilisation for any of the test conditions investigated.

Table 2.2.2. Biostabilisation index resulting from natural biofilm and Xanthan Gum and Carrageenan extracted EPS as measured in this study. The biostabilisation index is defined relative to the erosion threshold of sand without EPS (Manzenrieder 1985).

	Uncolonised	***Median***	***Mean***	***Maximum***
Biofilm	*1*	*1.3*	*3.8*	*21.0*
	1.25 g·kg-1	*2.5 g·kg-1*	*5 g·kg-1*	*10 g·kg-1*
Xanthan Gum	*1.7*	*4.8*	*8.6*	*16.4*
Carrageenan	*0.6*	*1.5*	*3.5*	*7.4*
(10 g·kg-1)	*Dry mix*	*Saline*	*pH = 10*	*T = 10° Celsius*
Xanthan Gum	*27.6*	*15.2*	*10.3*	*7.8*
Carrageenan	*9.8*	*4.7*	*2.2*	*1.6*

Biostabilisation of the same sandy substrate due to natural biofilm colonisation and due to the addition of extracted EPS Xanthan Gum and Carrageenan compares well (Table 2.2.2). We find a mean biostabilisation index due to natural biofilm colonisation and development of almost four times that of the uncolonised sand. Such a biostabilisation index is within the reported range for fine sand (Dade et al. 1990; Vignaga et al. 2013). More specifically, 42% of the tested samples did not show biostabilisation compared to uncolonised sand while 10% of the measurements showed a tenfold biostabilisation relative to uncolonised sand (Figure 2.2.2). The presented cumulative probability distribution of critical erosion thresholds reflects the large spatial and temporal variations generally seen in natural biostabilised environments (Paterson 1989; Amos et al. 1998; Tolhurst et al. 1999; Tolhurst et al. 2003; Friend, Collins, and Holligan 2003). The biostabilisation index due to extracted EPS covers approximately the same range of erosion thresholds for the applied EPS contents. Xanthan Gum may be more suited to replicate the higher biostabilisation observations of natural biofilms due to the increased erosion thresholds for the highest applied content of 10g·kg^{-1}. Carrageenan may be more appropriate to replicate the lower biostabilisation observations of natural biofilms due to the small effect on erosion thresholds for low concentrations.

The concentrations of the EPS derived from the natural biofilm experiment (µg·g^{-1}) are about three orders of magnitude lower than the applied extracted EPS concentrations (mg·g^{-1}) to achieve the same biostabilisation effect. Two reasons may explain these differences. First, the applied phenol-sulphuric acid assay measures a carbohydrate fraction of the total EPS, along with low-weight sugars that are extracted with the polymeric material (Underwood, Paterson, and Parkes 1995). Along with the sensitivity of the EPS extraction methodology to a host of conditions (Perkins et al. 2004), this

may be part of the explanation for the lower EPS concentrations in the natural biofilm samples. Second, sediment sampling for EPS concentration analysis typically involved scraping off the top centimetre of the substrate. However, it has been shown that EPS content in nature is highest at the sediment surface (top 200 µm) and decreases with depth (Taylor and Paterson 1998). Our sediment sampling strategy is likely to have diluted the EPS concentration, which may offer another explanation for the lower EPS concentrations in the natural biofilm samples.

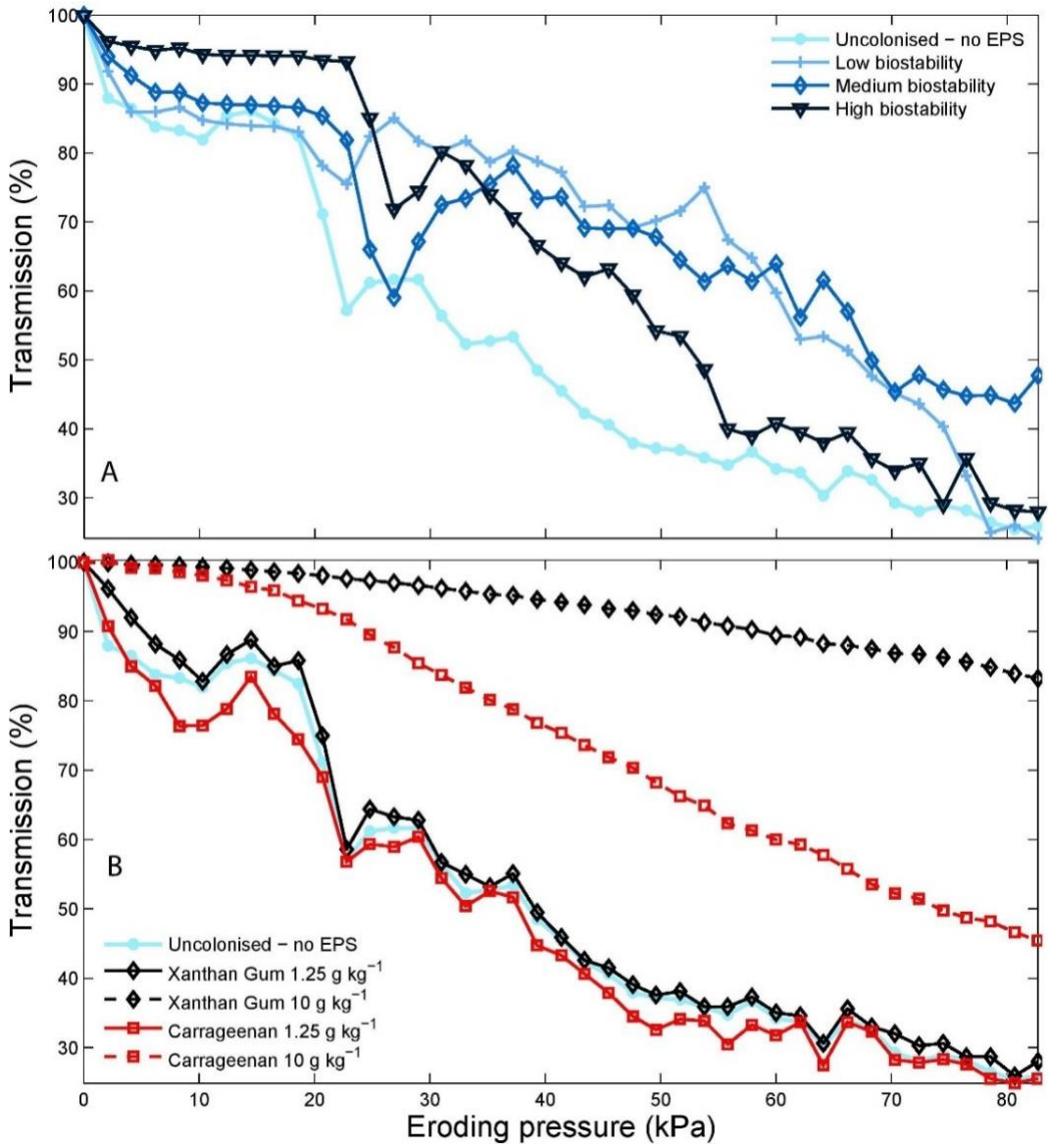

Figure 2.2.10. CSM erosion profiles for sediment with different degrees of biostability due to natural biofilm colonisation (A) and due to different Xanthan Gum and Carrageenan extracted EPS contents (B).

Erosion profiles for low concentrations of extracted Xanthan Gum and Carrageenan are similar to those measured from the natural biostabilised sediments (Figure 2.2.10). For higher concentrations of Carrageenan and particularly Xanthan Gum, the erosion rate is reduced relative to the natural biostabilised samples. In contrast to the natural samples where EPS concentration decreases with depth (Taylor and Paterson 1998), the extracted EPS were mixed homogenously with depth in this study. As a consequence, the erosion rate for high concentrations of extracted EPS has been reduced more than would be found under natural conditions. To overcome this and to better replicate

natural biofilm-mediated erosion behaviour, it may be more appropriate to apply extracted EPS only on the surface in future studies. This will result in the highest EPS concentrations at the sediment surface that decreases with depth depending on the porosity and saturation of the substrate.

Recommended protocols

The methodologies described herein for preparing engineered sediments and the resultant biostabilisation may serve as protocols to guide the design of future studies that aim to represent biological cohesion. In essence, biostabilisation effects of Xanthan Gum and Carrageenan extracted EPS behave linearly (Figure 2.2.4) and are therefore predictable. Different concentrations of these extracted EPS may be used to replicate the temporal and spatial variations generally seen in biostabilisation due to natural biofilm colonisation. Other than biostabilisation, no differences in application or behaviour between Xanthan Gum and Carrageenan were observed in this study. Furthermore, the sensitivity analysis performed in this study showed that the effectiveness of Xanthan Gum and Carrageenan for the stabilisation of sediment, not only depends on the applied concentration, but is also sensitive to the preparation procedure, time after application and environmental conditions. The results for the time elapsed after initial application tests were obtained for samples that dried out between measurements. Temporal behaviour of extracted EPS may be different when the engineered sediments remain wet for the duration of the test, which requires further research. The sensitivity of engineered sediments to salinity, pH and temperature found in this study indicates that a high level of control of these environmental variables is required for reliable application of extracted EPS in flume facilities.

Physical modelling of the complex flow, sediment transport and ecological interactions within aquatic ecosystems is key to bridge the divide between field observations and numerical models (Thomas et al. 2014; Gerbersdorf and Wieprecht 2015). The implementation of biological processes into sediment transport equations that have traditionally been modelled as abiotic systems is expected to result in better predictions of sediment dynamics (Black et al. 2002; Righetti and Lucarelli 2007; Gerbersdorf et al. 2011; Parsons et al. 2016). Our study confirms that Xanthan Gum and Carrageenan extracted EPS are not perfect analogues of natural biofilms (Perkins et al. 2004), but they are capable of introducing realistic biological cohesion into flume facilities in a fast and controlled manner for a range of commonly used conditions. The reduction in experimental time here is significant since the maximum biostabilisation effects of natural biofilm can easily take 5 weeks or more to achieve, whereas extracted EPS can be introduced at the same time as the sediment minimising time to set-up an experiment. Similarly, growth patterns, particularly the effect of increasing biostabilisation can easily be reproduced in a stepwise manner by introducing greater concentrations of the extracted EPS. Although this study has focused on replicating one aspect of natural biofilm behaviour only, future physical modelling studies employing extracted EPS may provide important insights into the role of biological cohesion in sediment dynamics, and how these may be altered in a changing climate.

2.3 ADHESION FORCES OF SURROGATE EPS (LEIBNIZ UNIVERSITÄT HANNOVER)

2.3.1 Objectives

Knowledge of the biomechanical properties of biofilms is crucial to develop surrogates that adequately replicate natural biofilm properties in erosion experiments. In these experiments a novel technique is applied to determine the adhesiveness (i.e. the glue-like effect) of different commercially available rheology modifiers (xanthan gum, agar agar, sodium alginate and guar gum) as EPS surrogates to compare these material properties with results previously obtained from a study of natural biofilms.

To determine adhesion, a modified version of the MagPI system (first published by Larson et al., 2009 see also Thom et al., 2015) developed in an earlier project is used. This system is called the MagPI-IP (Magnetic Particle Induction – Image Processing) and the enhancements enable the measurement of adhesion at the mesoscale (millimetre to centimetre) on submerged surfaces both quickly and reliably. The method has been successfully applied recently to determine adhesive properties of developing biofilms cultivated under different environmental conditions and at different seasons (Thom et al., 2016).

The aim of this section is to provide protocols on design criteria for surrogate biofilms based on the measured surface adhesion.

2.3.2 Experiments

Measuring setup (MagPI-IP)

To determine adhesion forces, ferromagnetic particles (FP, 0.20 < d < 0.35 mm) are dropped on the biofilm surface where they come into contact with the EPS and stick to it with a strength that is proportional to the surface adhesion forces of the biofilm. These particles are then immediately attracted by an electromagnet at increasing magnetic forces which is positioned at a vertical distance of 4 mm above the particles. The retrieval of the FP from the surface is recorded by a camera system and the data is later processed with a MATLAB© program. A mean pull-off force can be calculated from the mechanical force exerted by the electromagnet which is calculated by calibration and the quantity of particles attracted for each step change in the applied magnetic force. Also, the surface adhesion force can be calculated ($A_{s,30}$ in N/m²) from the deadweight of the particles (derived from measurements on non-adhesive surfaces) and the area of contact between the particles and the adhesive surface (so far an assumption is used: sinking depth of FP into the adhesive is 30% of their diameter). Figure 2.3.1 shows the measuring setup.

Surrogates

Four different rheology modifiers that are commonly used as food additives were tested as part of this project. These substances have two useful characteristics: (i) they are partly also produced by bacteria (e.g. xanthan gum) and come as a powder which can be easily mixed with water in different concentrations to modify the mechanical properties that they impart to the mixture; and (ii) they are relatively inexpensive and easily purchased in large quantities. The following modifiers are tested for their adhesive capacities: xanthan gum, agar agar, guar gum (XG, AG, GG, all purchased from buxtrade.com), sodium alginate (SA, specialingredients.com) and xanthan gum (XG, FuFeng). For the adhesion measurements, all surrogates are mixed as described in section 2.3.4. To elucidate the impact of concentration (powder/water) on adhesiveness the following concentrations (C) were tested: 0.3, 1.0 and 1.5 %.

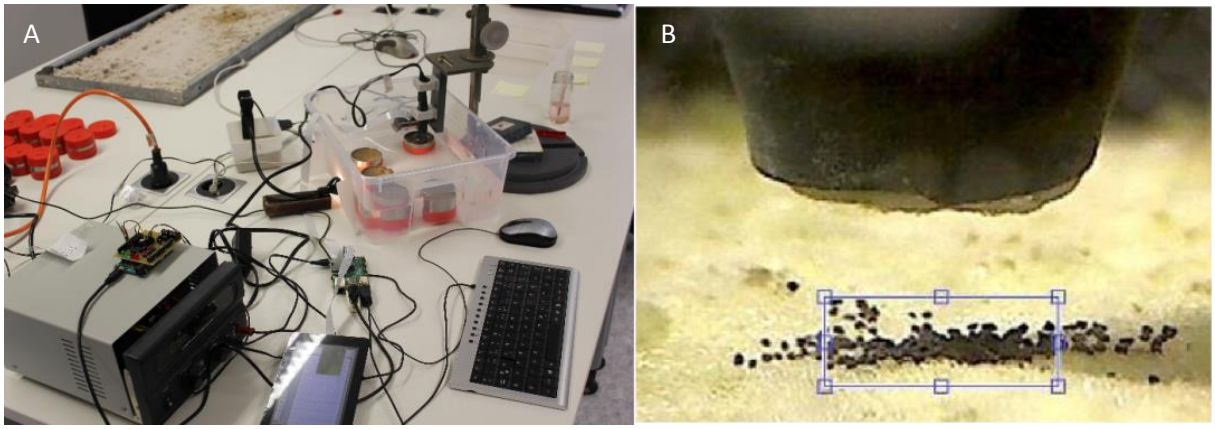

Figure 2.3.1 The MagPI-IP to measure surface adhesion forces. A) The electromagnet attached to a micromanipulator for height adjustment and screen showing the process of FP retrieval recorded by a submerged camera. B) An example image for evaluation. The rectangle shows the area with magnetic particles which is used to calculate the mean pull-off force.

Natural biofilms

In addition to the surrogate materials, natural biofilms were also tested. Sediment cores were taken from a site close to the Wadden Island of Schiermonnikoog. After sampling, the cores were kept at 4 °C in darkness for five months before the adhesion measurements were conducted. Adhesion was measured on a) samples without a visible biofilm, b) samples with visible biofilm and c) samples with initial vegetation (see Figure 2.3.2). In the latter case the initial vegetation was cut away just prior to the experiments to avoid trapping of particles and increase their visibility.

Figure 2.3.2 Sediment cores from Schiermonnikoog. Left: samples without a visible biofilm, Middle: samples with visible biofilm and Right: samples with initial vegetation.

2.3.3 Results and Discussion

Surrogates

Figure 2.3.3 (Left) shows the behaviour of the mean adhesion ($3 < n < 5$) versus the concentration (C). Except for agar and guar gum the adhesion of the surrogates increases with concentration. Both sodium alginate and xanthan gum cover a wide range of values ($1.8 < A_{s,30} < 6.0$ Nm^{-2}) which is also in the range of measured values from cultivated biofilms (see Thom et al., 2016). However, xanthan gum is more sensitive to changes in concentration than sodium alginate. Furthermore, sodium alginate does not break apart in pieces when exposed to increased bed shear stress but forms a mat-like structure in the range of reported concentrations and at a mix of 1.5 g EPS/ 6g sediment.

Even though the differences are small, the two types of xanthan gum (sourced from different suppliers) behave differently. This is particularly apparent when looking at the heterogeneity of the measurements expressed as coefficient of variation (CV = standard deviation/mean value). Adhesion of the xanthan gum purchased from buxtrade has a relatively low CV of 10-11% and the results are thus easily reproducible. In contrast, XG (FuFeng) and all other surrogates have considerably higher CV values: XG FuFeng = 20 – 43%, sodium alginate: 29 – 36%, guar gum 13 – 35%, agar agar: 16 – 29%. Figure 2.3.3 (Right) illustrates the means and standard deviations at C = 1.0 %. In fact, it was surprising that especially for the XG (FuFeng) a few particles remained on the sticky surface while the majority was already attracted at lower magnetic forces. While this behaviour was also observed for natural biofilms and mainly attributed to physical trapping (e.g. between filaments) the same cannot be true for the surrogate surfaces as the surfaces were flattened before the measurements.

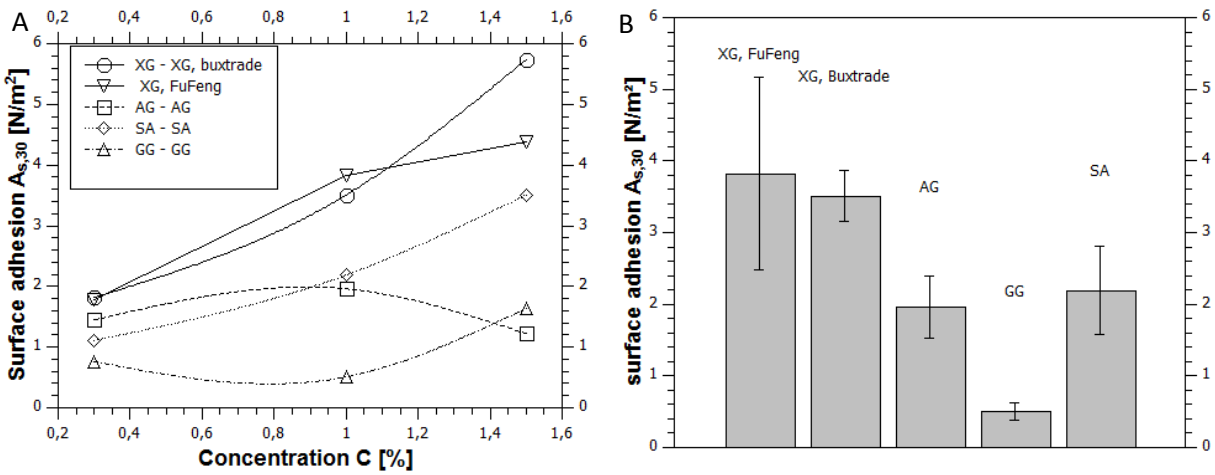

Figure 2.3.3 Measured adhesion on surrogate surfaces. A) Mean surface adhesion plotted against the concentration of dissolved EPS powder in water. B) Mean surface adhesion and standard deviation of different surrogates at C = 1%.

The results demonstrate that XG/SA have similar surface adhesion forces to natural biofilms and may therefore be suitable candidates for further research on biostabilisation. Due to the mat-forming capacity of sodium alginate it may be particularly suitable for use as surrogate for mat-forming biofilms. On the other hand, XG may be best-suited to reproducing aggregate forming biofilms. However, observations from ongoing experiments also suggest that XG may be suitable for reproducing mat-forming biofilms, particularly when using increased ratios of EPS/sediment.

Natural biofilms

From visual inspection, the storage conditions (5 months at 4°C) did not result in dramatic changes in the vegetation. As can be seen in Figure 2.3.2 both the greenish colour of the biofilm as well as the colour of vegetation were surprisingly well conserved. However, if the storage conditions influenced the biomechanical properties could not be investigated but should be addressed in the future.

Figure 2.3.4 illustrates the measured surface adhesion forces of the natural sediment samples. Mean values range from 0.2 to 2.4 N/m². Sediment cores with visible biofilms had the highest values while the adhesion on sediment cores without visible biofilms is negligible (< 1.0 N/m²). Figure 2.3.4 also shows the standard deviation from n = 4 to 7 measurements. Relating the standard deviation to the mean values the highest heterogeneities were found on the samples with non-visible biofilms (CV 37%) to be explained by one obviously adhesive outlier ($A_{s,30}$ = 1.4 Nm^{-2}). In contrast CV values for samples with visible biofilms and initial vegetation were comparably low (CV = 23% and 19%

respectively) and generally in the lower range of CV values determined for XG, FuFeng. Consequently, this variability could be used to simulate the natural heterogeneity of biofilms, but this suggestion still needs further research and more data from natural biofilms.

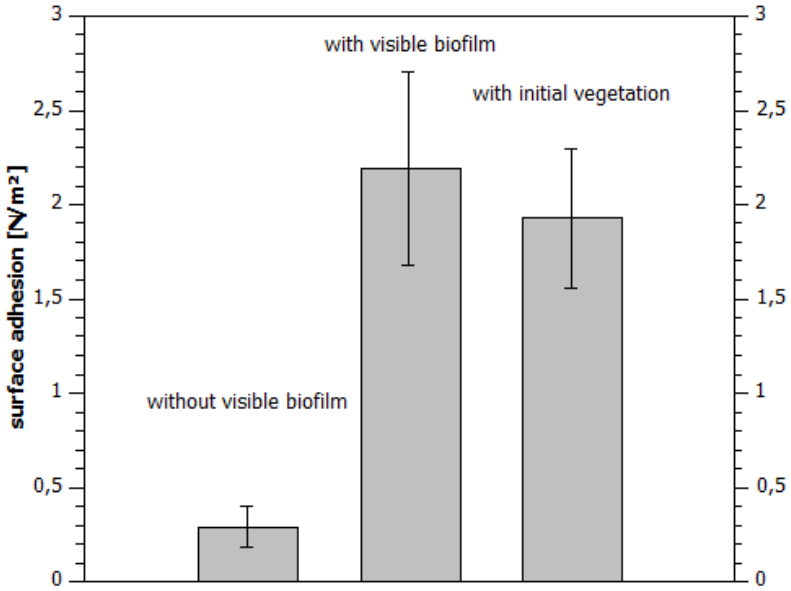

Figure 2.3.4 Mean surface adhesion measured on natural biofilm samples (+standard deviation)

2.3.4 Recommended Protocols

Based on the results reported in the previous sections the following protocols have been developed to give guidance on a) what to consider when measuring adhesion on surrogate and natural biofilm surfaces and b) how to derive design criteria for biofilm surrogates based on these measurements. Further the protocols point at remaining research needs to be addressed in future to replicate and investigate the adhesiveness of natural biofilms.

Protocol on adhesion measurements of surrogates and natural biofilms

Conducting adhesion measurements using the MagPI-IP device has proved to be a promising approach to studying the material properties of biofilms. Although the method is still in its infancy, it has the potential to enable very detailed analysis which will be necessary for developing effective surrogates and derive scaling laws. The most obvious downside is that few researchers have conducted adhesion measurements and therefore the data are still very limited.

This section describes how to conduct adhesion measurements to reduce potential errors in future studies: The surrogates come as a powder which is mixed with water at the desired concentrations. The water temperature is equivalent to the room temperature and normal tap water is used. It is important to carefully mix the powder using e.g. a stirring blender (see Figure 2.3.5). The resulting EPS is then mixed with sediment (in this study beach sand d<1.4 mm was used) to prevent the EPS from floating away (the bulk density of EPS is approximately 1000 kg/m³, i.e. similar to water). In this study 1.5g of EPS was mixed to 6g of sand.

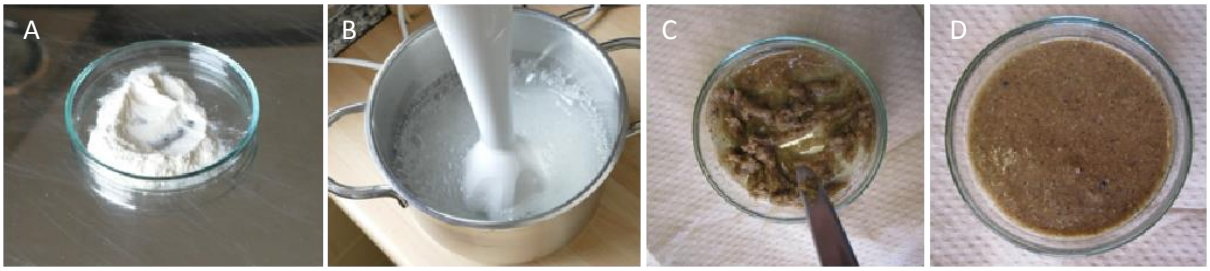

Figure 2.3.5 Mixing procedure. From left to right: A) The surrogate powder is weighted. B) The powder is mixed with water using a stirring blender (~2 mins to destroy larger aggregates). C) The resulting EPS is carefully mixed to sediment (here beach sand) until the dry sediment is completely coated with EPS. D) The surface of the EPS-sediment mix is flattened.

Even though this ratio should in theory not impact the measured adhesiveness it appears to be critical for the depth of the particles sinking into the adhesive. This behaviour is part of ongoing research and thus it is recommended to follow the given ratio of 1.5/6 EPS/sediment. Subsequently, the EPS/sediment mix is poured into a petri dish, the surface is flattened, and the petri dish is immediately submerged in water to conduct the MagPI-IP measurements (to prevent the EPS from winnowing, see Parsons et al., 2016). Ideally, measurements should be replicated on the same sample to derive the spatial heterogeneity as well as being replicated on different samples which have been mixed separately to characterise differences in preparation procedures. A reasonable number of replicates is between 3-5. After measurements are completed, the surface should be checked for magnetic particles that have not detached from the surface ('leftovers') since they may indicate that a) the adhesion is beyond the range of the force of the electromagnet and/or b) the surface adhesion is highly heterogeneous.

Taking core samples of biostabilised sediments is an approach for studying natural biofilms. Ideally the biostabilised sediment samples should fill the whole volume of the core so that they can readily be used for adhesion measurements. After collection, sample cores should be stored in moist, cold and dark conditions with measurements ideally being taken immediately after sample collection to minimize the risk of disturbance. Even samples with surface vegetation can be analysed simply by cutting the vegetated parts. As demonstrated above, adhesive biofilms may not be directly observable thus measurements should be made on different locations on the sample surface. Furthermore, it is important to have many replicates as natural biofilms are highly heterogeneous. Lastly, instead of tap water, the natural water should be used to submerge the samples.

Suggestion on deriving design criteria from adhesion measurements

The first question that should be addressed is whether the biofilm to be mimicked is mat- or aggregate forming. An initial test for this behaviour is to remove the upper layer and holding it between the fingertips. If the biofilm behaves like illustrated in Figure 2.3.6, it can be described as being a mat-forming biofilm and an appropriate surrogate (here sodium alginate or XG at high concentrations) can be selected. In this case, it is likely that cohesion plays a more important role than adhesion (see Vignaga et al., 2012). If the biofilm easily falls apart and cannot be taken up like in Figure 2.3.6, measured adhesion forces can be used as basis for the design of a surrogate.

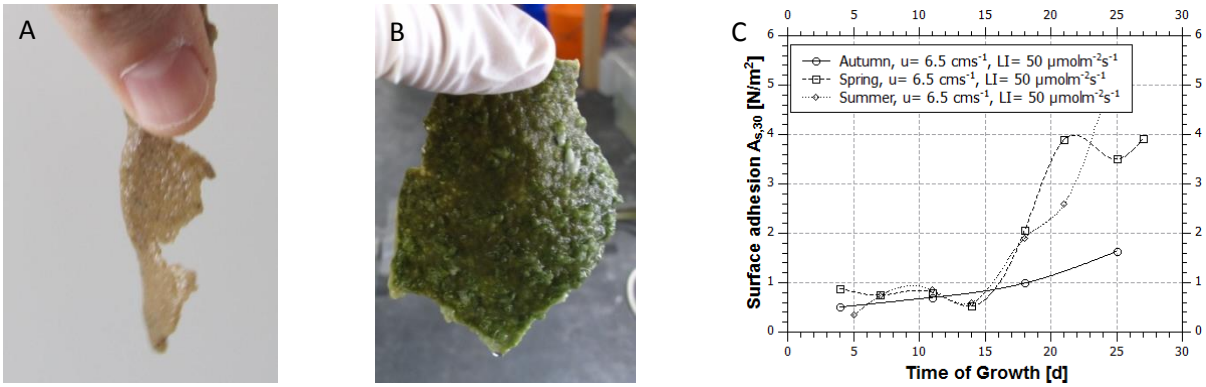

Figure 2.3.6 A): Sodium Alginate forms a mat-like structure. B) A mat-like structure from a biofilm cultivated in an ecohydraulic flume. C) Surface adhesion of developing biofilms cultivated under identical environmental conditions but with river water from different seasons. Data & images from: Thom (in prep).

The next step is to compare the measured adhesion values between the surrogate and the natural counterpart. Measurements on biofilms cultivated in ecohydraulic flumes reveal surface adhesion forces ranging between 0.0 and 7.0 N/m² where the individual values depend on the environmental conditions (light, temperature, flow velocity), the benthic community, the age of the biofilm and seasonal effects (Thom et al., 2016 and unpublished data, see also Figure 2.3.6 Right for an example). However, it should be noted that all data on adhesion that has been collected so far is only from the surface of biofilms and it is likely that adhesion forces of natural biofilms vary with depth, while surrogate adhesion might be constant. Considering the spatial heterogeneity of adhesion forces, the CV values should also be compared. For example, the XG purchased from buxtrade.com is highly homogeneous and therefore suitable for fundamental investigations, the xanthan gum from FuFeng might be more useful to mimic a natural heterogeneous biofilm.

3 PROTOCOLS FOR EXPERIMENTS WITH VEGETATION

3.1 BACKGROUND

Aquatic vegetation such as seagrasses, have been proven to provide natural coastal protection by wave attenuation, flow dampening and bed stabilisation (Gedan et al, 2010; Nepf, 2012a; Short et al, 2011). These coastal protection benefits originate from alterations to the local hydrodynamics due to the obstructive presence of vegetation which in turn influences bed sediment mobility and characteristics. Present research has initially assessed the properties of flow velocity and turbulence within and around aquatic vegetation, but further work is required to understand the influence of specific vegetation characteristics. An area of notably limited research exists in understanding the influence of differing vegetation flexibility.

Despite the notable benefits of seagrass, a global loss is predicted due to climate change factors, such as warming waters and increased storminess. Further protection and expansion of seagrass meadows could incorporate natural engineering solutions as part of coastal defence strategies. . In response, it is crucial that research into the roles of aquatic vegetation is further developed to highlight its role in providing suitable and sustainable adaptations to coastal management under a changing climate. Further investigation of seagrass hydrodynamics and sediment mobility will allow further incorporation of coastal and aquatic vegetation into coastal management strategies.

3.2 EXPERIMENTAL ASSESSMENT OF SURROGATE FLEXIBLE SEAGRASS CANOPIES ON WAVE HYDRODYNAMICS (UNIVERSITY OF HULL / UNIVERSITY OF ABERDEEN)

3.2.1 Objectives

It is essential that coastal aquatic vegetation, is suitably represented in experimental research to improve understanding of the interaction with local hydrodynamics. At present, the assessment of coastal vegetation such as seagrass has largely been represented using surrogate vegetation in the form of rigid rods, with few accurately incorporating flexibility. The assessment of seagrass blade flexibility is a notably understudied area of research within flume experiments, and the limited existing studies largely look at a single comparison between rigid and flexible surrogate leaving limited understanding of the sea-grass flow interactions at a range of flexural rigidities. There is a recognised need to quantify systematically the role of vegetation flexural rigidity on flow structures and the link to sediment mobility.

Experimental research into the role of vegetation flexibility on wave hydrodynamics was conducted in the Aberdeen University Random Wave Flume (AURWF). This research aims to improve knowledge on the role of vegetation blade flexibility for wave induced flow velocities and turbulence, both above and within the canopy. Parameterisation of vegetation properties are validated by a previous field campaign in Rødsand Lagoon, Denmark, during August 2017. Links between field and flume are beneficial to facilitate comparable data acquisition under controlled conditions, which are otherwise difficult to obtain in the field. The quantification of flow and turbulence structures aims to provide an insight into in-canopy sediment behaviours for a range of wave conditions. Acquisition of near bed velocity measurements provide data that supports the assessment of potential sediment entrainment within seagrass canopies.

3.2.2 Background

Aquatic vegetation is classified as either emergent or submerged, depending on vegetation species and local conditions; this research focuses only on submerged seagrass vegetation. An expanse of seagrass along a coastline is referred to as a canopy or meadow. Seagrass encompasses a large group of aquatic vegetation with over sixty known species, resulting in global variation in geometric and biomechanical properties due to both the species, and the local environmental factors (de los Santos et al, 2016). In Europe, the most abundant species is *Zostera marina* (eelgrass) with additional co-existence of *Zostera noltti* (dwarf eelgrass), with two additional predominant species found in the Mediterranean: *Cymodocea nodosa* and *Posidonia oceanica* (Borum and Greve, 2004). Plant properties within the *Zostera*- communities have similar structural architecture, comprising of a short rigid sheath at the shoot base, and 2 to 5 flexible blades extending; as depicted in Figure 3.2.1 (Marbà et al, 2004).

Figure 3.2.1: (a) Simplified graphical representation of a typical seagrass plant structure. (b) Photograph of Zostera Marini collected in Rødsand Lagoon, Demark, in August 2017. The central plant shows the presence of rhizome at the base, along with older decaying brown leaves at the base.

The properties of a patch of seagrass can vary considerably, with factors not limited to but including: submergence ratio, stem density/geometry, and biomechanics. These variations result in differing flow and turbulence conditions, with wave forcing and flexibility particularly understudied. The assessment and quantification of flow mechanics within seagrass vegetation has previously been conducted using flume experimentation, field measurements, and numerical modelling; including assessments of living and surrogate vegetation.

Measurements within the field are more limited than physical and numerical model research due to limitations with conducting in-situ measurements. Flume experiments provide a solution to collect data that is not viable in the field, while also allowing isolation and assessment of the importance of differing vegetation properties and forcing conditions present in nature.

Natural Living Plants

A number of studies have conducted experiments using living seagrass, however this type of research is limited due to issues associated with organism survival in these artificial environments (Johnson et al., 2014). Despite these difficulties, research has been conducted using living plants,

providing an understanding of patch hydrodynamics that are representative of natural biomechanics, thus providing comparison between flume and field. However, a limitation of using living vegetation in flume research is the inability to vary individual plant properties in order to improve understanding of individual factors and controls.

Table 3.2.1 provides a summary of published data on *Zostera* marina properties of individual blades and sheaths, canopy scale characterises and local environmental settings. This data summary provides vital parametrisation for experimental research set-up highlighting the natural variation within just one species of seagrass. An extensive dataset published by de los Santos et al (2016) provides comparisons between 23 different species of seagrass.

Surrogate Vegetation

As an alternative to the use of natural vegetation, the majority of recent flume studies have opted to use artificial materials to mimic natural vegetation, referred to as: surrogate-, prototype-, or mimic-vegetation. The use of surrogate vegetation enables greater investigation and control over natural variables. Previously, seagrass has been modelled using rigid rods, or flexible polymer ribbons. A substantial proportion of published research comprises of the assessment of hydrodynamic flow alteration due to the presence of these surrogates under unidirectional flow, with less research studying wave dominated flows.

Rigid rods provide a simplistic understanding of hydrodynamics, but do not incorporate the complex movement present with flexible blades. Subsequently, there is a need to assess the effect of flexible surrogates on hydrodynamics. The use of flexible surrogate vegetation requires consideration of best-practice to suitably represent natural biomechanics, while allowing isolated assessment of natural variables. Guidance on the use of surrogates can be gained from the experience of previous research such as Ghisalberti and Nepf (2002) and guides such as Frostick et al (2014). As a result of this, there are a limited number of studies that have attempted to directly replicate the natural vegetation properties within a surrogate, including some but not all of the following properties: mass density and Young's moduli. While some studies have attempted to replicate natural biomechanics, it is almost impossible to find a commercially available material that fulfils the specific mechanical properties present in nature. Further research and material development would be required to produce exact replica vegetation surrogates. As an alternative, surrogates may be chosen to maintain fundamental parameters as best as possible, including: Young's modulus, mass density and main geometrical characteristics.

Blade flexibility can be considered in a more holistic sense to assess patterns of hydrodynamic difference between rigid and flexible scenarios. Many studies highlight the significant difference associated with the use of a flexible blade in comparison to a rigid surrogate, thus promoting the importance of including flexible blades.

Table 3.2.1. Summary of published data on Zostera marina geometry and patch characteristics for various species and spatial and temporal samples

Literature Source	Sample Date (mm-yyyy)	Sample Location		Submergence Ratio (h/H)	Water Depth (cm) [H]	Canopy Height (cm) [h]	Number of Samples	Blade Length (cm)	Sheath Length (cm)	Blade Width (cm)	Shoots per m^2	Blades per m^2	Blades Per Shoot
de los Santos (2016)	Jun-10	Cádiz, Spain		*NR*	<100	*NR*	28	27.3 ± 6.8	*NR*	4.58 ± 0.71	NR	NR	NR
Abdelrhman (2007)	NR	Beaufort, USA	1	NR	NR	NR	NR	69 ± 6.4	*Refer to source publication page 88 and 89 for regression analysis data.*			1190	NR
	NR		2	NR	NR	NR	NR	36 ± 10.4				574	NR
	NR		3	NR	NR	NR	NR	54 ± 8.1				515	NR
	NR		4	NR	NR	NR	NR	28 ± 6				1293	NR
Gambi et al (1990)	August 1986[1]	San Juan Island, USA		Na	Na	Na	20	7.9 ± 3.5	3.68 ± 0.47	0.28 ± 0.04	Na	NR	3.9 ± 0.76
Gambi et al (1988)	*Sep-86*	San Juan Island, USA		0.6425[†] to 0.37[†]	40 to 70	25.7 ± 8.3	20	19.0 ± 10.1	7.1 ± 1.7	0.5± 0.1	508 ± 117	NR	3.9 ± 1.2
	Sep-86			<0.958[†]	>100	141.7 ± 22.6	20	95.8 ± 41.5	40.8 ± 3.8	0.84 ± 0.09	140 ± 34	NR	3.6 ± 0.5
	*12-1986**			1.37[†] to 0.78[†]	40 to 70	Na	10	Fertile Shoot Height: 54.8 ± 6.2			0.8 ± 1.3	Na	Na
	01-1987*			1.2[†] to 0.68[†]	40 to 70	Na	10	Fertile Shoot Height : 48.3 ± 11.5			NR	Na	Na
	02-1987*			1.06[†] to 0.60[†]	40 to 70	Na	10	Fertile Shoot Height : 42.2 ± 12.1			NR	Na	Na
Fonseca and Bell (1998)	Spring-1991	North Carolina, USA		NR	-	*Above Ground Biomass: $\bar{x}$ = 77g (max= 247g)*					$\bar{x}$ = 329 (max = 810)	NR	NR
	Autumn-1991			NR	-	*Above Ground Biomass: $\bar{x}$ = 21g (max= 85g)*					$\bar{x}$ = 185 (max = 442)	NR	NR
	Spring 1992			NR	-	*Above Ground Biomass: $\bar{x}$ = 131g (max= 611g)*					$\bar{x}$ = 423 (max = 1133)	NR	NR
	Autumn-1992			NR	-	*Above Ground Biomass: $\bar{x}$ = 15g (max= 67g)*					$\bar{x}$ = 175 (max = 512)	NR	NR
Hansen and Reidenbach (2013)	*Jun-10*	South Bay, Virginia, USA		NR	See pub.	25 ± 5	*Var*	21 ± 8	NR	0.3 ± 0.1	560 ± 70	4.8± 1.3	4.8 ± 1.3
	Oct-10			NR	See pub.	23 ± 5	*Var*	19 ± 7	NR	0.2 ± 0.1	350 ± 50	3.0 ± 0.9	3.0 ± 0.9
	Jan-11			NR	See pub.	16 ± 5	*Var*	13 ± 7	NR	0.2 ± 0.1	310 ± 60	2.6 ± 1.0	2.6 ± 1.0
	Mar-11			NR	See pub.	15 ± 3	*Var*	12 ± 5	NR	0.2 ± 0.1	350 ± 90	4.0 ± 1.4	4.0 ± 1.4
	Jun-11			NR	See pub.	29 ± 8	*Var*	23 ± 11	NR	0.2 ± 0.1	440 ± 140	4.2 ± 1.2	4.2 ± 1.2
Hansen and Reidenbach (2012)	June – July 2010	South Bay, Virginia, USA	1	0.15[†] to 0.12[†]	140 to 180	NR	158	21 ± 8	NR	0.29 ± 0.08	560 ± 70	NR	NR
			2	0.20[†] to 0.16[†]		NR	176	28 ± 13	NR	0.41 ± 0.12	390 ± 80	NR	NR
			3	0.24[†] to 0.19[†]		NR	73	16 ± 9	NR	0.26 ± 0.07	150 ± 80	NR	NR

Abbreviations: *Var = variable;* $\bar{x}$ = mean; NR = not reported; See pub. = see source publication for full details. Numbers are mean value ± Sd.

[1] Data for living juvenile plants selected for flume experiment, therefore not fully representative of field values.

[†] Value calculated from data to provide indication. * Fertile Shoots only

Natural Biomechanical Properties

The flexible rigidity of vegetation can be considered as being governed by three main factors: drag, buoyancy, and modulus of elasticity (Ghisalberti and Nepf, 2002). Nepf and Vivoni (2000) categorised aquatic vegetation into four regimes that express ranging motion characteristics in unidirectional flow: (1) Rigid (erect with no movement), (2) gently swaying, (3) strong coherent swaying featuring monami and (4) prone. Furthermore, Nikora (2010) distinguishes aquatic plants as: (1) *tensile plants,* which are highly flexible and are controlled by tensile forces; and (2) *bending plants*, that at more ridged and controlled by bending forces. These forces and material properties are used to ensure biomechanical similarity when selecting a vegetation surrogate for flume experimentation. Some previous studies have also assessed flexible rigidity in terms of blade bending angle (Abdelrhman, 2007), or alteration in submergence ratio at differing flow velocities (Fonseca et al., 2007).

This research will utilise field data to quantify surrogate vegetation properties; justification via field records is sometimes neglected within flume experiments. Ghisalberti and Nepf (2002) have detailed an approach to ensure mathematical dynamic similarity of surrogate seagrass to a 'prototypical' *Zostera marina* meadow. This approach ensures the scaled surrogate seagrass has a modulus of elasticity (E) in the region of E = 300 $MN.m^{-2}$, which Ghisalberti (2000) states is comparable to nature, and based upon review of four sets of published field data with particular emphasis given to values recorded in Massachusetts Bay by Chandler *et al* (1996). Supporting data from Lei and Nepf (2016) reports field data to show E = 260$MN.m^{-2}$. The plant geometric properties chosen by Ghisalberti (2000) are in general agreement with the values independently chosen for use in this research. The present research study uses the available field data on plant mechanics to provide guidance on relating dynamics of the chosen surrogates to that of natural seagrass using the formulae of Ghisalberti and Nepf (2002) to assess: (i) λ_1 - the ratio of buoyancy force to rigidity force, and (ii) λ_2 – the ratio of drag force to rigidity force. It should be noted that seagrass biomechanical properties are variable by species, along with influence due to the local environmental setting and notable flow velocity for λ_2. While no significant difference in blade modulus of elasticity between seasons has been recorded, it has been found that variability in nutrient availability will significantly alter blade elasticity and strength (La Nafie *et al*., 2012).

Published records of direct measurements of modulus of elasticity remain sparse for *Zostera Marina,* and most seagrass species. Table 3.2.2 provides an insight into published values of flexibility, however the quantification of flexibility is inconsistent with the use of elastic young's modulus (E), bending's young's modulus (EI), or more generic statements. The units also vary, and are sometimes absent, therefore, it is vital to take care and consider the fragmentation in published results when developing experimental plans that incorporate assessment of biomechanical properties, especially with respect to scaling.

While this review has primarily focused on *Zostera marina*, de los Santos *et al* (2016) assessed the mechanical properties of one third of the known seagrass species globally, and reported a 23-fold variation in blade stiffness across species. This demonstrates the natural variation in flexible rigidity within nature; the influence of this on localised hydrodynamics will be investigated in this research. All records report seagrass as being positively buoyant, however, discontinuity in calculation and inconstancy in approach of stating rigidity, along with variable use of units within published work

creates difficulty in drawing comparisons. It has been recorded that the sheath of *Zostera Marina* is approximately twice as stiff as the blade (Fonseca et al., 2007).

Natural variation in biomechanical stiffness can also occur because of blade health, whereby healthy living tissue is more flexible than dead tissue (Niklas, 1999). Niklas (1999) further notes that plants naturally adapt to the loading imposed on them.

Table 3.2.2 - Summary of published values of seagrass flexibility

Literature Source	***Species***	***Flexibility***
de los Santos 's (2016)	*Z. marina*	*"Stiffness" = 1.2E+08 Pa*
Folkard (2005)	*P. oceanica*	*Young's Modulus (E) = 4.7E+08Pa*
Fonseca et al (2007)	*Z. marina*	*Bending Young's Modulus (EI) = 7.998E-08 s.d.= 2.462E-07 [no units].*

Further quantification of seagrass flexibility can be obtained through combining data, sometimes from multiple sources, to calculate blade flexibility. Lei and Nepf (2016) appear to have calculated an estimated value of E by dividing out the inertia (I) element of the EI. A known leaf length is 0.15m, following linear regression from Abdelrhman (2007) suggests a thickness of 1E+04m, subsequently resulting in an estimation of E = 2.7E+08 (Pa m4).

Application to Flume Research

As previously mentioned, the flexible rigidity of surrogate vegetation used in flume experiments is often considered in a generalised context, rather than being informed by direct field measurements (Folkard, 2011). This is potentially due to a limited number of published values of seagrass flexural rigidity along with natural variation in flexible rigidity due to species and local environmental factors (Lei and Nepf, 2016). As a result, a flume study by Paul et al (2016) did not inform mechanics of surrogate vegetation from field data, but instead used blades of various flexible rigidities to assess the differences in the associated drag force. However, there is a benefit to this approach by providing results that are not restricted to one species of vegetation occurring in one location, thus providing wider application of results.

The importance of incorporating vegetation flexibility is highlighted following reports by Koch and Gust (1999) that show that the movement of flexible vegetation allows greater wave penetration into the canopy. Assessment of flexibly is also vital in determining wave attenuation, following findings by El Allaoui (2016) that flexible surrogates had a lower capacity to attenuate waves in comparison to rigid surrogates. Under unidirectional turbulent flow the dynamic movement of flexible blades, and results in phenomena such as monami: a waving motion of blades at the canopy top, which occurs when instantaneous drag at the canopy top overcomes the buoyancy and rigidity forces of the canopy blades under unidirectional flow. This results in the formation of a depression in the canopy surface that travels progressively with vortex movement (Nepf, 2012a). Furthermore, the dynamic movement of flexible blades alters the drag and resistance within a water column, which in turn sets the velocity and internal turbulence structures (Ghisalberti and Nepf, 2005). The assessment of flexible canopy behaviour under oscillatory flow remains far more limited, and requires detailed measurements to determine the role of vegetation flexibility.

Influence of Blade Flexibility on Hydrodynamics

In order to assess the influence of blade biomechanics on hydrodynamics, blade behaviour can be represented through several dimensionless numbers (Luhar and Nepf, 2011; 2016):

- Cauchy Number (Ca) - a ratio between hydrodynamic forcing and blade stiffness restoring forces.
- Buoyancy Parameter (B) – the ratio in which blade reconfiguration due to buoyancy or stiffness.
- Keulegan-Carpenter number (KC) – quantification of the ratio between internal and drag forces, and the wave orbital excursion relative to blade length.

Existing research has predominantly drawn comparison between rigid blades relative to flexible blades. This has highlighted notable differences in hydrodynamics, but the quantified role of blade flexibility on changes in hydrodynamics, or identifying thresholds of change, remain currently undetermined.

The dynamic movement of flexible vegetation is known to alter flow structures in comparison to a rigid patch. Flexible vegetation streamlines with flow due to the process of blade reconfiguration or bending under load, thus acting as a predominant process involved in alteration to local hydrodynamics (Nepf, 2012a). Ghisalberti and Nepf (2006) recorded that in comparison with rigid vegetation, flexible blades resulted in a 40% reduction in turbulent momentum transport in the shear layer. Nepf (2007) confirmed that the value of canopy drag is fundamental to vortices penetration, and later reported that the presence of monami causes turbulence to penetrate further into the canopy, thus increasing in-canopy velocities (Ghisalberti and Nepf, 2009). However, the momentum transfer is reduced under the presence of monami due to vortices being weaker and smaller (Ghisalberti and Nepf, 2006). Alternatively, it may be possible that the highly flexible blade bending either due to low flexural rigidity, or under high velocity forcing, will result in a dense canopy top layer that prevents the vertical exchange of momentum associated with vortex penetration as suggested by Nepf and Vivoni, (2000). The work of Ghisalberti and Nepf (2006), has begun to assess this, but has not investigated varying blade flexibilities or conditions. The development of coherent flow structures associated with submerged aquatic vegetation requires additional research to further understand their dynamic and kinematic properties over time, and due to the monami effect in regards to flexural rigidity.

Luhar and Nepf (2011) considered the reconfiguration of two flexible blades due to dominance of buoyancy and stiffness restoring forces, concluding that when reconfiguration is stiffness dominated, drag is directly proportional to $U^{4/3}$ (U = horizontal velocity). This research was conducted for an isolated singular blade, and additional research is required to assess if this relationship holds for vegetation within an established patch. Assessments of differences in drag forces have shown form drag is lowered in comparison to rigid surrogates because of flexibility, resulting in viscous drag (Nikora, 2010). The velocity and turbulence within a canopy is subsequently influenced by drag forces, which in turn effects the resuspension of sediment (Ghisalberti and Nepf, 2005; Luhar et al, 2008).

Paul et al (2016) found that blades of differing stiffness played a more important role than biomass on drag forces under varying velocities as a result of blade reconfiguration. It was also highlighted that stem to stem interaction within a patch can increase drag forces. Supporting experiments by Albayrak et al (2012) identified the importance of reconfiguration, and noted that blades with

greater flexibility experienced lower drag forces that increased quasi-linearly with velocity. However, blades of greater rigidity experienced higher drag forces that increased as a function of velocity squared: although this research was devoid of waves. Experiments that have collected direct measurements on blade drag have often assessed a singular, or very small patch of stems, for a singular flexibility of blade.

An assessment of blade flexibility by Houser et al (2015) considered the influence of flexibility on the drag coefficient of the canopy (C_D) for three blade rigidities: Rigid, Semi-Flexible, and Flexible. This research showed that C_D reduced with increasing flexibility. The calculated C_D is not a direct measurement on a physical blade, but estimated from wave dissipation, while this provides an overall indication of canopy drag, it does not provide a detailed assessment of hydrodynamics. The use of different materials for semi-flexible and flexible blades introduced a difference in buoyancy of over one order of magnitude, which is expected to notably influence the restoring forces of the blades and thus the drag (Luhar and Nepf, 2011). Furthermore, the flexible blade buoyancy is around five times greater than the approximate value of natural seagrass.

Majoribanks et al (2016) has highlighted through numerical modelling that while current hydrodynamic understanding is valid for semi-rigid blades, there are additional turbulence parameters occurring due to blade flapping in highly flexible blades, which is largely un-quantified in physical settings. Further research is required to quantify the boundaries of blade rigidity on turbulence penetration into canopy, for conditions that include wave parameters comparable to nature. There is a requirement for experimental research to constrain the extent of blade flexural rigidity on turbulence dissipation, this would be improved further if drag measurements were acquired to separate and quantify the forces role, in energy dissipation.

Limited research has been conducted on the flow associated with blade flexibility, especially within the canopy. Dijkstra and Uittenbogaard (2010) have developed a numerical model to assess the influence of highly flexible blades on flow structure, demonstrating that greater flexibility results in higher in-canopy velocities and increased bed shear stress, but did not elaborate much further on the hydrodynamic changes. Their model was validated by direct force transducer measurements on plastic strips with three flexibilities. It should be noted that differing materials and thus buoyancy were used, while only the very flexible plastic was buoyant in water, a property synonymous of nature. Bed roughness was calculated from velocities profiles, and the model would therefore benefit from direct measurements of bed shear stress. It is noted within the paper that the model would be improved with the addition of greater flexibilities and flow velocities, improving the applicability to nature and assessment of seagrass resilience.

An extensive experimental study by Paul et al (2016) assessed the influence of blade flexibility and drag, while also varying biomass, and drawing comparison against change in frontal area (ah) due to blade reconfiguration. This study recorded direct drag measurements, but it should be noted that the surrogate vegetation tested was not a continuous meadow, but five individual elements (1cm wide) with 2 to 8 blades attached, essentially replicating an isolated stem in a vast (7m wide) open body of water; a set up that is incomparable to nature. Paul et al (2016) concluded that drag force increases with orbital velocity, without statistical analysis, the results appear to show a linear trend, however differences between flexibility is not clear.

Luhar and Nepf (2016) have also assessed the dynamics of an isolated blade and noted that numerically modelled blade behaviour does not always conform to reality. A phase transition between force dominated and stiffness dominated conditions within a wave cycle was observed, resulting in unsteady blade behaviour. During this transition, the blade rapidly moves in an upstream direction described as a 'springing back' motion, accompanied by vortex shedding from the blade, resulting in increased drag for this short time period. The recording of this occurrence highlights the need to further study the role of blade flexibility, as the springing back motion will change with blade stiffness and also wave parameters.

There has been limited assessment of within canopy hydrodynamic behaviour, especially under wave forcing for flexible vegetation. This has predominantly been due to the complexities and measurement technique limitations associated with conducting in-canopy data collection; therefore this research will use a combination of strategic methodical approaches in experimental design coupled with Laser Doppler Anemometry (LDA) measurement techniques in scenarios where blade flexibility obstructs data collection. A significantly limited area of research exists regarding the complexity associated with flexible blades, with a notable knowledge gap surrounding the understanding of surrogate blades of differing flexibility on local hydrodynamics: specifically, vortex penetration depth and bed shear stress, and dynamics of turbulence structurers.

3.2.3 Experiments

Experimental research into the influence of vegetation flexibility on hydrodynamics will be conducted at the Aberdeen University Random Wave Flume (AURWF). The flume has a length 20m, width 0.45m, and depth 0.90m (standing water depth of 0.70m). A patch of artificial surrogate vegetation spanning the entire channel width along a 7.50m section, will provide an area, in the patch centre uninfluenced by boundary effects. The patch will be located 5.50m from the wave paddle, allowing a sufficient distance for wave conditions to stabilise. This experimental work aims to evaluate sediment mobility potential inferred from turbulence and TKE, but will not include a mobile sediment bed.

Flexible Surrogate Vegetation Properties

The variable properties within this research comprise of the surrogate vegetation (stem flexibility and density), and flow conditions (wave parameters). While a common European species of seagrass (*Zostera marina*) was used to inform this experimental work, it is important to note that exact vegetation geometric characteristic and stem biomechanics are variable across the world depending on species and local conditions. Detailed technical information of seagrass biomechanics remain limited, and it is therefore difficult to replicate or accurately generalise this vegetation. This research tests a range of blade flexibilities, thus providing results that can be applied to a range or seagrass species and environments.

The required vegetation properties within this study were obtained through bespoke production of a surrogate vegetation patch, allowing full control of: (i) Blade Mechanics: flexibility and buoyancy, and (ii) Patch Geometry: blade length, width and thickness; stem density and geometry. Field data of *Zostera marina* was used to provide guidance to contextualise the chosen materials, and maintain properties such as buoyancy. As a result, this research modelled vegetation using surrogates with reasonable mechanical properties scaled using the dynamic similarity formulae developed by Ghisalberti and Nepf (2002). This research follows previous experimental work on flexible vegetation

whereby strips of LDPE or HDPE polymers were attached directly to the flume floor, or to a ridged sheath (Luhar and Nepf, 2016; Pujol and Nepf, 2012).

The flexible blades in this research were produced from readily available polypropylene (PP) polymer sheets, cut into 4mm wide strips (herein referred to as *blades*). PP is buoyant in water (0.91 $g.cm^{-3}$) and has a modulus of elasticity of 850MPa. In order to assess the effect of flexibility on hydrodynamics, four blade thicknesses (0.12mm, 0.2mm, 0.5mm, and 1.0mm) resulted in four test canopies. The approach of varying blade flexibility through the use of materials with differing thickness has been conducted by several previous flume experiments (Albayrak *et al*, 2012; Paul *et al*, 2016). In the case of Paul *et al* (2016) assessment was made to evaluate the subsequent impact of biomass change due to blade thickness increases, but the conclusion was drawn that stiffness rather than biomass was the driving force in flow-velocity relationship.

Dijkstra and Uittenbogaard (2010) also used the approach of varying thickness, while Houser *et al* (2015) used entirely different materials to vary flexibility. This research opted to use the same material but vary thickness, thus maintaining mechanical similarity as best as possible with the exclusion of stiffness. Notable consideration to maintain buoyancy will be made to ensure that the occurrence of restoration force changes due to stiffness and not buoyancy.

Two patch densities were tested within this research, providing a comparison between dense and sparse patch scenarios. The geometry will remain the same and symmetrical for both patch densities, thus ensuring comparability. One submergence ratio (vegetation height (h) / water depth (H) =0.34) was tested, providing a representative comparison to field conditions.

Wave Climates

Natural seagrass canopies are subjected to variable wave climates that are often wind-driven, and controlled by localised conditions such as water depth and seasonal meteorology (Fonseca et al., 1982; Koch and Gust, 1999). This flume research investigated three regular wave scenarios to investigate a range of conditions and vegetation behaviour, along with the associated wave hydrodynamics: T=1.6s H=0.18m, T=1.6s H=0.09m, T=1.1s H=0.19m.

Previous research assessing vegetation under wave hydrodynamics has assessed a range of wave frequencies and magnitudes. Table 3.2.3 indicates a range of example studies and the wave conditions investigated.

Table 3.2.3 - Example wave conditions assessed in previous experimental flume research 'NR' indicated data Not Reported

Reference	***Water Depth (m)***	***Frequency (Hz)***	***Period (s) [or length]***	***Wave Hmax (m)***
Fonseca et al (2007)	*0.25*	*0.50*	*2.0*	*0.045*
		0.38	*2.6*	*0.100*
Fonseca and Cahalan (1992)	*0.06 to 0.30*	*2.50*	*0.4*	*NR*
		1.43	*0.7*	*NR*
Luhar and Nepf (2016)		*0.5*	*2.0*	*0.02*
		0.5	*2.0*	*0.04*
		0.5	*2.0*	*0.06*
		0.5	*2.0*	*0.08*
		0.7	*1.4*	*0.04*
		0.7	*1.4*	*0.08*
		0.9	*1.1*	*0.04*
		0.9	*1.1*	*0.08*

Instrumentation

Measurement techniques will provide information on flow structures, including turbulence and Turbulent Kinetic Energy (TKE) with assessment of vertical spatial variation within the patch.

LDA (Laser Doppler Anemometry)

LDA measurements permit measurement of internal hydrodynamics within the canopy at a high temporal resolution, without physical intrusion into the water column or requirement to remove vegetation. Published LDA measurements within aquatic vegetation are limited, and most focus on assessment of rigid vegetation surrogates (Nepf *et* al, 1997; Lowe *et al* 2005; Okamoto and Nezu, 2010). Ghisalberti and Nepf (2002) have previously conducted LDA measurements at near surface parameterisation for flexible vegetation. There is a very limited record of LDA measurements within a flexible vegetation canopy due to the difficulty in preventing obstruction of the laser beams. Ghisalberti and Nepf (2002) demonstrated, the use of a rigid sheath at the base of each stem, as found in nature, to produce a clear line of sight near the bed; a technique incorporated into this research. Additional datasets of this sort will be highly beneficial to improve understanding of near bed turbulence properties and associated sediment entrainment thresholds.

The majority of current research has avoided the difficulties associated with LDA measurement through the use of ADV instrumentation (Li *et al*, 2013; Chen *et al* 2013; Ghisalberti and Nepf, 2006; Tinoco and Coco, 2016). However, ADV measurement requires a void in the canopy for the physical instrument to take measurements. Ikeda and Kanazawa (1996) have shown that the removal of a small canopy section does not have a significant impact on the flow structures. While it is believed ADV does not affect the results, the use of LDA would ensure there is no alteration to the canopy or physical intrusion of measuring device within the flow.

Twin-Wire Wave Gauges

The result of wave attenuation due to the presence of submerged vegetation has been widely documented for both rigid and flexible vegetation surrogates. This research will collect supporting wave gauge data to allow for data analysis. Furthermore this will provide datasets for an additional aspect of this research: the influence of variability in blade flexibility on wave attenuation. Several wave gauges will be placed throughout the canopy, with a control gauge prior to the canopy edge.

Video Analysis

The use of video cameras located outside the flume will allow for visual assessment of blade dynamic behaviour throughout the wave period. Image analysis will allow assessment of variability of submergence ratio due to blade deflection resulting from the various wave scenario properties.

3.3 EXPERIMENTAL INVESTIGATIONS OF KELP HYDRODYNAMICS (NTNU)

3.3.1 Objectives

Vegetation is present in most aquatic environments, affecting many physical, chemical, and biological processes across a wide range of spatial and temporal scales (e.g. Nikora et al., 2012). Benthic assemblages of marine macroalgae and seagrasses are good examples, as they can be a net source of dissolved organic carbon vital for the microbial food web in the nearshore water column (Barrón et al., 2004; Wada and Hama, 2013). Kelp forests are also known to be among the most productive marine macrophyte communities (Reed et al., 2015; Smale et al., 2013), and thanks to their nutritional and ecological properties, macroalgae are cultivated world-wide to produce food, biofuel, cosmetics, or other agricultural products (see e.g. Stévant et al. 2017). Marine macrophytes are also increasingly used as a water quality regulator in Integrated Multi-Trophic Aquaculture systems (see e.g. Stévant et al. 2017). Simultaneously, vegetated canopies generate and regulate turbulent processes, playing a major role in the natural environment (e.g. wave dampening, Løvås and Tørum (2001); Möller et al. (2014); Carus et al. (2016)). As a consequence, aquatic vegetation, macroalgae and seaweeds in particular, is increasingly considered in engineering applications and bio-inspired coastal management strategies to face the future changes of hydrodynamic regimes triggered by global changes (Temmerman et al., 2013).

Figure 3.3.1– Left: Fish community living around a forest of L. digitata/hyperborea outside Finnøy in Møre, Norway (photo: Kjell Magnus Norderhaug). Right: SES' pilot seaweed farm with L. saccharina outside Frøya, Norway (© Seaweed Energy Solutions AS).

However, several challenges remain to be tackled when it comes to understanding the large-scale interactions between macrophyte forests or seaweed farms with their physical environment. One of the reasons for this is the need for a deeper understanding of the fluid forces acting on vegetation elements to derive meaningful representations of vegetation in hydrodynamic models (e.g. Henry 2016, Vettori 2016, Whittaker et al. 2015). In continuation of some investigations initiated by Henry

et al. (2016), two projects conducted by Norvik (2017) and Sjødal Olsen (2017) were designed to investigate the dependency of drag forces on different levels of complexity of macrophyte morphology. For doing so, these projects relied on the development and the refinement of new surrogate production protocols for the characterization of seaweed hydrodynamics in hydraulic and hydrodynamic laboratories, as such environments usually do not allow for the introduction of biological material.

Figure 3.3.2 – Surrogates of L. saccharina as developed by Norvik (2017). Both surrogates are cut with the same shape out of a thin PVC sheet, and undulation on the side of the blades are realized with a heat treatment process. Taken from Norvik (2017).

These two projects addressed the same issue, i.e. the plant flow mechanical interactions, but from two different angles as Sjødal Olsen (2017) focused on the representation of a benthic organism (i.e. attached to the seafloor – *Laminaria digitata*), while Norvik (2017) investigated a seaweed farm configuration (i.e. seaweeds attached to a structure – *Laminaria saccharina*).

3.3.2 Experiments

Following the work of Vettori (2016) on L. saccharina, Norvik (2017) investigated the effect of increased macrophyte complexity on its hydrodynamics when attached to a submerged structure (seaweed farm). After some initial work on the basic mechanical and morphological properties of L. saccharina (in collaboration with the MACROSEA project at SINTEF Ocean), Norvik (2017) characterized the drag forces and behaviour of two simplified blade morphologies, flat and undulated, both with uniform thickness. Although seaweeds are typically subject to the action of both current and waves, these investigations focused only on steady unidirectional flows. The experiments were conducted in the towing tank of the Marine Cybernetics laboratory, at the Department of Marine Technology - NTNU. Two setups were used; one with a single vertical profiled rod piercing the surface, allowing to measure forces on surrogates attached on a single point, and one with a horizontal cylinder that allowed for the test of a rope-like situation. This cylinder was perforated on its wake-side to be able to perform flow visualizations by dye-injections (for more details, see Norvik, 2017). The kelp surrogates were attached to the single-point or the bar set-up and towed at various constant speeds in the basin. Drag forces on the towed structure were recorded by a single point load-cell (PW2C manufactured by HBM). Flow visualisations and the characterization of surrogate reconfiguration were based on underwater video footage made with a Go Pro camera, and these results were compared with the drag force measurements. The kelp

surrogates were cut out of a PVC sheet material, and two model sizes were tested for each simplified morphology. Two surrogate sizes were tested, and for each size, half of the models were heat treated to produce undulations on the side of the blades.

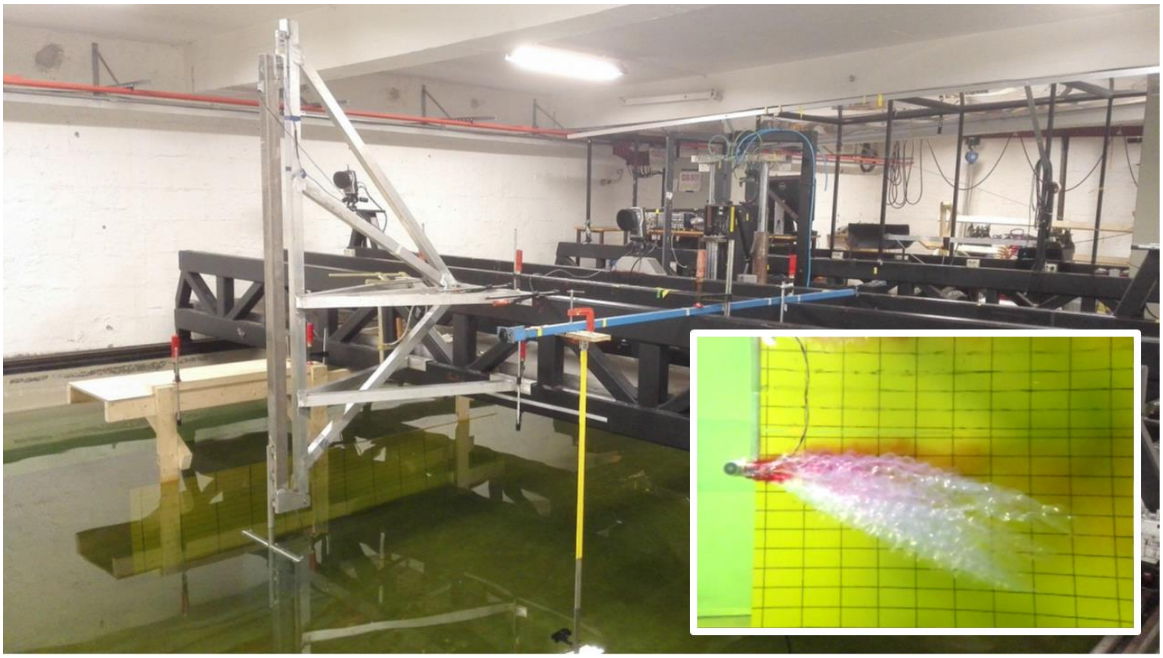

Figure 3.3.3 – Illustration of the experimental setup developed and used by Norvik (2017). The surrogates are attached to the submerged horizontal bar and towed in the basin. Dye is injected through the horizontal cylinder. Taken from Norvik (2017).

In parallel, Sjødal Olsen (2017) followed the work initiated by Henry (2016) on *L. digitata* and investigated the potential effects of varying biomechanical properties of a macrophyte on its interactions with a steady current. Surrogates with different materials and simplified shapes were used to simulate some idealized variations of the kelp biomechanical properties described by Henry (2018). The surrogate behaviour was monitored using video recordings, and drag forces were measured at the foot of the surrogate placed at the bottom of a flume (similar set-up as used by Henry et al., 2016). Extensive Acoustic Doppler Velocimetry measurement were carried out in the flume to document the flow conditions applied in the experiments. The surrogates were manufactured according to a moulding/casting protocol developed by Henry (2016). A mould was made by 3D-milling two thick Plexiglas plates, based on a digital model of a simplified shape of the kelp *Laminaria digitata*. Three kelp models were then casted in three different silicone materials, ranging from shore hardness 20A to 90A. Due to time limitations, the kelp model surrogate 60A was the only one investigated regarding drag forces. The plant models were tested with five different velocities from 0.05 m/s to 0.34 m/s to observe plant-flow interactions and drag forces. The dynamic reconfiguration of the surrogates was recorded from different angles with three cameras. Further detail about the experimental set-up can be found in Sjødal Oslen (2017).

3.3.3 Results and Discussion

Preliminary results from Norvik (2017)'s investigations suggest that there are major differences in the drag measurements and flow circulation patterns around the flat surrogates and the undulated surrogates of *L. saccharina.* Flat surrogates had the tendency to exhibit a strong fluttering behaviour

when tested separately, or to clump together when tested in a patch configuration. These movements are not observed in natural conditions for the species considered (C. Norvik and A, Lien, personal communications), thus suggesting that this type of surrogate does not represent the dynamics of the original macrophyte in a satisfactory way. Given that the undulated model has a shape more similar to the typical morphology of *L. Saccharina*, and that its qualitative behaviour is similar to the one observed in field situations, Norvik (2017) suggested that surrogates taking into account the blade undulation of the kelp offers a better representation of the mechanical interactions observed in nature. However, due to the surrogate material available at the time, the surrogate produced had a higher flexural rigidity and a higher density than real kelps. In addition to the limitation of the materials commercially available, Norvik (2017) pointed out that the stems were cut out of the same material as the blades, leading to a decrease of the stem's flexural rigidity of the kelp surrogate (not quantified in this study). This may have affected the behaviour of the surrogates, as the stem is the organ of the macrophyte that transfers the mechanical stresses from the blade to the support. Thus, Norvik (2017) identified some aspects to further improve when producing kelp surrogates for investigating seaweed farm hydrodynamics, namely:

- More effort should be given to identifying commercially available materials with the correct properties for mass production of surrogates.
- The reproduction of special morphological features such as undulations and critical mechanical parts of the plant, such as the stipe may have a major impact on the hydrodynamics and should therefore be reproduced accurately.
- The heat treatment of existing material is a promising technique with a limited time cost to shape and mass-produce surrogates with complex geometries.

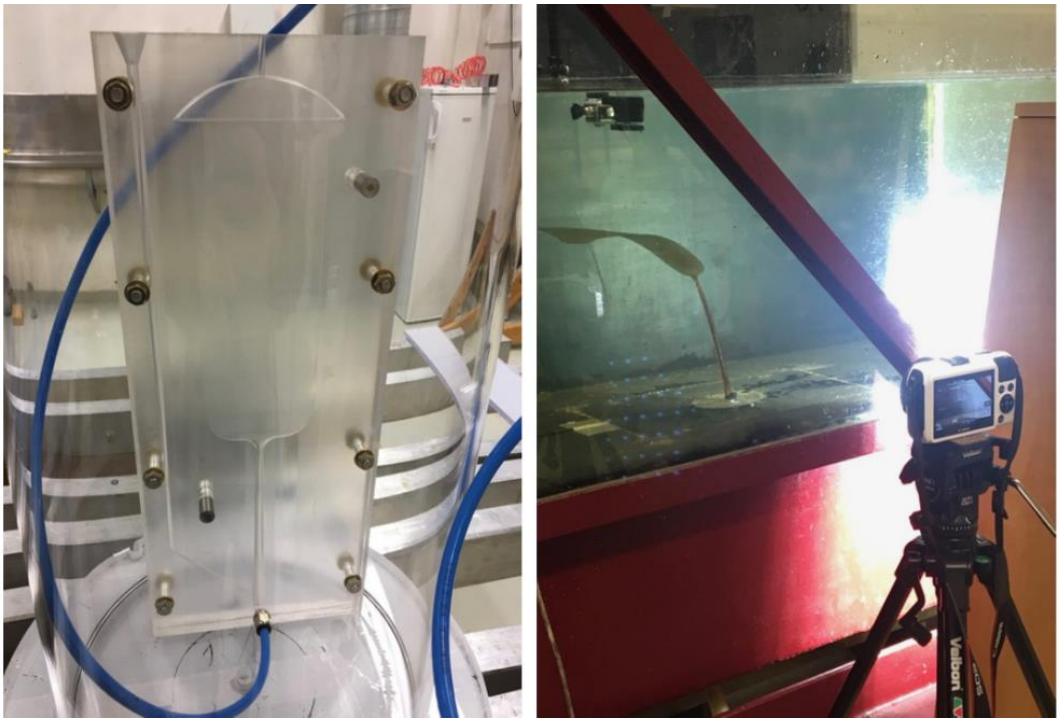

Figure 3.3.4 – Mould and test of a surrogate in Sjødal Olsen (2017)'s preliminary experiments. Taken from Sjødal Olsen (2017).

In parallel, Sjødal Olsen (2017) documented the different degrees of reconfiguration of the surrogate models depending on their flexibilities, in the case of a kelp attached to the seafloor. Transverse oscillations of the tip of the stem of the surrogates were observed and attributed to Vortex-Induced-Vibrations of the stem. The frequencies of oscillation characterised converge towards a similar value around 1.5 Hz as the flow velocity increased. However, vortex shedding frequencies derived for a vertical cylinder were plotted for comparison against the observed frequencies of the plant models, but did not match. The preliminary results presented by Sjødal Olsen (2017) would require some additional investigations to explain the observations made. However, Sjødal Olsen (2017) showed the relevance of the use of a moulding-casting approach to produce plant surrogates.

3.3.4 Conclusions and outlook

The main purpose of these two preliminary projects was to implement new surrogate production techniques that allows for further investigations of the basic processes of plant-flow interactions. Two distinct methods were developed, one by shaping an existing material and one by developing a moulding-casting technique. Both methods were successful in terms of the surrogate production, with the first approach more suited to mass production of idealised surrogates and the second for small production of special surrogates with varying mechanical properties. Further analysis would be required to quantify the hydrodynamic performance of these surrogates. Some of these additional investigations have been carried out at NTNU and SINTEF Oceans, based on the preliminary studies of Norvik (2017) and Sjødal Olsen (2017). As the analysis of the datasets obtained in ongoing, results and details about the final protocols used is still to be published.

4 PROTOCOLS FOR EXPERIMENTS WITH ANIMALS

4.1 BACKGROUND

In semi-enclosed areas, such as bays and estuaries, a strong feedback exists between benthic fauna evolution and sediment dynamics. So-called "ecosystem engineers", benthic populations modify suspended matter deposition by bio-filtration and increase sedimentation by bio-deposition of pseudo-faeces. In turn, hydro- and sediment dynamics directly impact the fauna environmental conditions. However, the complexity of this feedback remains extremely difficult to be addressed in the natural environment. Therefore, new laboratory experiments have been carried out to investigate the feasibility of simulating interactions between benthic fauna with mud/sand dynamics under waves and currents.

4.2 EXPERIMENTAL STUDY OF SEDIMENT-BIOTA INTERACTIONS UNDER WAVE-CURRENT CONDITIONS: APPLICATION TO THE ECOSYSTEM ENGINEER SPECIES *CREPIDULA FORNICATA* (IFREMER)

4.2.1 Objectives

Benthic and pelagic coupling in coastal and estuarine areas is a key mechanism for primary production dynamics, dissolved and particulate matter fluxes (e.g. sediments, nutrients, contaminants) and energy transfers within food webs. The relative importance of benthic and pelagic primary producers for sustaining benthic invertebrate communities depends on many factors (water depth, hydrodynamics, bed coverage, nutrient availability and benthic biodiversity).

Physical (biotope) and biological (biota: flora and fauna) compartments have often been investigated from separate disciplinary approaches. However, many studies have highlighted the strong non-linearities of hydro-bio-geochemical processes due to physical-biological interactions (e.g. Graf and Rosenberg, 1997; Murray et al., 2002). Benthic species can change the sediment habitat by physical processes (e.g. bed roughness, sediment trapping) and biological processes (e.g. bioturbation, biofiltration and biodeposition) (Orvain et al., 2004).

Most of the studies on sediment suspension associated with biological activities have focused on intertidal areas; however, subtidal areas have been less frequently investigated with biotopes dominated by "ecosystem engineer" species. Such species modify their habitat and increase the complexity of hydro-bio-sediment interactions at the water-sediment interface (e.g., Orvain and Sauriau, 2002; Reise, 2002; Widdows and Brinsley, 2002; Le Hir et al., 2007).

The *Crepidula* (*Crepidula fornicata*) is a gregarious invasive gastropod originating from the eastern coast of the USA, which has expanded along the European coasts since the 1980's. It largely impacted the colonised ecosystems and changed the seafloor nature, especially in the Bay of Brest "BoB" (NW France). After 40 years of proliferation, this "engineer" species shaped original benthic habitats characterized by heterogeneous sediment nature (mud/sand) and varying densities of dead and living shells. Studies investigating *Crepidula*-biotope interactions proposed three main processes driving the bio-sediment dynamics within such habitats: (i) the hydrodynamics at the bed level, (ii) the sediment erodibility, and (iii) the biodeposition induced by biofiltration (Barrilé et al., 2006;

Moulin et al., 2007; Beudin et al., 2013). In addition, such environments represent areas that are advantageous for biofilm development, which also impacts on sediment erodibility.

Crepidula habitats are associated with complex hydrodynamic forcing, such as wind- tide- and wave-induced currents, cohesive (mud) and non-cohesive (sand) sediment bed coverage and changing organic matter contents. However, the complexity of the physical-biological feedback remains extremely difficult to be addressed in the natural environment and previous laboratory experiments have not integrated the entire range of forcing. Therefore, new laboratory experiments have been carried out to investigate the interactions between the *Crepidula* shellfish with mud/sand dynamics under waves and currents.

The specific aims of this study are:

- to experiment the feasibility of simulating realistic sediment dynamics interacting with a living benthic fauna, based on a mesocosm facility;
- to quantify the key processes driving the sediment dynamics associated with a benthic population;
- to distinguish the physical and biological mechanisms responsible for sediment dynamics (erosion and settling) in conducting comparative tests with shell absence and presence (dead and alive);
- to summarize the precautions that need to be accounted for when experimenting with cohesive sediment and living fauna.

4.2.2 Experiments

This study reports on an annular flume experiment in which current and waves can be generated over a mixed sediment bed, i.e. mud and sand, with living benthic fauna in seawater.

Experimental set-up

Experiments were carried out during 5 weeks (May 2017) in the "Polludrome" flume tank of the CEDRE (CEntre de Documentation de Recherche et d'Expérimentation sur les pollutions accidentelles des eaux, Brest – France, http://wwz.cedre.fr/en/About-Cedre/Facilities-and-equipment/Experimental-devices/Flume-tank). The flume tank is 1.4 m high, 0.6 m wide and 13 m long, representing a surface of 8 m^2 (Figure 4.2.1). In the present study, the water level was fixed at 0.9 m, a turbine located 0.3 m above the bed generated currents reaching 0.25 m/s. A wave maker generated wave heights reaching 0.17 m for wave periods lower than 3 s, inducing an orbital wave velocity around 0.25 m/s. Such forcing generated tide- and wave-induced currents representative of the BoB environmental conditions over *Crepidula* habitats.

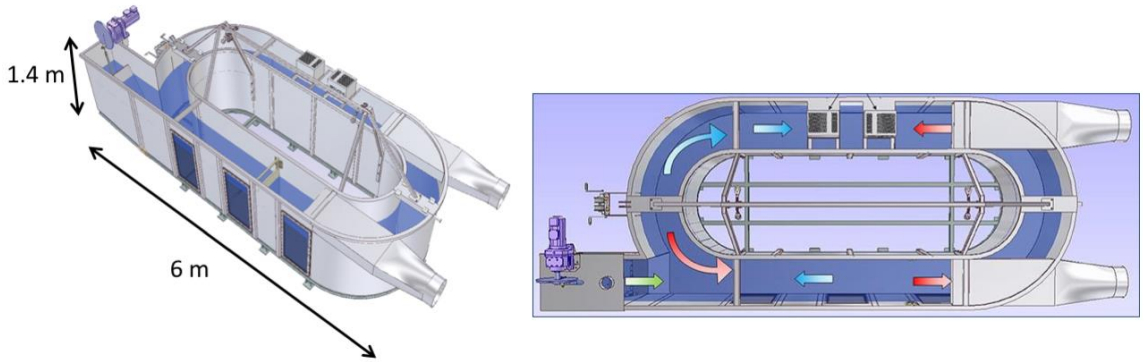

Figure 4.2.1. CEDRE's annular flume tank "Polludrome" generating current and waves over mud/sand bed and seawater.

The 10 cm thick bed was composed of a natural sandy mud collected in BoB at the location where the *Crepidula* shells were collected (d_{10} = 2 µm, d_{50} = 18 µm, d_{90} = 130 µm, representing the 10, 50 and 90 percentiles of the sediment grain size distribution, respectively). Dead and living *Crepidula* were dredged from natural dead and living shell banks, respectively, and distributed along the full length of the flume to assure the bed cover homogeneity. In the experiments, shell densities corresponded to the highest densities observed in the BoB, reaching 12 kg/m^3 and 16 kg/m^3 for dead and living *Crepidula* banks, respectively. The number of shells is approximately the same for dead and living *Crepidula*, but the density is higher for the living due to the weight of the gastropod. Therefore, the physical perturbation, in terms of bed roughness, should be similar between dead and living shell tests.

Experimental conditions

To investigate the physical and biological mechanisms responsible for sediment dynamics, comparative tests were conducted with shell absence and presence (dead and alive) for different hydrodynamic conditions. The first series of tests (series 0) were conducted for a bare sediment bed; the second series (series 1) were conducted with the same sediment bed as series 0 with dead shells; then the dead shells were removed from the flume and the series 2-4 were conducted with the same sediment as series 0 and 1, but with living shells (Figure 4.2.2).

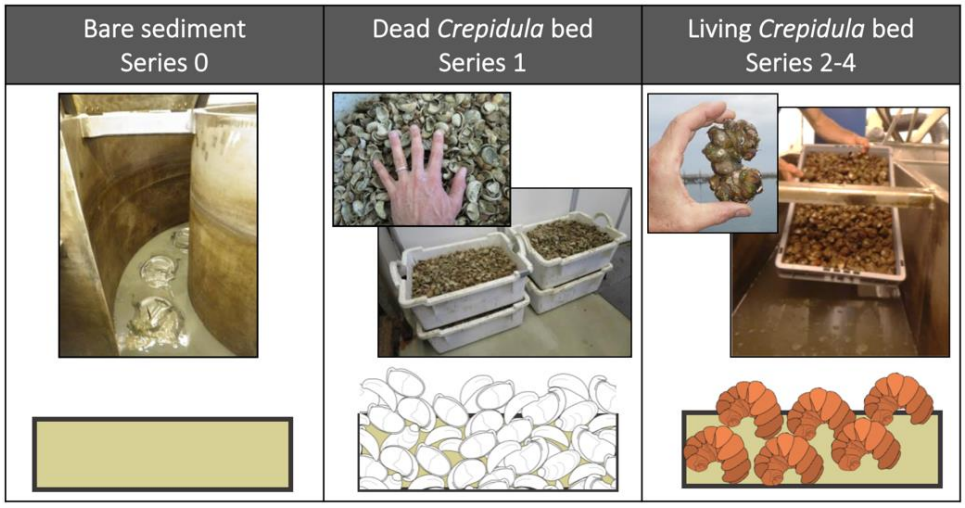

Figure 4.2.2. Tests conducted in the flume: (left panel) with a bare sediment (series 0), (centre panel) with dead shells (series 1) and (right panel) with living shells (series 2-4).

For each series, different hydrodynamic conditions were generated (Figure 4.2.3**Error! Reference source not found.**). The AM scenarios were aimed at generating an increasing current velocity, as a tidal current, from 0 to 0.25 m/s with steps of 0.05 m/s and duration of one hour. Scenarios 'a' and 'c' were identical; in scenario 'b' waves were generated in addition of the current. No forcing was generated during the PM scenarios to investigate the sediment settling without current- and wave-induced resuspension.

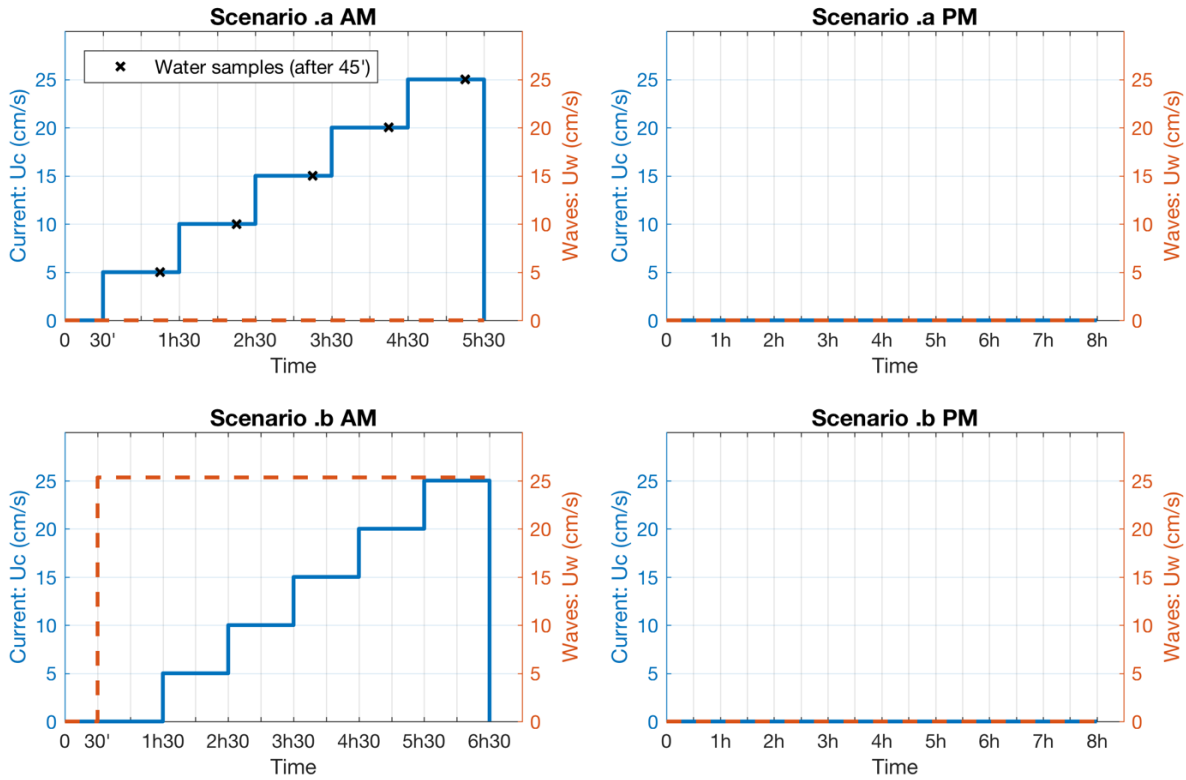

Figure 4.2.3. Hydrodynamic conditions generated for the different scenarios 'a' and 'b'. Scenario 'c' is the same as 'a'

Instrumentation and measurements

The sediment and shells were distributed along the flume, but the measurement section was located in front of the centre window opposite the current generator (Figure 4.2.1). The hydrodynamics was quantified from two velocity measurements (Acoustic Doppler Velocimeter, ADV) in the middle of the flume section at 0.13 and 0.38 m above the bed, sampling continuously at 10 Hz. The sediment dynamics was quantified with four turbidimeters (Optical Backscatter Sensors, OBS), located near the flume wall on the same section as the ADVs, at 13, 18, 23 and 38 cm above the bed. OBSs sampled continuously at 2 Hz. Moreover, the backscatter index derived from the signal to noise ratio (SNR) of the ADVs gave information on the turbidity level as well.

In addition to these continuous measurements, water samples were regularly collected during the experiments at the OBS elevations for different current velocities (Figure 4.2.3 and Table 4.2.1). Water samples were used to quantify the concentration of Suspended Particulate Matter (SPM) expressed in g/l, to calibrate the optical (OBS) and acoustic (ADV) turbidity measurements. The Organic Matter (OM) content was measured by loss of ignition, and the SPM size distribution was

measured by a LISST (Laser In-Situ Scattering and Transmissometery) after being deflocculated via ultra-sonication over 2 minutes.

Table 4.2.1. Experiment planning for tests without shells (series 0), with dead shells (series 1) and with living Crepidula (series 2-4). Timing of water and bed sampling are registered, as well as sediment bed reworking.

Series	Experiment days						
	1	2	3	4	5	6	7
Series 0 (no shell)		Bed mixing		Series 0.a water sampling. bed sampling	Series 0.c		
	8	9	10	11	12	13	14
Series 1 (dead)			Series 1.a water sampling	Series 1.b	Series 1.c		
	15	16	17	18	19	20	21
Series 2 (alive)	Bed mixing bed sampling	Series 2.a water sampling	Series 2.b	Bed mixing			
	22	23	24	25	26	27	28
Series 3 (alive)		Series 3.a	Series 3.c				
	29	30	31	32	33	34	35
Series 4 (alive)	Series 4.a	Series 4.b	Series 4.c water sampling	Bed sampling			

Bed sediment samples were collected for grain size analysis in front of each window, i.e. at the ADV and OBS measurement location and 1.5 m downstream and upstream, for different series. Video recording of the bed substrate was carried out at the beginning of every test for low current conditions, when the turbidity level was sufficiently low to ensure the visibility through the muddy water. The experiment planning is represented in Table 4.2.1.

4.2.3 Results

The results of the experiments are first presented in terms of sediment grain size distribution within the bed, and SPM size distribution and organic matter content in the water column. Secondly, results of hydrodynamics and SPM dynamics for different tests are presented. As the sediment bed had been actively reworked between the series 1 and 2, to remove the dead shells, the duration for the consolidation of the muddy sediment was not the same before each series. Therefore, the difference in sediment resuspension that were observed between the series could be related to different sediment erodibility associated with different level of consolidation. As a consequence, the results are mainly focusing on the settling phase (scenarios PM) where the initial conditions where similar.

Sediment bed grain size

The sediment grain size analysis within the bed is based on sediment samples collected at the ADV and OBS measurement location, i.e. centre window, and 1.5 m downstream and upstream (Figure 4.2.4, Table 4.2.1). A MALVERN laser granulometer was used to measure the grain size distribution. The muddy bed presented small changes between the different locations due to local heterogeneity (not shown); however, the grain size distribution remained very similar all along the experiments

with a main peak around 7 µm, as illustrated Figure 4.2.4 with the initial (blue) and final (yellow) tests at the centre location.

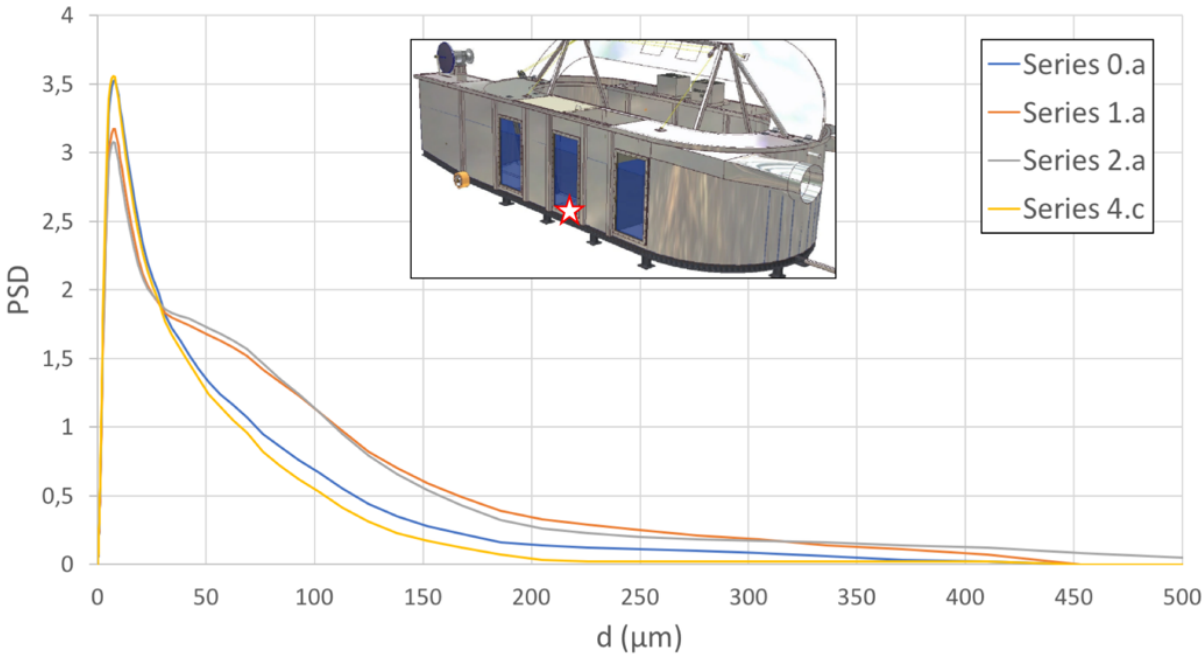

Figure 4.2.4. Sediment grain size distribution at the measurement location (see red star in the small panel) from the beginning (series 0.a) to the end (series 4.c) of the experiments.

SPM size

The SPM size distribution was measured with the LISST from the water samples collected during the different series (Table 4.2.1). The deflocculated particle size is presented for the highest current velocity (0.25 m/s) in series 1.a, 2.a and 4.c for the four OBSs (Figure 4.2.5), with OBS 1 to 4 elevated from the near-bed to the mid-water column, respectively. The particle size was distributed following two modes: a first mode around 2 µm, corresponding to the lowest detection limit of the LISST; and a second mode that shifted from 15 to 8 µm between the beginning and the end of the experiments. However, based on additional measurements of the series 1.a samples for different current velocities, the second mode was observed to vary between 8 and 15 µm. Therefore, it is difficult to conclude on an effective change of SPM size distribution during the experiments.

Organic matter content

The OM content derived from the water samples by loss of ignition of the SPM mass can be expressed in absolute value (mg/l) or in relative value (%) by normalizing by the total SPM mass, as in Figure 4.2.6. The OM content can affect fine particle flocculation in strengthening the floc cohesion. The influence of OM content on flocculation is more related to the relative value than the absolute value, which depends on the SPM concentration. The relative OM content did not change significantly between the tests without shells (series 0.a) and with dead shells (series 1.a). However, it increased significantly at the end of the experiments (series 4.c): from 14% to 30% for low current velocities (<0.1 m/s) and from 13% to 18% for high current velocities (0.25 m/s). Such an increase can be explained by the detrital OM content secreted by the *Crepidula* during series 2-4.

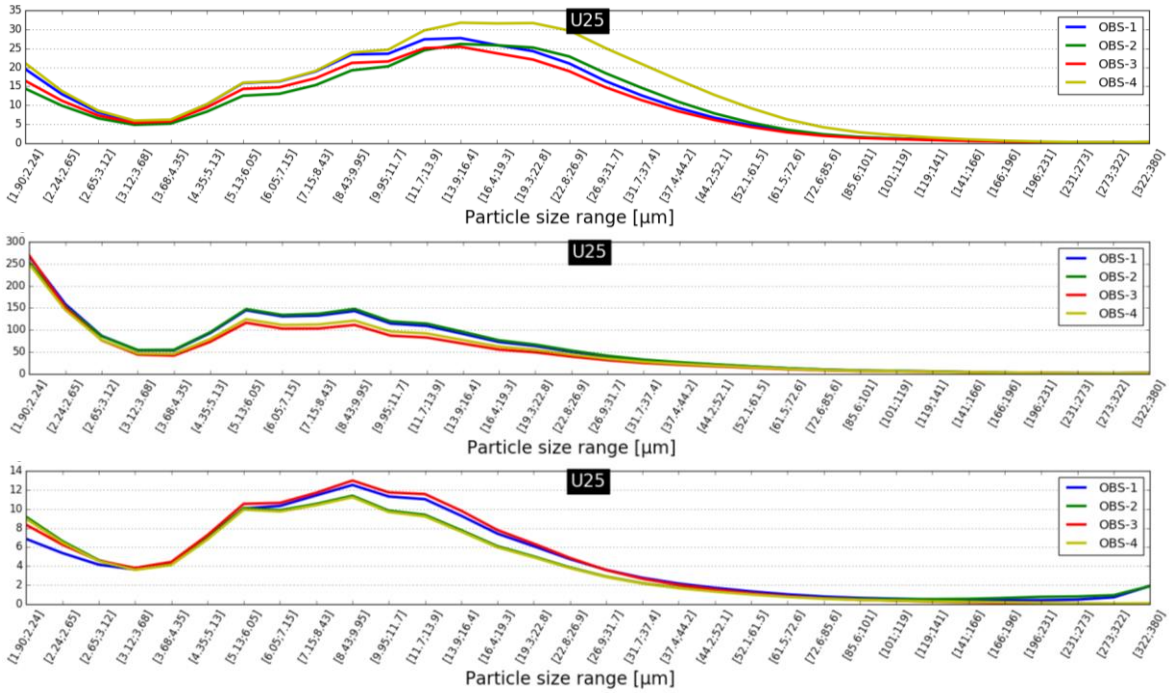

Figure 4.2.5. Power Spectral Density (PSD) of the deflocculated SPM size distribution for (top panel) series 1.a, (centre panel) series 2.a and (bottom panel) series 4.c at the highest current velocity (0.25 m/s) for the four OBSs.

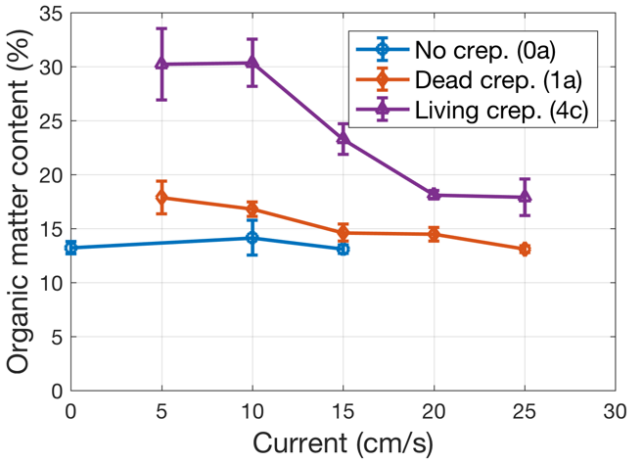

Figure 4.2.6. Relative organic matter content into the water column versus the current velocity for series 0.a, 1.a and 4.c. Symbols and brackets represent the average and standard deviation, respectively, of water samples collected at the four OBS elevations.

Calibration

The optical (OBS) and acoustic (SNR) turbidity measurements, expressed respectively in Volt and dB, were calibrated in SPM concentrations (mg/l) based on water sample filtrations (Figure 4.2.7). The linear regression slope between OBS and SPM increased slightly from the beginning (series 0.a) to the end (series 4.c) of the experiments, which could imply small changes in particle nature. As the optical turbidity measurement is more sensitive to fine particles, a weaker OBS signal (in Volt) for a given SPM concentration may be associated with larger particles. Such a trend was more pronounced for the ADV calibration, with a stronger SNR signal (in dB) for the series 4.c. The acoustic turbidity measurement is also substantially influenced by the particle type. For a given SPM

concentration, a SNR increase (in dB) may be associated with larger or denser particles. This is characteristic of flocculation processes.

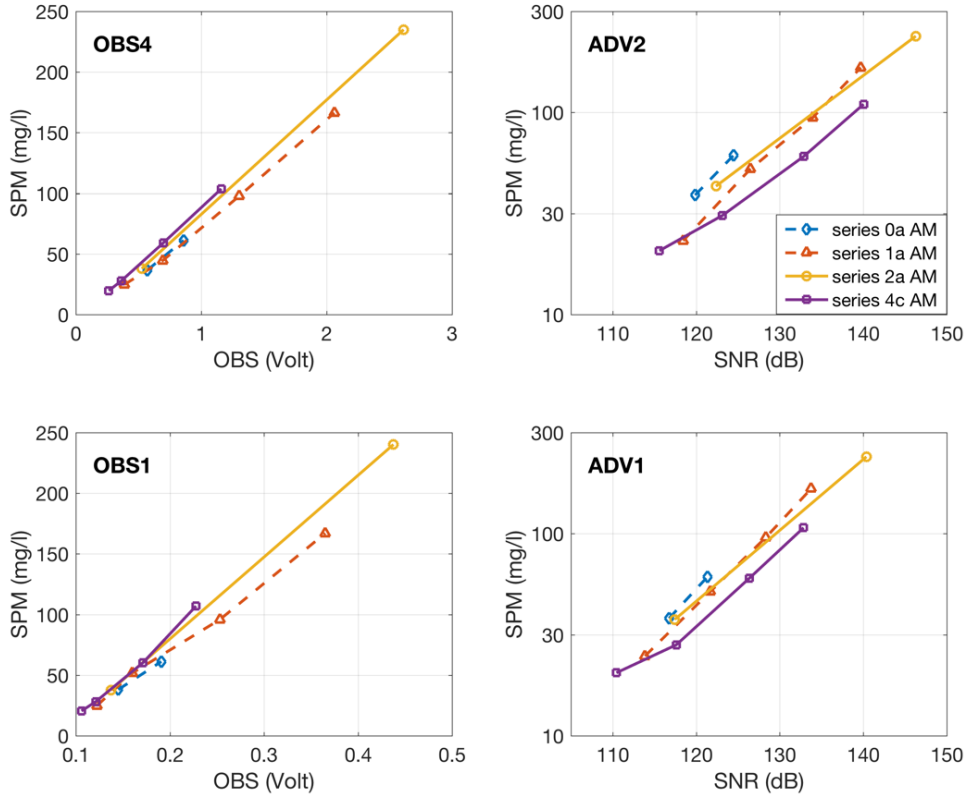

Figure 4.2.7. Calibration tests between SPM concentration measured from water sample filtration and (left panels) optical (OBS) and (right panels) acoustic (SNR) turbidity measurements, for (top panels) mid-water column and (bottom panels) near-bed elevations.

Hydrodynamics

The hydrodynamic results are presented in Figure 4.2.8(a, b, e and f) for the scenarios 'c', i.e. current only, of series 0, 1, 3 and 4 (see Table 4.2.1). The current velocity at the mid-water column elevation was significantly lower with the dead shell bed cover (series 1.c, red) than with the bare sediment bed (series 0.c, blue) (Figure 4.2.8a). This is in agreement with previous experimental studies illustrating the decreasing current velocity due to the increasing bed roughness induced by *Crepidula* shells (Moulin et al., 2007). However, such a behaviour was not observed at the near-bed elevation (Figure 4.2.8b), that may be explained by local heterogeneities of the shell cover.

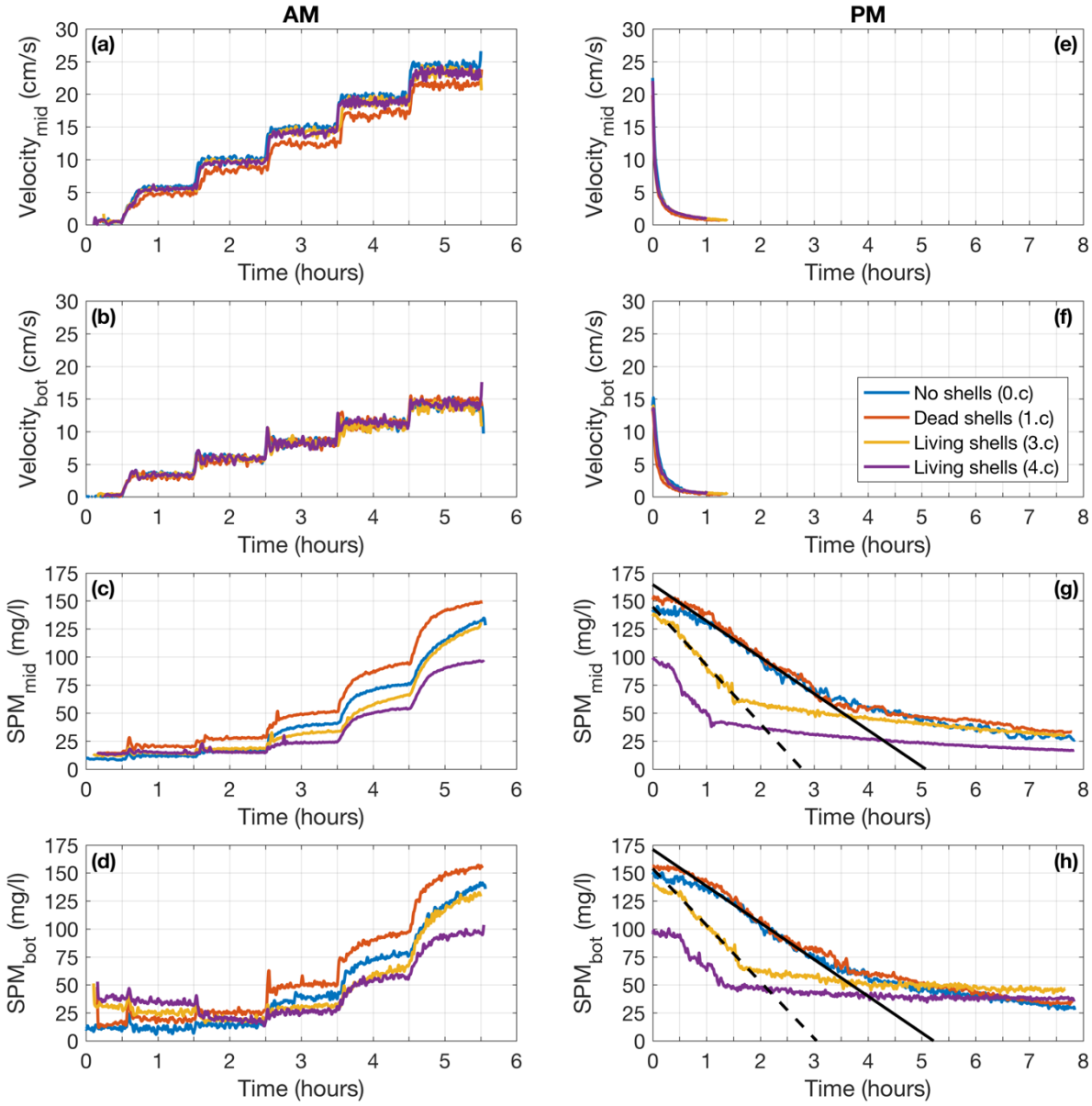

Figure 4.2.8 Hydrodynamics and SPM dynamics for scenarios 'c' with current only (AM, left panels) and without forcing (PM, right panels) for series 0, 1, 3 and 4 (see Table). Velocity measurements (a, e) at the mid-water column elevation, ADV2 and (b, f) at the bottom near the bed, ADV1. SPM concentration measurements (c, g) at the mid-water column elevation, OBS4 and (d, h) at the bottom near the bed, OBS1.

With living *Crepidula* bed covers (series 3.c, orange; 4.c, purple), the current velocity was smaller than with the bare sediment bed, but larger than with the dead shell bed cover. The bed roughness induced by living shells is lower than the dead shells due to the smooth chains that form the living *Crepidula*. In addition, living shells are heavier than dead shells and sink deeper in the bed, reducing the current flow perturbation.

The PM scenarios were carried out in the continuity of the AM scenarios by stopping the hydrodynamic forcing (Figure 4.2.8e and f). It resulted in a quick decrease of the current velocity, with a current slower than 0.05 m/s after 10 minutes.

SPM dynamics

As with the hydrodynamic analysis, the SPM dynamics is presented for the scenarios 'c' of series 0, 1, 3 and 4 (Figure 4.2.8c, d, g and h). In scenarios AM with the increasing current velocity, the sediment suspension, resulting from the current-induced erosion, was larger with dead shell beds than with the bare sediment bed (Figure 4.2.8c and d). This is in agreement with the larger bed roughness observed with dead shells, enhancing sediment resuspension. Contrastingly, the SPM concentration measured with the living *Crepidula* bed covers did not exceed the values reached with the bare sediment bed; whereas the bed roughness was observed to be larger. Different hypothesis related to physical and biological processes can explain such a behaviour:

i. the muddy bed consolidation, more advanced at the end of the experiments (series 3.c and 4.c), increasing the bed sediment concentration and increasing the critical shear stress for erosion that limits sediment resuspension;
ii. the *Crepidula* activity, as biofiltration, that enhances sediment settling (i.e. biodeposition) and reduces SPM concentration;
iii. the biofilm development (e.g. microphytobenthos) associated with an increased OM content, stabilizing the bed and reducing the sediment erodibility that reduces sediment resuspension;
iv. the SPM flocculation, associated with an increased OM content, which enhances sediment settling and reduces SPM concentration.

Unfortunately, core samples of the sediment bed were not collected during the experiments and OM content within the sediment were not measured. Consequently, it is not possible to have a quantification of sediment consolidation and biofilm development for the different series. As sediment erodibility, driving the SPM dynamics, could not be properly characterized during scenarios AM, the relative influence of physical and biological processes on SPM dynamics is mainly investigated through the analysis of the sediment settling without forcing (scenarios PM).

Following the sediment suspension in scenarios AM, the sediment settling is analysed from the SPM decrease in scenarios PM (Figure 4.2.8g and h). Three different phases were observed during the settling experiments: the SPM concentration slowly decreased during the first phase (e.g. $t \approx 0$-0.5 h in series 1.c, Figure 4.2.8g); then, it decreased faster during the second phase ($t \approx 0.5$-3.5 h), before decreasing more slowly in the last phase ($t \approx 3.5$-7.5 h). Such a behaviour is associated with the settling of particles at different velocities during the decantation. Interestingly, the SPM dynamics of series 0.c and series 1.c, with no shells and dead shells, respectively, were very similar. As expected, the dead shell bed cover did not affect the sediment settling. In contrast, the decantation during the tests with living *Crepidula* (series 3.c and 4.c) was significantly faster, especially in the second phase. These results point out that bed covers with living shells substantially affect the SPM settling.

SPM settling velocity

To quantify the settling velocity of sediment particles during the different tests, an original method based on SPM concentration measurements is proposed. This method is similar as the settling column experiment proposed by Owen (1976); however, instead of measuring the settling velocity distribution from the cumulated mass weighed at the bottom of the column, in this study it is proposed to quantify the sediment mass from the measured SPM concentration (OBS). Nevertheless, this is based on the assumption of a homogeneous SPM concentration into the water column.

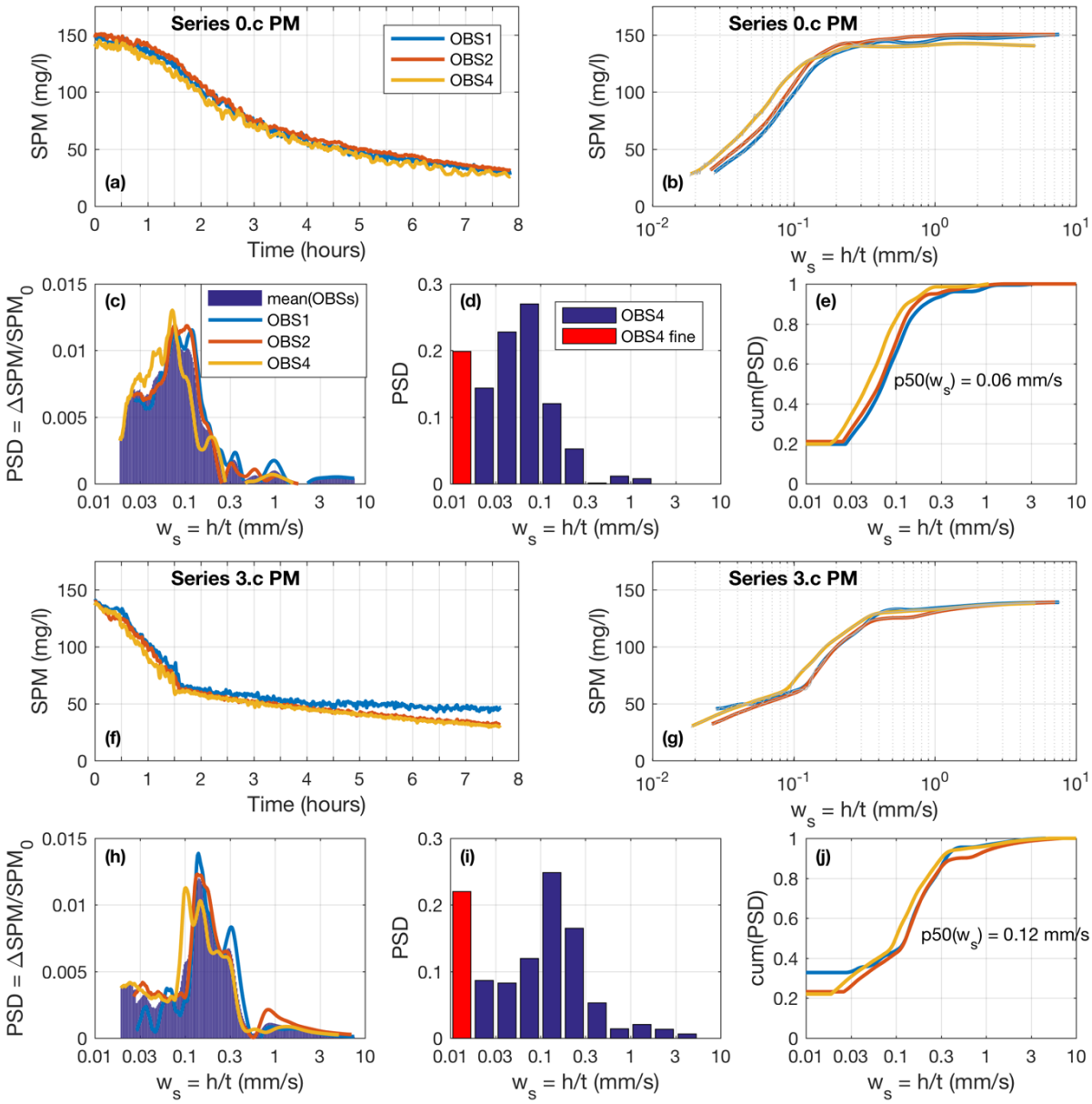

Figure 4.2.9. Method to estimate a settling velocity distribution from SPM concentration measurements. (a-e) Series 0.c PM, i.e. bare sediment bed, and (f-j) Series 3.c PM, i.e. living shell bed cover; analysis for OBS1 (blue), OBS2 (red) and OBS4 (yellow). (a, f) Time evolution of SPM concentration, (b, g) Time evolution of SPM concentration, with time expressed as a settling velocity w_s, (c, h) Power Spectral Density (PSD) of settling velocity w_s, derived from graphs in panels b and g, respectively, (d, i) example of settling velocity distribution (PSD) discretized with 11 velocity classes, and (e, j) cumulated PSD of settling velocity w_s, with the median value p50(w_s) for all the OBSs.

In a decantation test (e.g. series 0.c PM, Figure 4.2.9a), the time (t) can be expressed as a settling velocity $w_s = h/t$, with h the distance between the OBS elevation and the water surface (Figure 4.2.9b). Next, a decrease of the SPM concentration ΔSPM_i during a time step Δt_i can be associated with a settling velocity class $w_{s,i}$. The Power Spectral Density (PSD) of the settling velocity distribution is then derived from the ΔSPM_i distribution normalized by the initial concentration SPM_0 (Figure 4.2.9c). As the final SPM concentration (SPM_f) did not decrease to zero at the end of the experiments (e.g. SPM_f = 30 mg/l at t_f = 7h45, $w_{s,f}$ = 0.02 mm/s, Figure 4.2.9a and b), a low settling

velocity class characterizing very fine particles is added to the measured distribution (red class in Figure 4.2.9d).

This method can be applied to the different OBS measurements and the resulting cumulated distributions of w_s provide statistics, as the median settling velocity (e.g. p50(w_s) = 0.06 mm/s, Figure 4.2.9e), for the different tests. Applied on the series 3.c PM (Figure 4.2.9f-j), this method leads to a median settling velocity of 0.12 mm/s. It implies that the SPM settling, i.e. the sediment decantation, was twice as large with the living *Crepidula* bed compared to the bare sediment bed.

The synthesis of the settling velocities corresponding to series 0, 1, 3 and 4 clearly highlights the above-mentioned trend (Figure 4.2.10). However, these velocities have to be related to the initial SPM concentration (SPM0), as w_s is known to increase with SPM0 due to flocculation processes (e.g. Van Leussen, 1994). In these experiments, w_s increased almost linearly with SPM0. In addition, w_s was significantly larger for the tests with living *Crepidula* (series 3 and 4) than without shell (series 0) and with dead shells (series 1).

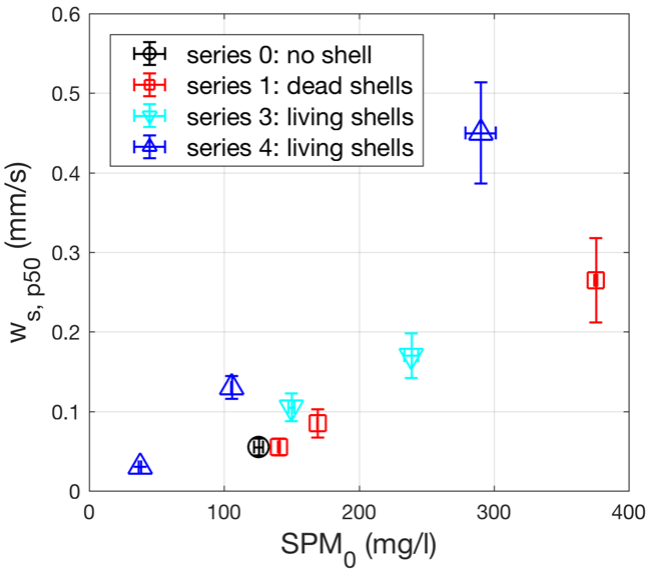

Figure 4.2.10 Synthesis of median settling velocity $ws_{,p50}$ versus initial SPM concentration SPM0 for the settling tests (scenarios PM) of series 0, 1, 3 and 4. Symbols and brackets represent the average and standard deviation, respectively, of settling velocities derived from OBS 1, 2 and 4.

4.2.4 Discussion

The SPM settling velocity increased for the tests with living *Crepidula* (Figure 4.2.8). This observation can result from two main processes: (i) the biofiltration of the *Crepidula* and (ii) the flocculation that would be larger with the living shell bed cover.

Biofiltration

According to Barillé et al. (2006), the filtration induced by *Crepidula* can reach 0.76±0.05 l/h/g_{dry} (i.e. 2.11×10^{-4} ±0.14×10^{-4} m^3/s/kg), based on the shell dry weight. It is estimated that the dry weight represents approximately 5% of the total weight of the *Crepidula* (flesh and shell). With a *Crepidula* density of 16 kg/m^2 within the flume, and assuming that all the shells were filtrating, it leads to a

biofiltration-induced settling velocity $w_{s,filt}$ = 0.17±0.01 mm/s. This value may partly explain the w_s changes observed during the experiments (Figure 4.2.8).

During the series 3 and 4, video recording of the bed revealed the development of black and white patches characteristic of sediment anoxia and microbial biofilm development, respectively, that could result from dying *Crepidula*. In addition, at the end of the experiments (day 32) most of the *Crepidula* chains were observed to be broken, characterizing dead shells. Therefore, it is doubtful that the *Crepidula* kept a biofiltration activity as intense in series 4 as in series 3; however, the settling velocity was observed to be larger in series 4 than in series 3 (Figure 4.2.8). It would suggest that the increasing settling velocity for the tests with living *Crepidula* would result from another mechanism.

Flocculation

Cohesive sediment particles are known to flocculate, increasing their settling velocity. The flocculation is affected by SPM concentration, as observed in Figure 4.2.10, turbulence, salinity and OM content (e.g. Van Leussen, 1994). The turbulence and salinity conditions were similar for the different tests; nonetheless, the relative OM content was observed to be larger at the end of the experiments for series 4.c (Figure 4.2.6). It can be explained by the detrital OM content secreted by the *Crepidula* during series 2-4 and by the biofilm development, such as microphytobenthos and microbial microfilms.

The Backscatter Index (BI) derived from the acoustic turbidity measurement is related to the SPM concentration (Figure 4.2.11a); however, a shift is observed between the different tests, implying different types of particles. Based on the sonar formulation, assuming a constant water attenuation and a negligible sediment attenuation (SPM concentration lower than 400 mg/l), BI can be associated with a median particle size. This median diameter is derived from the distribution in number of particles and not from the distribution in mass of particles. It is observed that for a given concentration, the median SPM size was larger for series 4, suggesting that the larger settling velocity could result from larger flocculation processes (Figure 4.2.11b).

Classical settling velocity formulations, such as Stokes' law (Stokes, 1901), are based on a mass median diameter; however, it is not straightforward to obtain this diameter from a number median diameter. For instance, it is estimated that a number median diameter ranging from 8 to 11 µm, would correspond to a mass median diameter ranging from 20 to 80 µm. Based on the Stokes' law, it corresponds to a settling velocity ranging from 0.06 to 0.3 mm/s. These results imply that the flocculation can increase the settling velocity by a factor of 5; therefore, it represents an important mechanism that could explain the larger settling velocities observed with the living *Crepidula* bed covers (Figure 4.2.8).

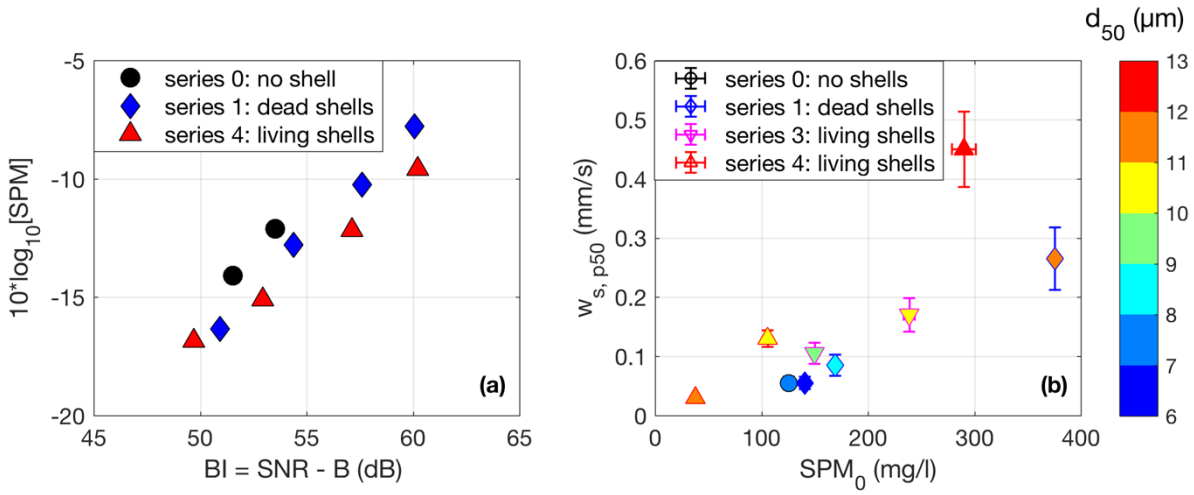

Figure 4.2.11. (a) SPM concentration versus backscatter index BI; (b) same caption as Figure 4.2.10, with the number median floc diameter d50 in colour.

Wave forcing

Tests with wave forcing in addition to current forcing were carried out (series 1.b, 2.b and 4.b,Table 4.2.1). The wave-induced bottom velocity U_w in the flume ($U_{w,f}$ = 0.25 cm/s, wave height H_f = 0.17 m and period T_f = 2.4 s for a water depth h_f = 0.9 m) corresponds to typical wind-wave conditions observed in the Bay of Brest ($U_{w,BoB}$ = 0.25 cm/s, H_{BoB} = 0.6 m, T_{BoB} = 6 s, h_{BoB} = 10 m). Therefore, the wave-induced bed shear stress in the experiments was similar as in nature.

These tests resulted in sediment erosion and SPM concentration significantly larger than with the current forcing alone. However, the wave influence on sediment erosion was difficult to analyse for the different series due to the sediment bed that was not at similar consolidation levels. For instance, the SPM concentration during series 2.b AM (day 17) was drastically larger than during series 1.b AM and 4.b AM because of the low consolidated bed previously reworked (day 15,Table 4.2.1). During the decantation tests (scenarios PM), the settling velocities were significantly larger than for current forcing alone due to larger initial SPM concentrations (not shown).

4.2.5 Recommended protocols

The experiments on sediment-fauna interactions presented in this study faced serious technical, physical and biological challenges:

- the presence of cohesive sediment (i.e. mud) induces consolidation and flocculation processes that make the analysis of sediment-biota interactions more complex;
- the organic matter content associated with microphytobenthos and microbial biofilm development, which is enhanced in muddy bed, can affect the sediment erodibility and impact the SPM dynamics;
- the presence of living fauna requires good environmental conditions (e.g. water quality, oxygen, food supply) that determine the fauna activity;
- the stress experienced by the fauna in the experiments can affect their biological activity as well.

Based on the knowledge gained during this study, recommendations on the experimental protocols are proposed here below.

Sediment bed conditions
To compare the influence of biological processes on sediment erosion, it is necessary to have similar sediment bed conditions. As a muddy bed consolidates with time, comparative tests have to be carried out in the same timing following the bed mixing. In addition, sediment core samples can be collected to measure the water content, providing a proxy of the bed consolidation level. Moreover, measurement of OM content within the bed can provide insight into biofilm development that may change the sediment erodibility.

SPM size distribution
Deflocculated SPM size distribution was measured from water samples, providing the primary particle size distribution. However, the SPM size during the tests, characterizing flocculation processes, was not measured directly. The SPM size was deduced from the acoustic measurement and required strong assumptions. The deployment of a LISST into the flume would measure directly the SPM size, and thus, flocculation. Nonetheless, the substantial size of the instrument has to be considered to not excessively disrupt the current flow.

Environmental conditions
Many *Crepidula* were observed to be dead at the end of the experiments. It can result from different causes: anoxia near the bed, lack of food supply (nutrients, OM), excessive stress, etc. The water was oxygenated through eight air sources deployed into the flume when no forcing was applied. In addition, the OM content into the water was supposed to be sufficient for *Crepidula* to survive during the 15-day experiments. In spite of these precautions, the environmental conditions were not conducive to *Crepidula* survival. Additional analyses on the cause of *Crepidula* mortality have to be realized in order to improve the experimental protocols.

4.2.6 Conclusions
The influence of the *Crepidula* shellfish on SPM dynamics has been investigated through an experimental study considering current and wave forcing over a mixed sediment bed (i.e. mud and sand) in seawater. Comparative tests were conducted with bare sediment beds, dead shell bed covers and living shell bed covers in order to discriminate the physical and biological influence of shells on sediment erosion and settling.

Dead shell bed covers were observed to reduce the current velocity and increase the sediment suspension due to a larger bed roughness. Tests with living shell bed covers presented contrasted results with an increased bed roughness, but a limited sediment suspension. It can be related to the muddy bed consolidation, *Crepidula* biofiltration and biofilm development.

The SPM settling velocities were similar for the tests with bare sediment and with dead shells. However, it was noticeably faster for the tests with living shells. Such a behaviour can be explained by the increased biodeposition from *Crepidula* biofiltration and by the enhanced flocculation that may result from the larger organic matter content observed with living *Crepidula*.

These challenging experiments provided interesting and encouraging results on the physical modelling of sediment-fauna interactions. Nevertheless, this study raised many technical, physical and biological issues that have to be taken into account when dealing with cohesive sediment and living fauna.

5 REFERENCES

Abdelrhman, M. (2007). *Modeling coupling between eelgrass Zostera marina and water flow*. Marine Ecology Progress Series, 338, pp.81-96.

Albayrak, I., Nikora, V., Miler, O. and O'Hare, M. (2012). *Flow-plant interactions at a leaf scale: effects of leaf shape, serration, roughness and flexural rigidity*. Aquatic Sciences, 74(2), pp.267-286.

Amos, C.L., M. Brylinsky, T.F. Sutherland, D. O'Brien, S. Lee, and A. Cramp. 1998. *The Stability of a Mudflat in the Humber Estuary, South Yorkshire, UK*. Geological Society, London, Special Publications 139 (1). Geological Society of London:25–43. https://doi.org/10.1144/GSL.SP.1998.139.01.03.

Augspurger, C., and K. Küsel. 2010. *Flow Velocity and Primary Production Influences Carbon Utilization in Nascent Epilithic Stream Biofilms.* Aquatic Sciences 72 (2). SP Birkhäuser Verlag Basel:237–43. https://doi.org/10.1007/s00027-009-0126-y.

Barillé, L., Cognie, B., Beninger, P., Decottignies, P., & Rincé, Y. (2006). *Feeding responses of the gastropod Crepidula fornicata to changes in seston concentration*. *Marine Ecology Progress Series*, *322*, 169-178.

Barrón, C., Marbé, N., Terrados, J., Kennedy, H., Duarte, C.M. (2004). *Community metabolism and carbon budget along a gradient of seagrass (Cymodocea nodosa) colonization*. Limnol. Oceanogr. 49, 1642e1651.

Beudin, A., Chapalain G. & Guillou N. (2013). *Suspended sediment modeling in the bay of Brest impacted by the slipper limpet Crepidula fornicata*, in: Proceedings of Coastal Dynamics'13.

Bhaskar, P.V., and N.B. Bhosle. 2006. *Bacterial Extracellular Polymeric Substance (EPS): A Carrier of Heavy Metals in the Marine Food-Chain.* Environment International 32 (2):191–98. https://doi.org/10.1016/j.envint.2005.08.010.

Black, K. S., T. J. Tolhurst, D. M. Paterson, and S. E. Hagerthey. 2002. *Working with Natural Cohesive Sediments*. Journal of Hydraulic Engineering 128 (1):2–8. https://doi.org/10.1061/(ASCE)0733-9429(2002)128:1(2).

Borum, J. and Greve, T. (2014). *The four European seagrass species. In: J. Borum, C. Duarte, D. Krause-Jensen and T. Greve, ed., European seagrasses: an introduction to monitoring and management*. [online] The M&MS project, pp.1-8. Available at: http://imedea.uib-csic.es/icg/downloads/seagrass.pdf [Accessed 17 Jun. 2017].

Carus, J., Paul, M., Schr€oder, B., 2016. *Vegetation as self-adaptive coastal protection: reduction of current velocity and morphologic plasticity of a brackish marsh pioneer*. Ecol. Evol. 6, 1579e1589.

Chandler, M., Colarusso, P. and Buchsbaum, R. (1996). *A study of eelgrass beds in Boston Harbor and northern Massachusetts bays*. Office of Research and Development, U.S. Environmental Protection Agency, Narragansett, RI.

Chen, Z., Jiang, C. and Nepf, H. (2013). *Flow adjustment at the leading edge of a submerged aquatic canopy*. Water Resources Research, 49(9), pp.5537-5551.

Chenu, C., and J. Guérif. 1991. *Mechanical Strength of Clay Minerals as Influenced by an Adsorbed Polysaccharide*. Soil Science Society of America Journal 55 (4). Soil Science Society of America:1076. https://doi.org/10.2136/sssaj1991.03615995005500040030x.

Dade, W.B., J.D. Davis, P.D. Nichols, A.R.M. Nowell, D. Thistle, M.B. Trexler, and D.C. White. 1990. *Effects of Bacterial Exopolymer Adhesion on the Entrainment of Sand*. Geomicrobiology Journal 8 (1). Taylor & Francis Group:1–16. https://doi.org/10.1080/01490459009377874.

Decho, A.W. 1990. *Microbial Exopolymer Secretions in Ocean Environments: Their Role (S) in Food Webs and Marine Processes.* Oceanogr. Mar. Biol. Annu. Rev 28 (7):73–153.

de los Santos, C., Onoda, Y., Vergara, J., Pérez-Lloréns, J., Bouma, T., La Nafie, Y., Cambridge, M. and Brun, F. (2016). *A comprehensive analysis of mechanical and morphological traits in temperate and tropical seagrass species.* Marine Ecology Progress Series, 551, pp.81-94.

Dijkstra, J. and Uittenbogaard, R. (2010). *Modeling the interaction between flow and highly flexible aquatic vegetation*. Water

Droppo, I.G., N. Ross, M. Skafel, and S.N. Liss. 2007. *Biostabilization of Cohesive Sediment Beds in a Freshwater Wave-Dominated Environment.* Limnology and Oceanography 52 (2):577–89.

Dubois, M., K. A. Gilles, P. A. Rebers, and Smith F. 1956. *Colorimetric Method for Determination of Sugars and Related Substances*. Analytical Chemistry 28:350–56.

El Allaoui, N., Serra, T., Colomer, J., Soler, M., Casamitjana, X. and Oldham, C. (2016). *Interactions between Fragmented Seagrass Canopies and the Local Hydrodynamics*. PLOS ONE, 11(5).

Flemming, H. 2011. *The Perfect Slime.* Colloids and Surfaces B: Biointerfaces 86 (2):251–59. https://doi.org/10.1016/j.colsurfb.2011.04.025.

Flemming, H., and J. Wingender. 2010. *The Biofilm Matrix*. Nature Reviews Microbiology 8 (9). Nature Publishing Group:623. https://doi.org/10.1038/nrmicro2415.

Folkard, A. (2005). *Hydrodynamics of model Posidonia oceánica patches in shallow water*. Limnology and Oceanography, 50(5), pp.1592-1600.

Folkard, A. (2011). *Flow regimes in gaps within stands of flexible vegetation: laboratory flume simulations*. Environmental Fluid Mechanics, 11(3), pp.289-306.

Fonseca, M. and Cahalan, J. (1992). *A preliminary evaluation of wave attenuation by four species of seagrass*. Estuarine, Coastal and Shelf Science, 35(6), pp.565-576.

Fonseca, M., Koehl, M. and Kopp, B. (2007). *Biomechanical factors contributing to self-organization in seagrass landscapes*. Journal of Experimental Marine Biology and Ecology, 340(2), pp.227-246.

Friend, P.L., P. Ciavola, S. Cappucci, and R. Santos. 2003. *Bio-Dependent Bed Parameters as a Proxy Tool for Sediment Stability in Mixed Habitat Intertidal Areas*. Continental Shelf Research 23 (17):1899–1917. https://doi.org/10.1016/j.csr.2002.12.001.

Friend, P.L., M.B. Collins, and P.M. Holligan. 2003. *Day–night Variation of Intertidal Flat Sediment Properties in Relation to Sediment Stability*. Estuarine, Coastal and Shelf Science 58 (3):663–75. https://doi.org/10.1016/S0272-7714(03)00178-1.

Gambi, M. (1988). *Flowering in a Zostera marina bed off San Juan island (Washington, U.S.A.) during winter*. Aquatic Botany, 30(3), pp.267-272.

Gambi, M., Nowell, A. and Jumars, P. (1990). *Flume observations on flow dynamics in Zostera marina (eelgrass) beds*. Marine Ecology Progress Series, 61, pp.159-169.

Gedan, K., Kirwan, M., Wolanski, E., Barbier, E. and Silliman, B. (2010). *The present and future role of coastal wetland vegetation in protecting shorelines: answering recent challenges to the paradigm*. Climatic Change, 106(1), pp.7-29.

Gerbersdorf, S.U., H. Hollert, M. Brinkmann, S. Wieprecht, H. Schüttrumpf, and W Manz. 2011. *Anthropogenic Pollutants Affect Ecosystem Services of Freshwater Sediments: The Need for a 'triad plus X' Approach*. Journal of Soils and Sediments 11 (6). Springer-Verlag:1099–1114. https://doi.org/10.1007/s11368-011-0373-0.

Gerbersdorf, S U, and S Wieprecht. 2015. *Biostabilization of Cohesive Sediments: Revisiting the Role of Abiotic Conditions, Physiology and Diversity of Microbes, Polymeric Secretion, and Biofilm Architecture.* Geobiology 13 (1):68–97. https://doi.org/10.1111/gbi.12115.

Ghisalberti, M. (2000). *Mixing layers and coherent structures in vegetated aquatic flows.* Masters Thesis. Massachusetts Institute of Technology. Department of Civil and Environmental Engineering. [online] Available at: https://dspace.mit.edu/handle/1721.1/80938 [Accessed 18 Jun. 2017].

Ghisalberti, M. and Nepf, H. (2002). *Mixing layers and coherent structures in vegetated aquatic flows*. Journal of Geophysical Research, 107(C2).

Ghisalberti, M. and Nepf, H. (2005). *Mass Transport in Vegetated Shear Flows*. Environmental Fluid Mechanics, 5(6), pp.527-551.

Ghisalberti, M. and Nepf, H. (2006). *The Structure of the Shear Layer in Flows over Rigid and Flexible Canopies*. Environmental Fluid Mechanics, 6(3), pp.277-301.

Ghisalberti, M. and Nepf, H. (2009). *Shallow Flows Over a Permeable Medium: The Hydrodynamics of Submerged Aquatic Canopies*. Transport in Porous Media, 78(3), pp.385-402.

Graba, M., S. Sauvage, F.Y. Moulin, G. Urrea, S. Sabater, and J.M. Sanchez-Pérez. 2013. *Interaction between Local Hydrodynamics and Algal Community in Epilithic Biofilm.* Water Research 47 (7):2153–63. https://doi.org/10.1016/j.watres.2013.01.011.

Graf, G., & Rosenberg, R. (1997). *Bioresuspension and biodeposition: a review*. Journal of Marine Systems, 11, 269–278.

Hansen, J. and Reidenbach, M. (2012). *Wave and tidally driven flows in eelgrass beds and their effect on sediment suspension*. Marine Ecology Progress Series, 448, pp.271-287.

Hansen, J. and Reidenbach, M. (2013). *Seasonal Growth and Senescence of a Zostera marina Seagrass Meadow Alters Wave-Dominated Flow and Sediment Suspension within a Coastal Bay*. Estuaries and Coasts, 36(6), pp.1099-1114.

Henry, P.Y. (2016). *Parametrisation of aquatic vegetation in hydraulic and coastal research: The importance of plant biomechanics in the hydrodynamics of vegetated flows*. Norwegian University of Science and Technology, Dept. of Marine Technology, Doctoral thesis NTNU 2016:138 (IMT-5-2016).

Henry, P.Y., Aberle, J., Dijkstra, J., Myrhaug, D. (2016). *An integrated, multi-sensing approach to describe the dynamic relations between turbulence, fluid-forces, and reconfiguration of a submerged plant model in steady flow*s. EGU General Assembly 2016, 17-22 April 2016, Vienna (Austria), id. EPSC2016-7544.

Henry, P.Y. (2018). *Variability and similarities in the structural properties of two related Laminaria kelp species*. Estuarine, Coastal and Shelf Science, 200 pp395-405.

Houser, C., Trimble, S. and Morales, B. (2015). *Influence of Blade Flexibility on the Drag Coefficient of Aquatic Vegetation*. Estuaries and Coasts, 38(2), pp.569-577.

Hoyal, D.C.J.D., and B.A. Sheets. 2009. *Morphodynamic Evolution of Experimental Cohesive Deltas*. Journal of Geophysical Research 114:F02009. https://doi.org/10.1029/2007JF000882.

Ikeda, S. and Kanazawa, M. (1996). *Three-Dimensional Organized Vortices above Flexible Water Plants*. Journal of Hydraulic Engineering, 122(11), pp.634-640.

Johnson, M., Rice, S., Penning, W. and Dijkstra, J. (2014). *Maintaining the health and behavioral integrity of plants and animals in experimental facilities*. In: L. Frostick, R. Thomas, M. Johnson, S. Rice and S. McLelland, ed., Users Guide to Ecohydraulic Modelling and Experimentation: Experience of the Ecohydraulic Research Team (PISCES) of the HYDRALAB Network. Leidem, The Netherlands: CRC Press/Balkema, pp.9-21.

Kleinhans, M.G., W.M. van Dijk, W.I. van de Lageweg, D.C.J.D. Hoyal, H. Markies, M. van Maarseveen, C. Roosendaal, et al. 2014. *Quantifiable Effectiveness of Experimental Scaling of River- and Delta Morphodynamics and Stratigraphy*. Earth Science Reviews 133:43–61, doi:10.1016/j.earscirev.2014.03.001.

Kornman, B.A., and E.M.G.T. De Deckere. 1998. *Temporal Variation in Sediment Erodibility and Suspended Sediment Dynamics in the Dollard Estuary*. Geological Society, London, Special Publications 139 (1). Geological Society of London:231–41. https://doi.org/10.1144/GSL.SP.1998.139.01.19.

La Nafie, Y., de los Santos, C., Brun, F., van Katwijk, M. and Bouma, T. (2012). *Waves and high nutrient loads jointly decrease survival and separately affect morphological and biomechanical properties in the seagrass Zostera noltii*. Limnology and Oceanography, 57(6), pp.1664-1672.

Larson, F., Lubarsky, H., Gerbersdorf, S. U., & Paterson, D. M. (2009). *Surface adhesion measurements in aquatic biofilms using magnetic particle induction: MagPI*. Limnology and Oceanography: Methods, 7(7), 490–497.

Ledger, M.E., R.M.L. Harris, P.D. Armitage, and A.M. Milner. 2008. *Disturbance Frequency Influences Patch Dynamics in Stream Benthic Algal Communities*. Oecologia 155 (4):809–19. https://doi.org/10.1007/s00442-007-0950-5.

Le Hir, P., Monbet, Y., & Orvain, F. (2007). *Sediment erodability in sediment transport modelling: Can we account for biota effects? Continental Shelf Research*, *27*(8), 1116–1142. doi:10.1016/j.csr.2005.11.016.

Lei, J. and Nepf, H. (2016). *Impact of current speed on mass flux to a model flexible seagrass blade*. Journal of Geophysical Research: Oceans, 121(7), pp.4763-4776.

Li, Y., Anim, D., Wang, Y., Tang, C., Du, W., Yu, Z. and Acharya, K. (2013). *An open-channel flume study of flow characteristics through a combined layer of submerged and emerged flexible vegetation*. Ecohydrology, 7(2), pp.633-647.

Løvås, S.M., Tørum, A., 2001. *Effect of the kelp Laminaria hyperborea upon sand dune erosion and water particle velocities*. Coast. Eng. 44, 37e63.

Lowe, R., Koseff, J. and Monismith, S. (2005). *Oscillatory flow through submerged canopies: 1. Velocity structure*. Journal of Geophysical Research, 110.

Luhar, M., Rominger, J. and Nepf, H. (2008). *Interaction between flow, transport and vegetation spatial structure*. Environmental Fluid Mechanics, 8(5-6), pp.423-439.

Luhar, M. and Nepf, H. (2011). *Flow-induced reconfiguration of buoyant and flexible aquatic vegetation.* Limnology and Oceanography, 56(6), pp.2003-2017.

Luhar, M. and Nepf, H. (2016). *Wave-induced dynamics of flexible blades*. Journal of Fluids and Structures, 61, pp.20-41

Malarkey, J., J.H. Baas, J.A. Hope, R.J. Aspden, D.R. Parsons, J. Peakall, D.M. Paterson, et al. 2015. *The Pervasive Role of Biological Cohesion in Bedform Development*. Nature Communications 6 (February). Nature Publishing Group:6257. https://doi.org/10.1038/ncomms7257.

Manzenrieder, H. 1985. *Retardation of Initial Erosion under Biological Effects in Sandy Tidal Flats.* 1985 Australasian Conference on Coastal and Ocean Engineering. Institution of Engineers, Australia, 455.

Marbà, N., Duarte, C., Alexandra, A. and Cabaço, S. (2014). *How do seagrasses grow and spread?* In: J. Borum, C. Duarte, D. Krause-Jensen and T. Greve, ed., European seagrasses: an introduction to monitoring and management. EU project Monitoring and Managing of European Seagrasses (M&MS) EVK3-CT-2000-00044, pp.11-18.

Marjoribanks, T., Hardy, R., Lane, S. and Parsons, D. (2016). *Does the canopy mixing layer model apply to highly flexible aquatic vegetation?* Insights from numerical modelling. Environmental Fluid Mechanics, 17(2), pp.277-301.

Miler, O., Albayrak, I., Nikora, V. and O'Hare, M. (2011). *Biomechanical properties of aquatic plants and their effects on plant–flow interactions in streams and rivers*. Aquatic Sciences, 74(1), pp.31-44.

Möller, I., Kudella, M., Rupprecht, F., Spencer, T., Paul, M., van Wesenbeeck, B.K., Wolters, G., et al. (2014). *Wave attenuation over coastal salt marshes under storm surge conditions*. Nat. Geosci. 7, 727-731.

Moulin, F. Y., Guizien, K., Thouzeau, G., Chapalain, G., Mülleners, K., & Bourg, C. (2007). *Impact of an invasive species, Crepidula fornicata, on the hydrodynamics and transport properties of the benthic boundary layer.* Aquatic Living Resources, *20*, 15–31.

Murray, J. M. H., Meadows, A., & Meadows, P. S. (2002). *Biogeomorphological implications of microscale interactions between sediment geotechnics and marine benthos: a review*. *Geomorphology*, *47*(1), 15–30. doi:10.1016/S0169-555X(02)00138-1.

Nepf, H., Sullivan, J. and Zavistoski, R. (1997). *A model for diffusion within emergent vegetation*. Limnology and Oceanography, 42(8), pp.1735-1745.

Nepf, H. and Vivoni, E. (2000). *Flow structure in depth-limited, vegetated flow*. Journal of Geophysical Research: Oceans, 105(C12), pp.28547-28557.

Nepf, H., Ghisalberti, M., White, B. and Murphy, E. (2007). *Retention time and dispersion associated with submerged aquatic canopies*. Water Resources Research, 43(4).

Nepf, H. (2012a). *Flow and Transport in Regions with Aquatic Vegetation*. Annual Review of Fluid Mechanics, 44(1), pp.123-142.

Niklas, K. (1999). *A mechanical perspective on foliage leaf form and function.* New Phytologist, 143(1), pp.19-31.

Nikora, V. (2010). *Hydrodynamics of aquatic ecosystems: An interface between ecology, biomechanics and environmental fluid mechanics*. River Research and Applications, 26(4), pp.367-384.

Nikora, V., Cameron, S., Albayrak, I., Miler, O., Nikora, N., Siniscalchi, F., Stewart, M., Hare, M.O. (2012). *Flow-biota Interactions in Aquatic Systems*. Environmental Fluid Mechanics 10.1201/b12283e12 10.1201/b12283-12, IAHR Monographs. CRC Press, pp. 217e235.

Noffke, N., and D.M. Paterson. 2007. *Microbial Interactions with Physical Sediment Dynamics, and Their Significance for the Interpretation of Earth's Biological History*. Geobiology 6 (1). Blackwell Publishing Ltd:1–4. https://doi.org/10.1111/j.1472-4669.2007.00132.x.

Norvik, C. (2017). *Design of Artificial Seaweeds for Assessment of Hydrodynamic Properties of Seaweed Farms*. Dept. of Marine Technology – Norwegian University of Science and Technology. MSc thesis, 76p. http://hdl.handle.net/11250/2453424.

Okamoto, T. and Nezu, I. (2010). *Large eddy simulation of 3-D flow structure and mass transport in open-channel flows with submerged vegetations*. Journal of Hydro-environment Research, 4(3), pp.185-197.

Orvain, F., & Sauriau, P.-G. (2002). E*nvironmental and behavioural factors affecting activity in the intertidal gastropod Hydrobia ulvae.* Journal of Experimental Marine Biology and Ecology, 272(2), 191–216. doi:10.1016/S0022-0981(02)00130-2.

Owen, M. W. (1976). *Determination of the settling velocities of cohesive muds*.

Paul, M. and Amos, C. (2011). *Spatial and seasonal variation in wave attenuation over Zostera noltii*. Journal of Geophysical Research, 116(C8).

Paul, M., Rupprecht, F., Möller, I., Bouma, T., Spencer, T., Kudella, M., Wolters, G., van Wesenbeeck, B., Jensen, K., Miranda-Lange, M. and Schimmels, S. (2016). *Plant stiffness and biomass as drivers for drag forces under extreme wave loading: A flume study on mimics*. Coastal Engineering, 117, pp.70-78.

Pan, Y., A. Herlihy, P. Kaufmann, J. Wigington, J. van Sickle, and T. Moser. 2004. *Linkages among Land-Use, Water Quality, Physical Habitat Conditions and Lotic Diatom Assemblages: A Multi-Spatial Scale Assessment.* Hydrobiologia 515 (1–3):59–73. https://doi.org/10.1023/B:HYDR.0000027318.11417.e7.

Parsons, D.R., R.J. Schindler, J.A. Hope, J. Malarkey, J.H. Baas, J. Peakall, A.J. Manning, et al. 2016. *The Role of Biophysical Cohesion on Subaqueous Bed Form Size."* Geophysical Research Letters 43 (4):1566–73. https://doi.org/10.1002/2016GL067667.

Passow, U. 2002. *Transparent Exopolymer Particles (TEP) in Aquatic Environments*. Progress in Oceanography 55 (3):287–333. https://doi.org/10.1016/S0079-6611(02)00138-6.

Passy, S.I. 2001. *Spatial Paradigms of Lotic Diatom Distribution: A Landscape Ecology Perspective*. Journal of Phycology 37 (3):370–78. https://doi.org/10.1046/j.1529-8817.2001.037003370.x.

Paterson, D.M. 1989. *Short-Term Changes in the Erodibility of Intertidal Cohesive Sediments Related to the Migratory Behavior of Epipelic Diatoms.* Limnology and Oceanography 34 (1):223–34. https://doi.org/10.4319/lo.1989.34.1.0223.

Paterson, D.M. 1997. *Biological Mediation of Sediment Erodibility: Ecology and Physical Dynamics*. In Cohesive Sediments, 215–29. John Wiley Chichester, UK.

Paterson, D.M., R.J. Aspden, P.T. Visscher, M. Consalvey, M.S. Andres, A.W. Decho, J. Stolz, and R.P. Reid. 2008. *Light-Dependant Biostabilisation of Sediments by Stromatolite Assemblages*. PLoS ONE 3 (9). Springer-Verlag:e3176. https://doi.org/10.1371/journal.pone.0003176.

Perkins, R.G., D.M. Paterson, H. Sun, J. Watson, and M.A. Player. 2004. *Extracellular Polymeric Substances: Quantification and Use in Erosion Experiments.* Continental Shelf Research 24 (15):1623–35. https://doi.org/10.1016/j.csr.2004.06.001.

Pujol, D. and Nepf, H. (2012). *Breaker-generated turbulence in and above a seagrass meadow*. Continental Shelf Research, 49, pp.1-9.

Reed, D.C., Carlson, C.A., Halewood, E.R., Nelson, J.C., Harrer, S.L., Rassweiler, A., Miller, R.J. (2015). *Patterns and controls of reef-scale production of dissolved organic carbon by giant kelp Macrocystis pyrifera*. Limnol. Oceanogr. 60, 1996e2008. https://doi.org/10.1002/lno.10154.

Reise, K. (2002). *Sediment mediated species interactions in coastal waters*. *Journal of Sea Research, 48(2),* 127–141. doi:10.1016/S1385-1101(02)00150-8.

Righetti, M., and C. Lucarelli. 2007. *May the Shields Theory Be Extended to Cohesive and Adhesive Benthic Sediments?* Journal of Geophysical Research 112 (C5):C05039. https://doi.org/10.1029/2006JC003669.

Ros, M.D., J.P. Marín-Murcia, and Mar. Aboal. 2009. *Biodiversity of Diatom Assemblages in a Mediterranean Semiarid Stream: Implications for Conservation*. Marine and Freshwater Research 60 (1):14. https://doi.org/10.1071/MF07231.

Schmidt, H., M. Thom, L. King, S. Wieprecht, and S.U. Gerbersdorf. 2016. *The Effect of Seasonality upon the Development of Lotic Biofilms and Microbial Biostabilisation*. Freshwater Biology 61 (6):963–78. https://doi.org/10.1111/fwb.12760.

Short, F., Polidoro, B., Livingstone, S., Carpenter, K., Bandeira, S., Bujang, J., Calumpong, H., Carruthers, T., Coles, R., Dennison, W., Erftemeijer, P., Fortes, M., Freeman, A., Jagtap, T., Kamal, A., Kendrick, G., Judson Kenworthy, W., La Nafie, Y., Nasution, I., Orth, R., Prathep, A., Sanciangco, J., Tussenbroek, B., Vergara, S., Waycott, M. and Zieman, J. (2011). *Extinction risk assessment of the world's seagrass species*. Biological Conservation, 144(7), pp.1961-1971.

Sjødal Olsen, K. (2017). *Impacts of Mechanical Properties and Blade Morphology on Seaweed Hydrodynamics in Steady Flow*. Dept. of Marine Technology – Norwegian University of Science and Technology. MSc thesis, 77p. http://hdl.handle.net/11250/2453423.

Smale, D.A., Burrows, M.T., Moore, P., O'Connor, N., Hawkins, S.J. (2013). *Threats and knowledge gaps for ecosystem services provided by kelp forests: a northeast Atlantic perspective*. Ecol. Evol. 3, 4016e4038.

Stévant, P., Rebours, C., Chapman, A. (2017). S*eaweed aquaculture in Norway: recent industrial developments and future perspectives*. Aquaculture International, vol. 25 (4), pp 1373–1390.

Stokes, G. G. (1901). *Mathematical and Physical Papers*, Vol. III, University Press, Cambridge, p. 59.

Sutherland, T.F., C.L. Amos, and J. Grant. 1998. *The Effect of Buoyant Biofilms on the Erodibility of Sublittoral Sediments of a Temperate Microtidal Estuary*. Limnology and Oceanography 43 (2):225–35. https://doi.org/10.4319/lo.1998.43.2.0225.

Taylor, I.S., and D.M. Paterson. 1998. *Microspatial Variation in Carbohydrate Concentrations with Depth in the Upper Millimetres of Intertidal Cohesive Sediments*. Estuarine, Coastal and Shelf Science 46 (3):359–70. https://doi.org/10.1006/ecss.1997.0288.

Taylor, I.S., D.M. Paterson, and A. Mehlert. 1999. *The Quantitative Variability and Monosaccharide Composition of Sediment Carbohydrates Associated with Intertidal Diatom Assemblages*. Biogeochemistry 45 (3):303–27. https://doi.org/10.1007/BF00993005.

Temmerman, S., P. Meire, T.J. Bouma, P.M.J. Herman, T. Ysebaert, and H.J. De Vriend. 2013. *Ecosystem-Based Coastal Defence in the Face of Global Change.* Nature 504 (7478). Nature Research:79–83. https://doi.org/10.1038/nature12859.

Thom, M, H Schmidt, S.U. Gerbersdorf, and S. Wieprecht. 2015. *Seasonal Biostabilization and Erosion Behavior of Fluvial Biofilms under Different Hydrodynamic and Light Conditions.* International Journal of Sediment Research 30 (4):273–84. https://doi.org/10.1016/j.ijsrc.2015.03.015.

Thom, M., Schmidt, H., Wieprecht, S., & Gerbersdorf, S. U. (2015). *Biostabilization of fluvial sediments: An improved device to address an old problem*. In E-proceedings of the 36th IAHR World Congress. The Hague, Netherlands.

Thom, M., Schmidt, H., Wieprecht, S., & Gerbersdorf, S. U. (2016). *The role of surface adhesion in biostabilization processes*. Conference paper, ISRS, Stuttgart.

Thomas, R.E., M.F. Johnson, L.E. Frostick, D.R. Parsons, T.J. Bouma, J.T. Dijkstra, O. Eiff, et al. 2014. *Physical Modelling of Water, Fauna and Flora: Knowledge Gaps, Avenues for Future Research and Infrastructural Needs.* Journal of Hydraulic Research 52 (3). Taylor & Francis:311–25. https://doi.org/10.1080/00221686.2013.876453.

Tinoco, R. and Coco, G. (2016). *A laboratory study on sediment resuspension within arrays of rigid cylinders*. Advances in Water Resources, 92, pp.1-9.

Tolhurst, T.J., K.S. Black, S.A. Shayler, S. Mather, I. Black, K. Baker, and D.M. Paterson. 1999. *Measuring the in Situ Erosion Shear Stress of Intertidal Sediments with the Cohesive Strength Meter (CSM).* Estuarine, Coastal and Shelf Science 49 (2):281–94. https://doi.org/10.1006/ecss.1999.0512.

Tolhurst, T.J., M. Consalvey, and D.M. Paterson. 2008. *Changes in Cohesive Sediment Properties Associated with the Growth of a Diatom Biofilm.* Hydrobiologia 596 (1). Springer Netherlands:225–39. https://doi.org/10.1007/s10750-007-9099-9.

Tolhurst, T.J., G. Gust, and D.M. Paterson. 2002. *The Influence of an Extracellular Polymeric Substance (EPS) on Cohesive Sediment Stability*. In Proceedings in Marine Science, 5:409–25. https://doi.org/10.1016/S1568-2692(02)80030-4.

Tolhurst, T.J., B. Jesus, V. Brotas, and D.M. Paterson. 2003. *Diatom Migration and Sediment Armouring — an Example from the Tagus Estuary, Portugal*. In Migrations and Dispersal of Marine Organisms, 183–93. Dordrecht: Springer Netherlands. https://doi.org/10.1007/978-94-017-2276-6_20.

Underwood, G.J.C., D.M. Paterson, and R.J. Parkes. 1995. *The Measurement of Microbial Carbohydrate Exopolymers from Intertidal Sediments.* Limnology and Oceanography 40 (7):1243–53. https://doi.org/10.4319/lo.1995.40.7.1243.

Van Leussen, W. (1994). E*stuarine macroflocs and their role in fine-grained sediment transport*. Ph. D. Thesis, University of Utrecht.

Vettori, D. (2016). *Hydrodynamic Performance of Seaweed Farms: an Experimental Study at Seaweed Blade Scale*. University of Aberdeen. PhD thesis, 216p.

Vignaga, E., H. Haynes, and W.T. Sloan. 2012. *Quantifying the Tensile Strength of Microbial Mats Grown over Noncohesive Sediments*. Biotechnology and Bioengineering 109 (5):1155–64. https://doi.org/10.1002/bit.24401.

Vignaga, E., D.M. Sloan, X. Luo, H. Haynes, V.R. Phoenix, and W.T. Sloan. 2013. *Erosion of Biofilm-Bound Fluvial Sediments*. Nature Geoscience 6 (9):770–74. https://doi.org/10.1038/ngeo1891.

Vriend, Huib J. de, Mark van Koningsveld, Stefan G.J. Aarninkhof, Mindert B. de Vries, and Martin J. Baptist. 2015. *Sustainable Hydraulic Engineering through Building with Nature.* Journal of Hydro-Environment Research 9 (2):159–71. https://doi.org/10.1016/j.jher.2014.06.004.

Wada, S., Hama, T., 2013. *The contribution of macroalgae to the coastal dissolved organic matter pool*. Estuar. Coast. Shelf Sci. 129, 77e85.

Widdows, J., Lucas, J. S., Brinsley, M. D., Salkeld, P. N., & Staff, F. J. (2002). I*nvestigation of the effects of current velocity on mussel feeding and mussel bed stability using an annular flume*. *Helgoland Marine Research*, *56*(1), 3–12. doi:10.1007/s10152-001-0100-0.

Zanke, U.C.E. 2003. *On the Influence of Turbulence on the Initiation of Sediment Motion.* International Journal of Sediment Research 18 (1):1–15.